

SEP

SECRETARÍA DE  
EDUCACIÓN PÚBLICA



TECNOLÓGICO NACIONAL DE MEXICO

Instituto Tecnológico de Tlalnepantla

Asunto: **Constancia de Servicios**

**A Quien Corresponda:**

La que suscribe, **JEFA DEL DEPARTAMENTO DE RECURSOS HUMANOS** del Instituto Tecnológico de Tlalnepantla, hace **CONSTAR**, que labora en esta Institución el (a) C:


NOMBRE: **SOLIS ROMERO JOSÉ**  
FILIACIÓN: **SORJ630126781**  
C.U.R.P.: **SORJ630126HDFLMS05**  
CLAVE(S) PRESUPUESTAL(ES): **11301 14.02 E3863 00.0 141033 (A PARTIR DEL 1º/MAR/2003)**  
CATEGORÍA(S): **PROFESOR INVESTIGADOR TITULAR "C" (E.S) TIEMPO COMPLETO (40 HORAS)**  
TIPO DE NOMBRAMIENTO: **(10) BASE**  
FECHA DE INGRESO SEP: **1º DE SEPTIEMBRE DE 1986**  
FECHA DE INGRESO I. T. TLA.: **1º DE SEPTIEMBRE DE 1986**  
LICENCIAS: **SIN LICENCIAS**

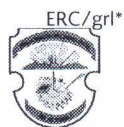
Se extiende la presente para los fines que el (a) interesado (a) convengan, en el Municipio de Tlalnepantla de Baz, Estado de México, a los dieciocho días del mes de junio del año dos mil dieciocho.

**ATENTAMENTE**

*EXCELENCIA EN EDUCACIÓN TECNOLÓGICA®  
"POR LA REALIZACIÓN TECNOLÓGICA DE MI PUEBLO"*

  
**M.T.I. ELEZER RÍOS CABALLERO**  
**JEFA DEL DEPARTAMENTO DE RECURSOS HUMANOS**

  
SECRETARÍA DE EDUCACIÓN PÚBLICA  
TECNOLÓGICO NACIONAL  
DE MÉXICO  
I.T. DE TLALNEPANTLA  
RECURSOS HUMANOS



INSTITUTO TECNOLÓGICO DE  
TLALNEPANTLA

CAMPUS TLALNEPANTLA  
Av. Instituto Tecnológico S/N  
Col. La Comunidad C.P. 54070  
Tlalnepantla de Baz, México  
Tel: 53900310 / 53900209

CAMPUS ORIENTE  
Av. Hermilo Mena S/N,  
Col. Lázaro Cárdenas La Presa C.P. 54187  
Tlalnepantla de Baz, México  
Tel: 53846464

www.itla.edu.mx





# SISTEMA EDUCATIVO NACIONAL

2003. Año del CCL Aniversario del Natalicio de Don Miguel Hidalgo y Costilla, Padre de la Patria



## SUBSECRETARÍA DE EDUCACIÓN SUPERIOR E INVESTIGACIÓN CIENTÍFICA

DIRECCIÓN GENERAL DE EDUCACIÓN SUPERIOR  
DIRECCIÓN DE INSTITUCIONES PARTICULARES DE EDUCACIÓN SUPERIOR

### RESOLUCIÓN DE REVALIDACIÓN DE ESTUDIOS

La DIRECCIÓN GENERAL DE EDUCACIÓN SUPERIOR, conforme a la atribución que le confiere el artículo 25 fracción XIII del Reglamento Interior de la Secretaría de Educación Pública, y con fundamento en lo previsto por los artículos 14 fracción III, 61 y 63 de la Ley General de Educación, así como en el Título Segundo del Acuerdo número 286, publicado en el Diario Oficial de la Federación el 30 de octubre de 2000, por considerar equiparables a un plan de estudios que se imparte en el Sistema Educativo Nacional, revalida a

**SOLIS ROMERO JOSÉ**

los estudios que realizó en The University of Sheffield, en Sheffield, en Reino Unido de Gran Bretaña e Irlanda del Norte, correspondientes al Grado de Doctor of Philosophy, expedido con fecha 16 de enero de 2003, según documentación integrada en esta Dirección General con la que se hizo la equiparación, y tomando en cuenta que se trata de estudios considerados por el Consejo Nacional de Ciencia y Tecnología (CONACYT) para el otorgamiento de beca, le tiene por acreditados los estudios de

### DOCTORADO EN INGENIERÍA MECÁNICA

México, D.F. a 14 de Noviembre de 2003

Expediente: 10-581-03



EL DIRECTOR DE INSTITUCIONES  
PARTICULARES DE EDUCACIÓN SUPERIOR

LIC. HÉCTOR LUIS NAVARRO PÉREZ

GLS/MPTO

CF01060

FOLIO

**A 190922**

CÉDULA 4001029

**SEP**



México D.F. 28 de Noviembre del 2003



FIRMA DEL TITULAR  
28/11/03

SECRETARÍA DE EDUCACIÓN PÚBLICA  
DIRECCIÓN GENERAL DE PROFESIONES

CÉDULA 4001029

EN VIRTUD DE QUE  
**JOSÉ  
SOLÍS  
ROMERO**

**CURP: SORJ630126HDFLMS05**  
CUMPLÓ CON LOS REQUISITOS EXIGIDOS POR LA LEY  
REGlamentARIA DEL ARTÍCULO 55 CONSTITUCIONAL  
RELATIVO AL EJERCICIO DE LAS PROFESIONES EN EL  
DISTRITO FEDERAL Y SU REGLAMENTO SE LE EXPIDE  
EN EDUCACIÓN DE TIPO SUPERIOR LA  
**CÉDULA**  
PERSONAL CON EFECTOS DE PATENTE PARA  
EJERCER PROFESIONALMENTE EN EL NIVEL DE  
**DOCTORADO EN  
INGENIERÍA MECÁNICA**



VÍCTOR EVERARDO BELTRÁN CORONA  
DIRECTOR GENERAL DE PROFESIONES

CEDULA 1964594

GRADO \_\_\_\_\_ REGISTRADO A FOJAS 092-45

DEL LIBRO A196

DE REGISTRO DE TITULOS PROFESIONALES Y  
GRUPO \_\_\_\_\_



S. E. P.  
DIRECCION GENERAL DE PROFESIONES  
DEPARTAMENTO DE REGISTRO  
Y EXPEDICION DE CEDULAS

FIRMA DEL INTERESADO

TGN.

SECRETARIA DE EDUCACION PUBLICA  
DIRECCION GENERAL DE PROFESIONES

1964594

EN VIRTUD DE QUE JOSE SOLIS  
ROMERO

CUMPLIO CON LOS REQUISITOS EXIGI-  
DOS POR LA LEY REGLAMENTARIA DEL  
ARTICULO 5º CONSTITUCIONAL EN  
MATERIA DE PROFESIONES Y SU REGLA-  
MENTO SE LE EXPIDE LA PRESENTE

CEDULA

CON EFECTOS DE PATENTE  
PARA EJERCER LA PROFESION DE

\*ENTRIA. EN CIENCIAS EN  
INGENIERIA MECANICA\*

MEXICO, D.F., A 29 DE JUN DE 19 94

  
EL DIRECTOR GENERAL DE PROFESIONES

LIC. MARIANO F. HERRAN SALVATTI



SUBSECRETARÍA DE EDUCACIÓN SUPERIOR  
DIRECCIÓN GENERAL DE EDUCACIÓN SUPERIOR TECNOLÓGICA

SECRETARÍA DE  
EDUCACIÓN PÚBLICA

SEP

México, D.F., 01/Diciembre/11

OFICIO No. 513.1.J/0755/11

**DR. JOSÉ SOLÍS ROMERO  
PRESENTE**

En uso de las atribuciones que me confiere la fracción XIII del artículo 19 del Reglamento Interior de la Secretaría de Educación Pública, he tenido a bien designarlo **Jefe de la División de Estudios de Posgrado e Investigación del Instituto Tecnológico de Tlalnepantla.**

Con la certeza de que su desempeño estará orientado por el respeto a las leyes, reglamentos y disposiciones que nos dan vida institucional y nos obligan a conducirnos en el marco del Código de Ética de los Servidores Públicos, le deseo el mayor de los éxitos en el ejercicio profesional de sus funciones.

**ATENTAMENTE**  
"Excelencia en Educación Tecnológica"



**DR. CARLOS ALFONSO GARCÍA IBARRA  
DIRECTOR GENERAL**

SECRETARÍA DE EDUCACIÓN PÚBLICA  
DIRECCIÓN GENERAL DE  
EDUCACIÓN SUPERIOR TECNOLÓGICA  
DIRECCIÓN GENERAL

C.C.P. Ing. Arnoldo Solís Covarrubias.- Coordinador Sectorial de Promoción de la Calidad y Evaluación.  
Lic. Eduardo Jeramilla Serna.- Coordinador Sectorial de Planeación y Desarrollo del Sistema.  
Dr. Miguel Ángel Cisneros Guerrero.- Coordinador Sectorial Académico.  
Dr. Fernando Apolinar Córdova Calderón.- Coordinador Sectorial de Administración y Finanzas.  
Ing. Oscar Castellanos Hernández.- Director del Instituto Tecnológico de Tlalnepantla.  
Expediente.

CAGTASCUIMC/1105



Patriotismo 711 Edif. B 2º Piso, Col. San Juan, Deleg. Benito Juárez, C.P. 03730, México, D.F.;

Tels. Dir.: 36 01 86 31; Conmut.: 36-01-10-00 Ext.: 65030; e-mail: par0@sep.gob.mx

[www.dgest.poo.mx](http://www.dgest.poo.mx)



**"2011, Año del Turismo en México"**



SUBSECRETARÍA DE EDUCACIÓN SUPERIOR  
DIRECCIÓN GENERAL DE EDUCACIÓN SUPERIOR TECNOLÓGICA

SECRETARÍA DE  
EDUCACIÓN PÚBLICA



México, D.F., 01/Diciembre/11

OFICIO No. 513.1.J/0755/11

**DR. JOSÉ SOLÍS ROMERO  
PRESENTE**

En uso de las atribuciones que me confiere la fracción XIII del artículo 19 del Reglamento Interior de la Secretaría de Educación Pública, he tenido a bien designarlo **Jefe de la División de Estudios de Posgrado e Investigación del Instituto Tecnológico de Tlalnepantla.**

Con la certeza de que su desempeño estará orientado por el respeto a las leyes, reglamentos y disposiciones que nos dan vida institucional y nos obligan a conducirnos en el marco del Código de Ética de los Servidores Públicos, le deseo el mayor de los éxitos en el ejercicio profesional de sus funciones.

**ATENTAMENTE**  
"Excelencia en Educación Tecnológica"



**DR. CARLOS ALFONSO GARCÍA IBARRA  
DIRECTOR GENERAL**

SECRETARÍA DE EDUCACIÓN PÚBLICA  
DIRECCIÓN GENERAL DE  
EDUCACIÓN SUPERIOR TECNOLÓGICA  
DIRECCIÓN GENERAL

C.c.p. Ing. Arnoldo Solís Covarrubias.- Coordinador Sectorial de Promoción de la Calidad y Evaluación.  
Lic. Eduardo Jaramillo Serna.- Coordinador Sectorial de Planeación y Desarrollo del Sistema.  
Dr. Miguel Ángel Cisneros Guerrero.- Coordinador Sectorial Académico.  
Dr. Fernando Apolinar Córdova Calderón.- Coordinador Sectorial de Administración y Finanzas.  
Ing. Oscar Castellanos Hernández.- Director del Instituto Tecnológico de Tlalnepantla.  
Expediente.

CAGI/CJIMC/los



Patriotismo 711 Edif. B 2º Piso, Col. San Juan, Deleg. Benito Juárez, C.P. 03730, México, D.F.,  
Tels. Dir. 36 01 86 31, Conmut. 36-01-10-00 Ext. 65050, e-mail: [part@sep.gob.mx](mailto:part@sep.gob.mx)

[www.dgest.gob.mx](http://www.dgest.gob.mx)



RSBC 347 36  
Secretaría de Educación Pública  
2011.07.18  
Proceso Educativo

**SEP**

SECRETARÍA DE  
EDUCACIÓN PÚBLICA



**TECNOLÓGICO NACIONAL DE MÉXICO**  
Instituto Tecnológico de Tlalnepantla

ASUNTO: **Constancia de Nombramiento**

**A QUIEN CORRESPONDA**

Por este medio se hace constar que el **Dr. José Solís Romero**, se encuentra vigente en su Nombramiento como **Coordinador del programa de posgrado "Maestría en Ciencias de la Ingeniería"**, que ofrece la División de Estudios de Posgrado e Investigación, el cual fue otorgado con fecha **1° de febrero del 2016**.

Lo anterior, según aparece en el archivo de la División de Estudios de Posgrado e Investigación.

A petición del interesado y para los efectos que haya lugar, se extiende la presente en la Ciudad de Tlalnepantla de Baz, Estado de México, a los 9 días del mes de agosto de 2017.

**ATENTAMENTE**

*"Por la Realización Tecnológica de mi Pueblo"*

**DR. GUSTAVO FLORES FERNÁNDEZ**  
**DIRECTOR**



SECRETARÍA DE EDUCACIÓN PÚBLICA  
TECNOLÓGICO NACIONAL  
DE MÉXICO  
I.T. DE TLALNEPANTLA  
DIRECCIÓN

c.c.p. Archivo.



CAMPUS TLALNEPANTLA  
Av. Instituto Tecnológico S/N  
Col. La Comunidad C.P. 54070  
Tlalnepantla de Baz, México  
Tel: 53900310 / 53900209

CAMPUS ORIENTE  
Av. Hermilo Mena S/N,  
Col. Lázaro Cárdenas La Presa C.P. 54187  
Tlalnepantla de Baz, México  
Tel: 53846464

[www.ittla.edu.mx](http://www.ittla.edu.mx)





"2012, Año de la Lectura"

SUBSECRETARÍA DE EDUCACIÓN SUPERIOR  
DIRECCIÓN GENERAL DE EDUCACIÓN SUPERIOR TECNOLÓGICA  
INSTITUTO TECNOLÓGICO DE TLALNEPANTLA



SECRETARÍA DE  
EDUCACIÓN PÚBLICA



Tlalnepantla de Baz, Estado de México, 05/Septiembre/2012

OFICIO DIR. No1262 /09/2012

**DR. JOSE SOLÍS ROMERO  
P R E S E N T E**

Me permito comunicar a usted que a partir de esta fecha, he tenido a bien expedir su nombramiento como **Coordinador Maestría en Ingeniería Mecánica** dependiente de la División de Estudios de Posgrado e Investigación de este Instituto.

En el desempeño de su cargo, deberá observar, respetar y promover el cumplimiento de las Leyes, Reglamentos, Acuerdos y Disposiciones que norman la vida institucional de la propia Secretaría.

**ATENTAMENTE**  
*"Por la Realización Tecnológica de mi Pueblo"*

  
**ING. OSCAR CASTELLANOS HERNÁNDEZ  
DIRECTOR**



C.c.p.- Subdirección Académica  
Depto. de Recursos Humanos  
Archivo

OCH/app



**CAMPUS TLALNEPANTLA:**  
Av. Instituto Tecnológico s/n, Col. La Comunidad,  
Tlalnepantla de Baz, Edo. de Méx. C.P. 54070  
Tels. 5565-3099, 5565-2694, 5565-3261, 5390-0209,  
5390-0310 Fax. 5565-1421

[www.ittla.edu.mx](http://www.ittla.edu.mx)

**CAMPUS ORIENTE:**  
Hermilo Mena s/n Col. Lázaro Cárdenas La Presa,  
Tlalnepantla de Baz, Edo. de Méx. C.P. 54189  
Tel. 5384-6464





**El Sistema Nacional de Investigadores otorga al:**

**DR. JOSE SOLIS ROMERO**

**la distinción de**

**INVESTIGADOR NACIONAL NIVEL I**

**Durante el periodo del 1 de enero de 2010 al 31 de diciembre de 2012 en virtud de sus logros en la realización de trabajo de investigación original.**

**DR. JOSE ANTONIO DE LA PEÑA MENA  
SECRETARIO EJECUTIVO**

+HNr3hgg0uDWUPigExAezjYxpX8V2r5lbisuDfUgEYh+Kf0QBor=  
Documento firmado electrónicamente.

11 de diciembre de 2009



El Sistema Nacional de Investigadores otorga al

*DR. JOSE SOLIS ROMERO*

la distinción de

*INVESTIGADOR NACIONAL NIVEL I*

Durante el periodo del 1 de enero de 2013 al 31 de diciembre de 2016 en virtud de sus logros en la realización de trabajo de investigación original.

**DRA. LETICIA MYRIAM TORRES GUERRA**  
Secretaria Ejecutiva del SNI

BH4jvse18i=O7rkJm5JA=A118ro8DMD3uDNShq3rnet7D= Documento firmado electrónicamente. 2 de septiembre de 2012

Es copia ~~del~~ del original

*JOSE SOLIS ROMERO*



SECRETARÍA DE EDUCACIÓN PÚBLICA  
TECNOLOGÍA EDUCACIONAL  
SE-SEVIC  
I.T. DE TLAHUAPÁN  
SUBDIRECCIÓN ACADÉMICA

Vo.Bo.

*ING. JOSÉ RAÚL HERNÁNDEZ BAUTISTA*

[http://siicyt.main.conacyt.mx:9098/psc/REGCYT\\_I/EMPLOYEE/REGCYT:c-CYT\\_...](http://siicyt.main.conacyt.mx:9098/psc/REGCYT_I/EMPLOYEE/REGCYT:c-CYT_...) 18/10/2015



**El Sistema Nacional de Investigadores otorga al**

**DR. JOSE SOLIS ROMERO**

**la distinción de**

**INVESTIGADOR NACIONAL NIVEL I**

**Durante el periodo del 1 de enero de 2017 al 31 de diciembre de 2020 en virtud de sus logros en la realización de trabajo de investigación original.**

**Dra. Julia Tagüeña Parga  
Secretaría Ejecutiva del SNI**

xO8kJ5U3LqJHXYAGvdwaEGY2mJOr8ikMeupEU7468aDXIW+NLY=  
Documento firmado electrónicamente.  
9 de septiembre de 2016

ES COPIA FIEL DEL ORIGINAL

\_\_\_\_\_  
ING. JOSÉ RAÚL TIERNÁNDEZ GAUTISTA  
SUBDIRECTOR ACADÉMICO

ES COPIA FIEL DEL ORIGINAL

\_\_\_\_\_  
DR. JOSÉ SOLIS ROMERO



**El Sistema Nacional de Investigadores otorga al**

***DR. JOSE SOLIS ROMERO***

**la distinción de**

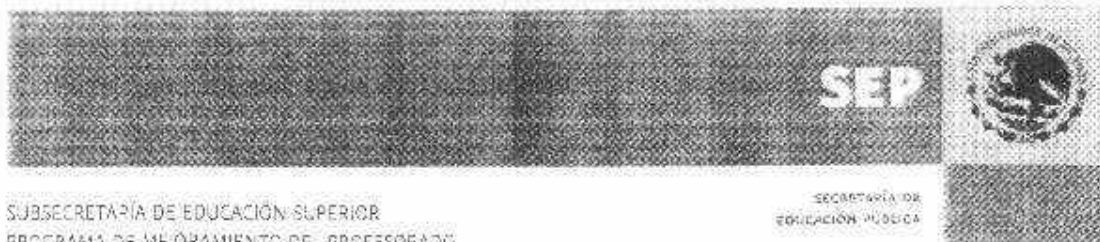
***INVESTIGADOR NACIONAL NIVEL I***

**Durante el periodo del 1 de enero de 2013 al 31 de diciembre de 2016 en virtud de sus logros en la realización de trabajo de investigación original.**

**DRA. LETICIA MYRIAM TORRES GUERRA**  
**Secretaria Ejecutiva del SNI**

BhHJwrse18I+OWrKJwm5JA==An1Bro8DMD3xDNSlhaq8lrret70=  
Documento firmado electrónicamente.  
2 de septiembre de 2012

2011 Año del Turismo en México



SUBSECRETARÍA DE EDUCACIÓN SUPERIOR  
PROGRAMA DE MEJORAMIENTO DEL PROFESORADO

SECRETARÍA DE  
EDUCACIÓN PÚBLICA

México, D. F., 20/ JUNIO/ 2011  
Oficio No. PROMEP/103.4/11/4632

Solis Romero José  
Instituto Tecnológico de Tlaxiahuacan  
Presente

Me complace informarle que el Comité Evaluador externo a PROMEP, de acuerdo con las Convocatorias 2011, resolvió positivamente su solicitud de Reconocimiento a Perfil Deseable.

En consecuencia, la SES acredita que usted tiene el perfil deseable para profesores de tiempo completo.

La acreditación tiene validez por 3 años a partir de esta fecha y servirá para los fines establecidos en la propia convocatoria.

En otro particular, aprovecho la oportunidad para enviarle un saludo.

Atentamente

M. en C. Guillermina Urbano Vidales  
Responsable de Coordinar el PROMEP

"Este programa es de carácter público, no es patrocinado ni promovido por partido político alguno y sus recursos provienen de los impuestos que pagan todos los contribuyentes. Está prohibido el uso de este programa con fines políticos, electorales, de lucro y otros distintos a los establecidos. Quien haga uso indebido de los recursos de este programa deberá ser denunciado y sancionado de acuerdo con la ley aplicable y ante la autoridad competente".



México, D. F., 10 de Diciembre de 2014  
Oficio No. DSA/103.5/14/10499

Solis Romero José  
Instituto Tecnológico de Tlalnepantla  
Presente

Me complace informarle que el Comité Evaluador externo al PRODEP, de acuerdo con las Convocatorias 2014, resolvió positivamente su solicitud de Reconocimiento a Perfil Deseable.

En consecuencia, la SES acredita que usted tiene el perfil deseable para profesores de tiempo completo.

La acreditación tiene validez por 3 años a partir de esta fecha y servirá para los fines establecidos en la propia convocatoria, en el entendido de que dejar de laborar en esta institución conlleva la cancelación del reconocimiento.

Sin otro particular, aprovecho la oportunidad para enviarle un saludo.

Atentamente



M. en C. Guillermina Urbano Vidales

Directora

“Año del Centenario de la Promulgación de la Constitución Política de los Estados Unidos Mexicanos”

Ciudad de México, 19 de Julio de 2017  
Oficio No. 511-6/17-9597

**Solis Romero José**  
**Instituto Tecnológico de Tlalneantla**  
**Presente**

Me complace informarle que el Comité Evaluador externo al PRODEP, de acuerdo con las Convocatorias 2017, resolvió positivamente su solicitud de Reconocimiento a Perfil Deseable.

En consecuencia, la SES acredita que usted tiene el perfil deseable para profesores de tiempo completo.

La acreditación tiene validez por 3 años a partir de esta fecha y servirá para los fines establecidos en la propia convocatoria, en el entendido de que dejar de laborar en esta institución conlleva la cancelación del reconocimiento.

Sin otro particular, aprovecho la oportunidad para enviarle un saludo.

**Atentamente**



**M. en C. María de Jesús Guillermina Urbano Vidales**

**Directora**

"Este programa es público ajeno a cualquier partido político. Queda prohibido el uso para fines distintos a los establecidos en el programa".

ES COPIA FIEL DEL ORIGINAL

  
DR. JOSÉ SOLÍS ROMERO

F-PROME-32/Rev-08



"2017, Año del Centenario de la Promulgación  
de la Constitución Política de los Estados Unidos Mexicanos"

Oficio núm. DP/034/17  
Dirección Adjunta de Posgrado y Becas  
Dirección de Posgrado

Ciudad de México, a 16 de febrero de 2017.

**Dr. José Solís Romero**  
**Coordinador**  
**Tecnológico Nacional de México**  
**Presente**

Estimado Dr. Solís:


Informo a usted que derivado del análisis del documento y medios de verificación recibidos en la Dirección de Posgrado, el Consejo Nacional de Posgrado (CNP) ha integrado al Padrón del PNPC el programa:

N° de Referencia	Programa	Institución
005417	Maestría en Ciencias de la Ingeniería	Tecnológico Nacional de México.

Al cumplir con las observaciones del Comité de Pares, el programa estará vigente hasta el 31 de diciembre del 2019 en el nivel de Reciente Creación.

Sin más por el momento, aprovecho la ocasión para enviarle un cordial saludo.

Atentamente,

  
M. en C. María Dolores Sánchez Soler  
Secretaría Técnica del Consejo Nacional de Posgrado  
Directora Adjunta de Posgrado y Becas

ES COPIA FIEL DEL ORIGINAL

  
DR. JOSÉ SOLÍS ROMERO

C.c.p. Dr. Luis Ponce Ramírez, Director de Posgrado.

*"Conacyt, conocimiento que transforma"*

"2011, Año del Turismo en México"

SUBSECRETARÍA DE EDUCACIÓN SUPERIOR  
DIRECCIÓN GENERAL DE EDUCACIÓN SUPERIOR TECNOLÓGICA  
COORDINACIÓN SECTORIAL ACADÉMICA  
DIRECCIÓN DE ESTUDIOS DE POSGRADO E INVESTIGACIÓN



SECRETARÍA DE  
EDUCACIÓN PÚBLICA



México, D. F., **17/noviembrel/2011**

**Oficio No. 513.2.2/3717/2011**

**ING. OSCAR CASTELLANOS HERNÁNDEZ**  
**DIRECTOR DEL INSTITUTO**  
**TECNOLÓGICO DE TLALNEPANTLA**  
**P R E S E N T E**

Por este conducto comunico a usted que el Dr. Carlos Alfonso García Ibarra, Director General de Educación Superior Tecnológica, mediante Oficio No. 513.1/2657/2011, ha autorizado la asignación de presupuesto 2011 para apoyo a la investigación a la institución a su digno cargo, lo anterior con base en las recomendaciones del Comité Evaluador de la Convocatoria de Investigación Científica y Tecnológica 2011, por lo cual hago de su conocimiento la información básica del proyecto de investigación.

Título del Proyecto	Clave
Comportamiento tribológico de aceros con tratamiento superficial de boruado, nitrurado y boronitrurado.	4450.11-P

Grupo de Investigación	
Director(a) Responsable	Dr. José Solís Romero
Colaboradores	Dr. Benjamín Vargas. A., M.C. Miguel A. Paredes R., M.C. Armando Gómez V.

Vigencia del proyecto: 12 meses	
Fecha de Inicio	Fecha de Término
03 de enero de 2012	31 de diciembre de 2012
Entrega de Informes	
Informe de Avance	Informe Final
01 al 30 de julio de 2012	01 al 31 de enero de 2013

La asignación del apoyo económico se realizará de acuerdo a la disponibilidad de los recursos que se tengan.



*Es copia Fiel del ORIGINAL  
del José Solís*



Patriotismo 711 Edif. B 2º Piso Col. San Juan Mixcoac, Del. Benito Juárez, C.P. 03730, México, D.F.,  
Tel. 055-36-01-86-00 Ext. 65048, 65066, e-mail: posgrado@dgest.gob.mx,  
www.dgest.gob.mx



"2015, Año del Generalísimo José María Morelos y Pavón"

México, D.F., **17/Marzo/2015**

Oficio No. M00.2.2/0543/2015

**ING. OSCAR CASTELLANOS HERNÁNDEZ**  
**DIRECTOR DEL INSTITUTO**  
**TECNOLÓGICO DE TLALNEPANTLA**  
**PRESENTE**

Con referencia al recurso asignado por la Coordinación Sectorial de Planeación y Desarrollo del Sistema, mediante el Oficio No. M00.3/0447/2015, para apoyo de la investigación en la institución a su digno cargo, y con base en las recomendaciones del Comité Evaluador de la Convocatoria 2015 de Proyectos de Investigación Científica, Aplicada, Desarrollo Tecnológico e Innovación, hago de su conocimiento la información básica del proyecto de investigación.

<b>Título del Proyecto</b>		<b>Clave</b>
Comportamiento mecánico y tribológico con y sin lubricación de los aceros S2100 y M2 revestidos por deposición con películas delgadas de carbón tipo diamante, hidrogenado (DLC) así como TiN, utilizando PVD-PECVD y su comparación con revestimiento de borur		5642 15-P
<b>Grupo de Investigación</b>		
Director(a) Responsable	José Solís Romero	
Colaboradores	Armando Gómez Vargas, Rodolfo Velázquez Mancilla, Miguel A. Paredes Ruedas, Víctor A. Castellano Escamilla	
<b>Vigencia del proyecto: 12 meses</b>		
Del 02 de mayo de 2015 al 02 de mayo de 2016		
<b>Entrega de Informes</b>		
1er. informe de Avance	Informe Final	
01 al 30 de noviembre de 2015	02 al 31 de mayo de 2016	

Cabe señalar que las partidas a continuación son enunciativas, para lo cual invariablemente al ejercerlas deberán ser justificadas en los proyectos de investigación.



"Año del Centenario de la Promulgación de la Constitución Política de los Estados Unidos Mexicanos"

Ciudad de México, 08/Agosto/2017

Oficio No. M00.2.2/3302/2017

**DR. GUSTAVO FLORES FERNÁNDEZ**  
**DIRECTOR DEL INSTITUTO TECNOLÓGICO DE TLALNEPANTLA**  
**PRESENTE**

Derivado de la asignación de presupuesto para los proyectos aprobados en la Convocatoria de Apoyo a la Investigación Científica y Tecnológica 2017-3 para los Institutos Tecnológicos Federales y Centros, hago de su conocimiento la información básica del proyecto de investigación:

<b>Título del Proyecto</b>	Optimización utilizando lógica difusa y diseño de experimentos tanto de los parámetros de procesamiento como del comportamiento tribológico de los aceros aleados y al carbón, revestidos mediante procesos de difusión (boronitrurado) y deposición (carbón cuasidiamante hidrogenado- HDLC).		
<b>Clave</b>	6353.17-P		
<b>Vigencia</b>	01 de septiembre de 2017 al 31 de agosto de 2018		
<b>Director(a) Responsable</b>	Solís Romero José		
<b>Entrega de Informes de Avance</b>	<b>1er. Informe</b>	<b>2do. Informe</b>	<b>3er. Informe</b>
	15 al 30 de diciembre de 2017	15 al 30 de marzo de 2018	15 al 30 de junio de 2018
<b>Entrega de Informe Final</b>	01 al 30 de septiembre de 2018		
<b>Monto aprobado</b>	<b>Partida 21701</b>	<b>Partida 31903</b>	<b>Total</b>
	\$250,000.00	\$ 0.00	\$250,000.00

**Partida 21701:** 21101, 21201, 21301, 21401, 21501, 22201, 23101, 23301, 23401, 23501, 23601, 23701, 23901, 23902, 24501, 24601, 24701, 24901, 25101, 25201, 25301, 25401, 25501, 25901, 26105, 29101, 29401, 29501 y 29801.

**Partida 31903:** 33301, 33304, 33601, 33901, 35301, 35401 y 35702.

Los informes técnicos de avance y final del proyecto deberán ser cargados en la plataforma de proyectos <https://dpiacad-tecnm.mx/proyectos/>, en el apartado correspondiente, de acuerdo al periodo establecido en este documento.

Sin otro particular, aprovecho la ocasión para enviarle un cordial saludo.



**ATENTAMENTE**

"EXCELENCIA EN EDUCACIÓN TECNOLÓGICA"

**DRA. YESICA IMELDA SAAVEDRA BENÍTEZ**  
**DIRECTORA DE POSGRADO, INVESTIGACIÓN E INNOVACIÓN**

SECRETARÍA DE EDUCACIÓN PÚBLICA  
TECNOLÓGICO NACIONAL  
DE MÉXICO  
DIRECCIÓN DE POSGRADO,  
INVESTIGACIÓN E INNOVACIÓN

YISB/ESGA/EFAB

"2011, Año del Turismo en México"



SUBSECRETARÍA DE EDUCACIÓN SUPERIOR  
DIRECCIÓN GENERAL DE EDUCACIÓN SUPERIOR TECNOLÓGICA  
COORDINACIÓN SECTORIAL ACADÉMICA  
DIRECCIÓN DE ESTUDIOS DE POSGRADO E INVESTIGACIÓN

SECRETARÍA DE  
EDUCACIÓN PÚBLICA

México, D. F., 01 / noviembre / 2011

Oficio 513.2.2/3349/2011

**ING. OSCAR CASTELLANOS HERNÁNDEZ**  
**DIRECTOR DEL INSTITUTO TECNOLÓGICO DE TLALNEPANTLA**  
**PRESENTE**

En relación a la solicitud de registro de proyectos de investigación, comunico a usted que esta Dirección a mi cargo ha registrado el proyecto 2011 que a continuación se menciona:

Título del Proyecto	Línea de Investigación	Clave de Registro
Comportamiento tribológico del hierro puro y acero 4140 con tratamiento superficial de borurado, nitrurado por plasma y boronitrurado.	Optimización de Sistemas Mecánicos	TLA-MIM-2011-104


Grupo de Investigadores	
Director(a) Responsable	Dr. José Solís Romero
Colaboradores	M.C. Miguel A. Paredes Rueda, M.C. Rodolfo Velázquez Mancilla, Dr. Benjamín Vargas Arista.

Vigencia del proyecto: 12 meses	
Fecha de Inicio	Fecha Término
01-feb-11	28-feb-12
Entrega de Informe	
Informe Final	
28 de marzo de 2012	

El control, seguimiento y evaluación de dicho proyecto, a través de informes de avance e informe final tanto de los aspectos técnicos como de los financieros, es responsabilidad de las unidades académicas y administrativas correspondientes del Instituto Tecnológico a su cargo. En este sentido, el director responsable del proyecto deberá entregar informes semestrales para verificar los resultados obtenidos en su Institución. Una vez que los informes académicos hayan sido avalados por las unidades correspondientes, deberá enviar a esta Dirección el archivo electrónico del informe final en disco compacto, así como las evidencias de los productos obtenidos en formato PDF, acompañado de un oficio de presentación por parte del Director de la Institución. Cabe mencionar que el formato del informe se encuentra disponible en el portal electrónico de la DGEST.

Sin más por el momento, aprovecho la oportunidad para enviarte un cordial saludo.

**ATENTAMENTE**  
**Excelencia en Educación Tecnológica**

  
**DRA. ANA MARÍA MENDOZA MARTÍNEZ**  
**DIRECTORA**

c.c.p. Archivo

AMMM: [initials]



**SECRETARÍA DE EDUCACIÓN PÚBLICA**  
**DIRECCIÓN GENERAL DE**  
**EDUCACIÓN SUPERIOR TECNOLÓGICA**  
**DIRECCIÓN DE ESTUDIOS DE**  
**POSGRADO E INVESTIGACIÓN**



Patriotismo 711 Edf. B 3° Piso, Ctra. San Juan Mixcoac, Del. Benito Juárez, C.P. 06700, México, D.F.

Tels. Central: 36-02 86-00 Ext. 63048, email: posgrado@dgest.gob.mx,

www.dgest.gob.mx





**V International Conference on Surfaces,  
Materials and Vacuum  
Tuxtla Gutiérrez, Chiapas  
September 24-28, 2012**

**Sociedad Mexicana de Ciencia y Tecnología  
de Superficies y Materiales**

The Conference Organizing Committee certifies that  
**JOSE SOLIS, JOAQUIN OSEGUERA, ARIOSTO MEDINA,  
ALBERTO CUEVAS**

presented the following poster contribution

**350- TRB  
"TRIBOLOGICAL EVALUATION OF PLASMA NITRIDED H13  
DIE STEEL"**

**Dr. Enrique Camps Carvajal  
President SMCTSM**

*Es copia FIEL DEL  
ORIGINAL  
del Jose Solis Portero*



SEP

SECRETARÍA DE  
EDUCACIÓN PÚBLICA

TECNOLÓGICO NACIONAL DE MÉXICO

INSTITUTO TECNOLÓGICO  
DE TLALNEPANTLA

CERTIFICACIÓN DE ACTA DE EXAMEN DE GRADO DE MAESTRIA



El suscrito Director del Instituto Tecnológico de Tlalnepantla, certifica que en el Libro para Actas de Examen de Grado de Maestría N° 1 autorizado el día 4 del mes de Agosto del 2014 por la Dirección de Servicios Escolares y Estudiantiles del Tecnológico Nacional de México, se encuentra asentada en la foja número 032 el Acta que a la letra dice:

En la ciudad de Tlalnepantla de Baz, Estado de México a los 15 días del mes de JUNIO, siendo las 14:20 horas, se reunieron en EDIFICIO DE POSGRADO AULA W1 del Instituto Tecnológico de Tlalnepantla, clave 15DIT0025M, el jurado integrado por:

Presidente(a): DOCTOR EN INGENIERIA MECÁNICA JOSÉ SOLIS ROMERO - CED 4001029

Secretario(a): DOCTOR EN INGENIERIA MECÁNICA OSCAR ARMANDO GÓMEZ VARGAS - CED 08705830

Vocal MAESTRO EN CIENCIAS EN INGENIERIA MECÁNICA MIGUEL ÁNGEL PAREDES RUEDA - CED 2384253

Y de acuerdo con las disposiciones reglamentarias en vigor, se procedió a efectuar el examen de Grado de Maestría a el (la) C. HECTOR DAVID DE REZA ESCAMILLA, número de control M03250291, aspirante al Grado de Maestro en INGENIERIA MECÁNICA

Tomando en cuenta el contenido de la tesis cuyo título es: COMPORTAMIENTO ELECTROQUÍMICO DE LOS RECUBRIMIENTOS HIDROGENADOS DE CARBÓN TIPO DIAMANTE Y CON SI SOBRE EL ACERO AL CARBÓN que fue dirigida por DOCTOR EN INGENIERIA MECÁNICA, JOSÉ SOLIS ROMERO, una vez concluido el examen oral, dictaminó que fuera Aprobado.

El (la) Presidente (a) del Jurado le hizo saber a el (la) sustentante el Código de Ética Profesional y le tomó la Protesta de Ley, una vez escrita y leída la firmaron las personas que en el acto protocolario intervinieron, para los efectos legales a que haya lugar, se asienta la presente.


Se extiende esta certificación a los 16 días del mes de JUNIO de 2017.

COTEJÓ

Jefe (a) del Departamento de  
Servicios Escolares

  
Ing. Reynaldo Olivares Gurroia

DIRECTOR

  
Dr. Gustavo Flores Fernández



SECRETARÍA DE EDUCACIÓN PÚBLICA  
TECNOLÓGICO NACIONAL  
DE MÉXICO  
I.T. DE TLALNEPANTLA  
DIRECCIÓN



# SUPERFICIES Y VACÍO

Una publicación de la

Sociedad Mexicana de Ciencia y Tecnología de Superficies y Materiales A.C.

Ciudad de México a 28 de noviembre de 2012.

## Editor

Miguel Meléndez  
Chvesta-IPN

## Barra de editores

Joe Green  
U. de Illinois

Wilfrido Calleja  
INAOE

Enrique Camps  
ININ

Luis Viña  
DFM-C-IV  
U. Autónoma de  
Madrid

Mario Farias  
IF-UNAM, Ensenada

María Carmen  
Asensio  
ICM-CSIC  
U. Autónoma de  
Madrid

Álvaro Pulzara Mora  
U. Nacional de  
Colombia, Manizales

Joseph Wojcik  
MSEL-NIST

Martin Flores  
U. de Guadalajara

Jesús Carrillo  
CIDS-BUAP

Satoshi Shimomura  
Universidad Ehime

Yvonne Primerano  
Universidad de São  
Paulo

## A Quien Corresponda

Por este conducto, hacemos constar que el Dr. José Solís Romero ha colaborado con la Revista Superficies y Vacío como revisor del trabajo: "*STUDY OF HARD LAYERS IN A STEEL BASED Cr-Mn*" (Ref. SV12-046).

La presente se extiende para los fines que al interesado convengan.

Atentamente,

Dr. Miguel Meléndez Lira  
Co-Editor



Tlalnepantla de Baz, Edo. de Méx., a 03/marzo/2016  
OFICIO DEPI 800/03/2016

**A QUIEN CORRESPONDA**


El que suscribe, Jefe de la División de Estudios de Posgrado e Investigación hace constar que los profesores-investigadores que se listan a continuación y que se encuentran adscritos a esta División, participaron durante los meses de octubre de 2015, así como **enero y febrero de 2016** en la elaboración del plan y programas de estudio de la Maestría en Ciencias de la Ingeniería, lo que inherentemente incluye el estudio de factibilidad para su apertura (se adjunta autorización del programa por parte del TecNM):

DR. VÍCTOR AUGUSTO CASTELLANOS ESCAMILLA  
DR- OSCAR ARMANDO GÓMEZ VARGAS  
DR. JOSÉ SOLÍS ROMERO  
DR. BENJAMÍN VARGAS ARISTA  
DR. IRINEO PEDRO ZARAGOZA RIVERA  
DRA. NADXIELI PALACIOS GRIJALVA  
DRA. VERÓNICA ESTRELLA SUÁREZ  
M.C. SANDRA SILVIA ROBLERO AGUILAR  
M.C. MIGUEL ANGEL PAREDES RUEDA  
M.C. RODOLFO VELÁZQUEZ MANCILLA

A petición de los interesados y para los efectos que haya lugar, se extiende la presente en la Ciudad de Tlalnepantla de Baz, Estado de México.


**A TENTAMENTE**

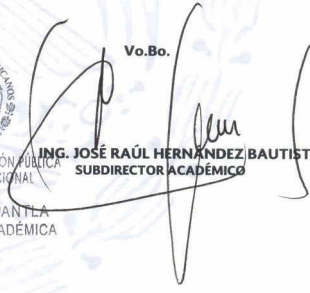
"Por la Realización Tecnológica de mi Pueblo"

  
**M.C. MIGUEL A. PAREDES RUEDA**  
JEFE DE LA DIVISIÓN DE ESTUDIOS DE POSGRADO E INVESTIGACIÓN

c.c.p. Ing. José Raúl Hernández Bautista  
Archivo.

JRHB/MAPR/nud\*

  
SECRETARÍA DE EDUCACIÓN PÚBLICA  
TECNOLÓGICO NACIONAL  
DE MÉXICO  
I.T. DE TLALNEPANTLA  
SUBDIRECCIÓN ACADÉMICA

**Vo.Bo.**  
  
**ING. JOSÉ RAÚL HERNÁNDEZ BAUTISTA**  
SUBDIRECTOR ACADÉMICO

México, D.F., 26/enero/2016

OFICIO No. M00/0019/2016

**DR. GUSTAVO FLORES FERNÁNDEZ**  
**DIRECTOR DEL INSTITUTO TECNOLÓGICO DE TLALNEPANTLA**  
**PRESENTE**

En cumplimiento de las fracciones I y II, del artículo segundo, del Decreto por el que se crea el Tecnológico Nacional de México, publicado en Diario Oficial de la Federación el 23 de julio de 2014, y de conformidad con el apartado 1.7. De la Apertura de Programas de Posgrado, establecido en los "Lineamientos para la operación de Estudios de Posgrado en el Sistema Nacional de Institutos Tecnológicos", que entraron en vigor el 18 de enero de 2013, y en virtud de que se han cumplido con los requisitos establecidos en los mismos lineamientos; he determinado aceptar y aprobar la apertura del Plan de Estudios de **Maestría en Ciencias de la Ingeniería**, con clave **MCING-2011-45**, en la Institución a su cargo, a partir de febrero de 2016, con la vigencia establecida en el inciso d) del mismo apartado 1.7 de los lineamientos, sujeta a las evaluaciones que esta Dirección General considere convenientes.

Sin otro particular, aprovecho la ocasión para enviarle un cordial saludo.

**ATENTAMENTE**  
EXCELENCIA EN EDUCACIÓN TECNOLÓGICA®



**Mtro. Manuel Quintero Quintero**  
**DIRECTOR GENERAL**



SECRETARÍA DE EDUCACIÓN PÚBLICA  
TECNOLÓGICO NACIONAL  
DE MÉXICO

**DIRECCIÓN GENERAL**

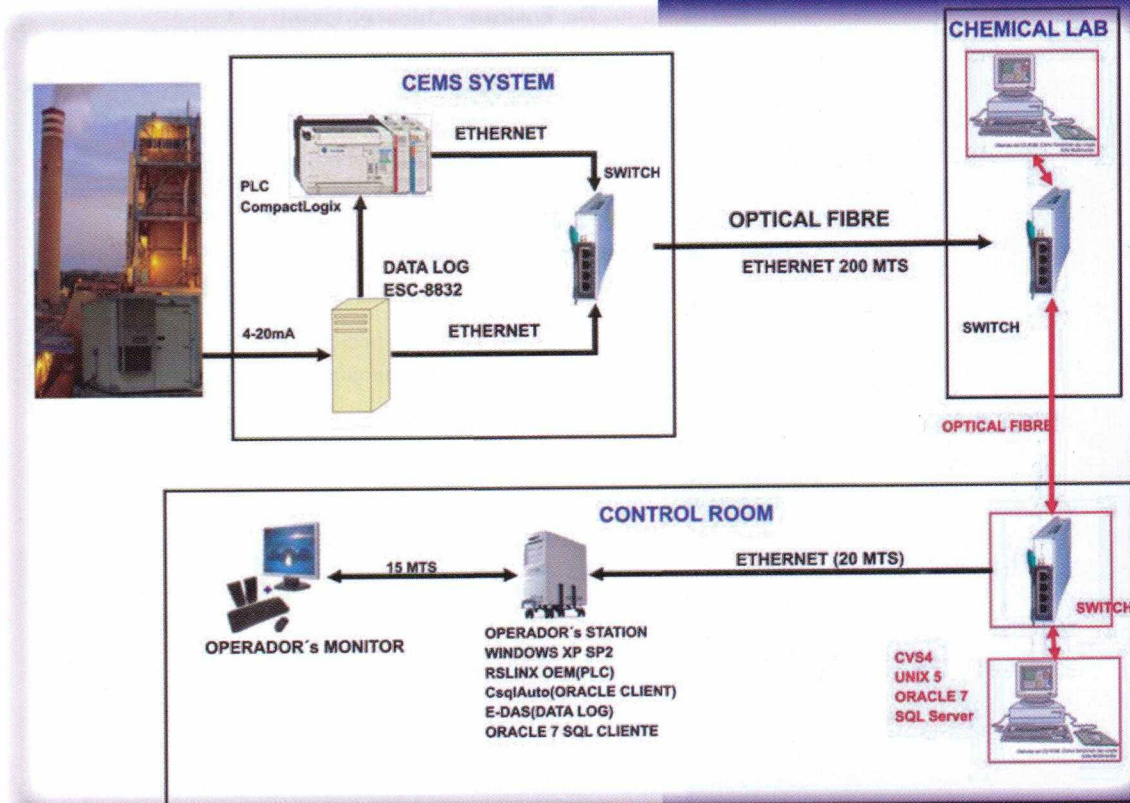
C.p. Mtro. Ignacio López Valdevinos - Secretaría Académica de Investigación e Innovación -Presente  
Archivo - Dirección de Posgrado, Investigación e Innovación -Presente

MQQ/IV/SGV

Revista de la Sociedad  
Mexicana de Ingeniería Mecánica

# INGENIERÍA MECÁNICA

## TECNOLOGÍA Y DESARROLLO



# Surface Roughness and Residual Stresses on the Fatigue Life of Shot Peened Components: Theoretical Determination

José Solís Romero<sup>1</sup>, Alfonso Anguiano García<sup>1</sup>, Antonio García Macedo<sup>2</sup>

<sup>1</sup>Instituto Tecnológico de Tlalnepantla. Departamento de Ingeniería Mecánica  
División de Estudios de Posgrado e Investigación  
josesolis@itesm.mx, ponchito\_jr@latinmail.com

<sup>2</sup>Instituto Tecnológico y de Estudios Superiores de Monterrey-CEM-DIA  
Departamento de Ingeniería Mecánica.  
josegarc@itesm.mx

## Abstract

The effects of the shot peening process on the fatigue damage are analysed and modelled. Surface roughness is modelled in a way that would increase the far-field stress. Compressive residual stresses translated as closure stresses which tend to reduce the application of the far-field stress by introducing this closure stress on the crack flanks and thus the propagation of the crack is expected to be somewhat reduced compared to the unpeened condition.

## Resumen

Se analizaron y modelaron matemáticamente los efectos del proceso de granallado que tienen en el daño por fatiga de materiales metálicos policristalinos. La rugosidad superficial se modeló de tal forma que incrementa el esfuerzo aplicado. Los esfuerzos residuales compresivos se convirtieron en esfuerzos de cerradura los cuales tienden a contrarrestar el esfuerzo aplicado dado que el esfuerzo de cerradura actúa en las caras de la grieta reduciendo la velocidad de propagación en comparación con aquellos componentes sin la aplicación del granallado.

## Keywords:

Controlled shot peening; fatigue life improvement; micromechanical model.

## Introduction

For many years controlled shot peening (CSP) was considered as a surface treatment of questionable benefits. This impression was fuelled by contradictory results from fatigue experiments [1,2]. It is now clear that the performance of CSP in terms of fatigue, depends on the balance between its beneficial (compressive residual stress and work hardening) and detrimental effects (surface roughening) [3,4]. Hence, in order to achieve a favourable fatigue performance, the role of the above effects has to be analysed and understood. To achieve such undertaking it is essential to consider their interaction with other parameters such as the nature of the target material and the loading conditions.

This work brings together two micromechanical models; one for notch sensitivity [5] and for fatigue life [6]. The former assesses the effect of surface roughening, whilst the latter incorporates the residual stress distribution and work hardening on fatigue life calculations. Combination of the two models allows the determination of the residual stress distribution to meet specific improvements in fatigue life (improvement life factor, ILF). Using the ILF methodology, the effects of CSP can be scrutinised against the stress level, the surface roughness and the ILF value.

## Modelling the Surface Roughness

On shot peened surfaces, cracks are likely to form at micro-

## Palabra claves:

Shot peening controlado; vida en fatiga; modelo micromecánico.

notches (dents). Early studies from Smith [7] and Tanaka [8] indicate that the propagation of cracks from notches depends on the bluntness of the notch, given by  $\sqrt{i/\rho}$  ( $\rho$  is the notch radius). Despite the numerous models published in the literature, an extended citation is given in [9], most models fail to provide a relationship between the geometry of the notch and the microstructure of the material. Such relationship was successfully provided by Vallellano et al [5,10]. According to their work, the nominal stress in a notched member is given by,

$$\sigma_i^{nom} = \frac{\sigma^{app}}{Z_i} \quad (1)$$

where  $\sigma^{app}$  is the applied stress,  $\sigma_i^{nom}$  is the distribution of the nominal stress ahead of the notch root as a function of the distance from the notch  $i$ , mapped as  $i=2a/D$ , and  $Z_i$  is the notch factor given by,

$$Z_i = \frac{\sqrt{i}}{\alpha + \beta} \left[ \frac{\bar{\beta}}{\lambda_i} + \frac{\bar{\alpha}}{\sqrt{1 + \lambda_i^2}} \right]^{1/2}$$

$$\lambda_i = \frac{1}{\alpha^2 - \beta^2} \left[ \alpha \sqrt{(\alpha + iD/2)^2 - \alpha^2 + \beta^2} - \beta (\alpha + iD/2) \right] \quad (2)$$

where  $i=1,3,5,\dots$



## Tribological performance of an H-DLC coating prepared by PECVD

J. Solís<sup>a,b,\*</sup>, H. Zhao<sup>a</sup>, C. Wang<sup>a</sup>, J.A. Verduzco<sup>c</sup>, A.S. Bueno<sup>a,d</sup>, A. Neville<sup>a</sup><sup>a</sup> *IBS, University of Leeds, School of Mechanical Engineering, Leeds, LS2 9JT, United Kingdom*<sup>b</sup> *SEPISS/TECNM/IT de Tlalpan, SEP-Mechanical Engineering, 54070, Edo. Méx., México*<sup>c</sup> *Instituto de Investigación en Metalurgia y Materiales, CIMOM, P.O. Box 408, 28000, Merida, Méx., México*<sup>d</sup> *Mechanical Engineering Department, Universidade Federal de São João Del Rei, 170 Praca Frei Orlando, 36307-352 São João Del Rei, Brazil*

## ARTICLE INFO

Article history:  
Received 1 January 2016  
Received in revised form 28 April 2016  
Accepted 29 April 2016  
Available online 2 May 2016Keywords:  
Hydrogenated diamond-like carbon  
Friction  
Wear  
AISI 52100 steel  
Dry sliding

## ABSTRACT

Carbon-based coatings are of wide interest due to their application in machine elements subjected to continuous contact where fluid lubricant films are not permitted. This paper describes the tribological performance under dry conditions of duplex layered H-DLC coating sequentially deposited by microwave excited plasma enhanced chemical vapour deposition on AISI 52100 steel. The architecture of the coating comprised C<sub>1</sub>, WC, and DLC (a-C:H) with a total thickness of 2.8 μm and compressive residual stress very close to 1 GPa. Surface hardness was approximately 22 GPa and its reduced elastic modulus around 180 GPa. Scratch tests indicated a well adhered coating achieving a critical load of 80 N. The effect of normal load on the friction and wear behaviours were investigated with steel pins sliding against the actual coating under dry conditions at room temperature (20 ± 2 °C) and 35–50% RH. The results show that coefficient of friction of the coating decreased from 0.21 to 0.13 values with the increase in the applied loads (10–50 N). Specific wear rates of the surface coating also decrease with the increase in the same range of applied loads. Maximum and minimum values were  $14 \times 10^{-4}$  and  $5.5 \times 10^{-4}$  mm<sup>3</sup>/N·m, respectively. Through Raman spectroscopy and electron microscopy it was confirmed the carbon-carbon contact, due to the tribolayer formation on the wear scars of the coating and pin. In order to further corroborate the experimental observations regarding the graphitisation behaviour, the existing mathematical relationships to determine the graphitisation temperature of the coating/steel contact as well as the flash temperature were used.

© 2016 Elsevier B.V. All rights reserved.

## 1. Introduction

The quality and functional characteristics of many engineering applications is determined by superimposed mechanical loads and particular requirements on their surface, such as wear resistance or low levels of coefficient of friction (CoF). The use of thin films as the non-stoichiometric hydrogenated amorphous carbon (a-C:H), also named hydrogenated diamond-like carbon (H-DLC), has become widespread for the improvement of performance/life of steel components [1,2], in which specific properties at particular locations are needed without compromising the bulk material strengths. Furthermore, these coatings are also being used as solid lubricants in the industrial field to improve tribological behaviours of machine components under very clean atmospheres or where fluid lubricants are not permitted. The progressive acceptance of

these coatings for the above purposes is due to the mechanical, chemical, electrical and optical properties they exhibit [3,4]. The deposition of DLCs is commonly obtained by plasma decomposition of a hydrocarbon-rich atmosphere at low substrate temperatures and high deposition rates. The latter is a major advantage for most steels because the annealing temperature is not reached (<200 °C), therefore substrate hardness is not affected. In spite of the outstanding properties of DLC coatings, the CoF and wear mechanisms depend significantly on the deposition method/parameters [1,5], variation in environment, either in vacuum or room atmosphere [6], relative humidity [7], the substrate and counterbody materials, the various coating architectures such as multiple or gradient layers, and very importantly, the wearing conditions, i.e. under dry, water, oil or a combination of these [8,9]. In the case of unlubricated conditions, the influence of loading and sliding velocity on the CoF and wear rates becomes essential. Sharma et al. [10] put forward variations in the CoF and wear for different loads on the Steel/DLC pair, under ambient and dry conditions. The CoF decrease with the increase of normal load for short sliding distances, and for long sliding distances, the CoF decrease with the decrease of normal load. Upon the steady state, there seems to be a convergence in the CoF

\* Corresponding author at: SEP/TECNM/Instituto Tecnológico de Tlalpan, Postgraduate Studies/Mechanical Engineering, Av. Constitución de 1857, S/N, Col. La Comunidad, 54070 Tlalpan, Edo. Méx., México.  
E-mail addresses: [jsolis@iita.edu.mx](mailto:jsolis@iita.edu.mx), [josesolis@nitium.com.mx](mailto:josesolis@nitium.com.mx) (J. Solís).

<http://dx.doi.org/10.1016/j.apsusc.2016.04.184>  
0169-4332/© 2016 Elsevier B.V. All rights reserved.





Contents lists available at ScienceDirect

Materials Letters

journal homepage: [www.elsevier.com/locate/matlet](http://www.elsevier.com/locate/matlet)

## Boro-nitriding coating on pure iron by powder-pack boriding and nitriding processes

O.A. Gómez-Vargas<sup>a</sup>, J. Solís-Romero<sup>b,\*</sup>, U. Figueroa-López<sup>a</sup>, M. Ortiz-Domínguez<sup>c</sup>, J. Oseguera-Peña<sup>a</sup>, A. Neville<sup>d</sup>

<sup>a</sup> Instituto Tecnológico y de Superior de Monterrey campus Estado de México, Carretera a Lago de Guadalupe km 3.5, 52926 Atizapán Edo. Méx., Mexico  
<sup>b</sup> SEP/INM Instituto Tecnológico de Toluca/Division of Postgraduate Studies/Department of Mechanical Engineering, Av. Mario Gallo, s/n, Col. La Compañía, Toluca, Edo. de México 54070, Mexico  
<sup>c</sup> Universidad Autónoma del Estado de Hidalgo, Campus Sahagún, Carretera Cd. Sahagún-Otumba s/n, Hidalgo, Mexico  
<sup>d</sup> IFS, University of Leeds, School of Mechanical Engineering, Leeds LS2 9JT, United Kingdom

## ARTICLE INFO

Article history:  
 Received 10 February 2016  
 Received in revised form 15 April 2016  
 Accepted 17 April 2016  
 Available online 20 April 2016

Keywords:  
 Boriding  
 Nitriding  
 Boro-nitriding  
 Powder-pack  
 Dry sliding

## ABSTRACT

To alleviate spallation and crack difficulties exhibited by a borided metallic surface when it is subjected to a normal, heavy and sliding load under dry conditions, a boron nitride coating was produced on pure iron in two stages: boriding the iron surface at 950 °C for 6 h and then nitriding the pre-borided iron at 550 °C for 6 h. The powder-pack technique was used in both stages. XRD measurements confirmed that the grown layers were nitrides and duplex borides. The produced diffusion of the layers reached 240 μm in depth as measured by SEM images. The measured microhardness across the case favoured the interphase cohesion between the iron nitrides and iron borides layers. Consequently, the multicomponent coating exhibited superior wear resistance to an applied normal load under dry sliding contact conditions in comparison to borided iron.

© 2016 Elsevier B.V. All rights reserved.

## 1. Introduction

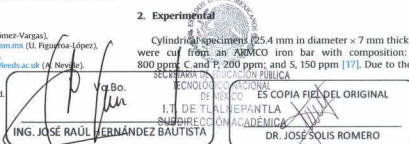
Hard coatings with carbides, borides and nitrides have been successfully utilised for engineering applications where specific properties at particular locations are required without compromising the bulk material strengths [1–5]. In particular, resistant layers of borides are produced in ferrous and non-ferrous materials through the well-developed process of boriding. In ferrous materials, this thermochemical diffusion treatment generally possesses superior hardening features than those found in conventional processes like carburizing, nitriding or chromising, due to the formation of single (Fe<sub>2</sub>B) or duplex (FeB + Fe<sub>2</sub>B) hard phases [3,6]. However, while the single Fe<sub>2</sub>B layer of ferrous materials promotes a surface with high compressive stresses, the FeB phase is very brittle and develops a surface subjected to high tensile stresses [2,7–9]. At the end of the boriding process when the temperature decreases to ambient, and if the duplex phase is produced in the boride layer, stresses from such phases can lead to crack formation at the FeB/Fe<sub>2</sub>B interface. This latter, due to those

phases exhibit different coefficients of thermal expansion, it can cause spallation leading to the separation of the duplex layer, or else crack formation can appear under mechanical strain or thermal and mechanical shocks [10,11]. On the other hand, the thermochemical process of nitriding is also used to improve the wear and corrosion resistance of engineering components, producing a hard case and a soft and tough core. Nevertheless, significant variation has been identified in the hardness gradient resulting in ablated tribological performances [12,13]. To mitigate the brittleness and those variations in microhardness, two multicomponent surface treatments such as boro-nitriding are being investigated. Nonetheless, very little work has been devoted to assess both the microstructural and mechanical characteristics of boron nitride coatings on ferrous materials [14–16]. In this study, boride-nitride layers on pure iron have been investigated. Aspects of the film formation and the characteristics of their mechanical response to static and dynamic loads (namely hardness and friction behaviour) under dry conditions were the focus of the study.

## 2. Experimental

Cylindrical specimens (25.4 mm in diameter × 7 mm thickness) were cut from an ARMCO iron bar with composition: Mn, 800 ppm; C and P, 200 ppm; and S, 150 ppm [17]. Due to the fact

\* Corresponding author.  
 E-mail addresses: [ogomez@itesm.mx](mailto:ogomez@itesm.mx) (O.A. Gómez-Vargas), [josel@ita.edu.mx](mailto:josel@ita.edu.mx) (J. Solís-Romero), [ufiguero@itesm.mx](mailto:ufiguero@itesm.mx) (U. Figueroa-López), [maria\\_ortiz@uaeh.mx](mailto:maria_ortiz@uaeh.mx) (M. Ortiz-Domínguez), [joseguar@itesm.mx](mailto:joseguar@itesm.mx) (J. Oseguera-Peña), [A.Neville@leeds.ac.uk](mailto:A.Neville@leeds.ac.uk) (A. Neville).  
<http://dx.doi.org/10.1016/j.matlet.2016.04.135>  
 0167-577X/© 2016 Elsevier B.V. All rights reserved.





## Original article

## Tribological properties of aluminium-clay composites for brake disc rotor applications

A.A. Agbeleye<sup>a,b,\*</sup>, D.E. Esezobor<sup>a</sup>, S.A. Balogun<sup>a</sup>, J.O. Agunsoye<sup>a</sup>, J. Solis<sup>b</sup>, A. Neville<sup>b</sup><sup>a</sup> Metallurgical and Materials Engineering Department, University of Lagos, Lagos, Nigeria<sup>b</sup> Institute of Functional Surfaces, School of Mechanical Engineering, University of Leeds, Leeds, UK

## ARTICLE INFO

## Article history:

Received 14 August 2017

Accepted 7 September 2017

Available online xxxxx

## Keywords:

Sliding wear

Surface analysis

Sliding friction

Hardness

Three-body abrasion

## ABSTRACT

In this paper, the mechanical and tribological behaviours of various compositions of aluminium 6063 alloy – clay (Al-clay) composites for brake pad applications were studied. The Al-clay composites with 5–30 wt% of clay particles of grain size of 60 BSS (250 microns) were developed through stir casting route. The wear characteristics of Al-clay in dry sliding conditions were subjected to a series of Denison T62 HS pin-on-disc wear tests. The action of two different loads (4 and 10 N), three sliding speeds of 200, 500 and 1000 rpm were investigated. The results of the mechanical and wear tests as well as the metallographic investigation of optical, scanning electron microscopy and energy dispersive X-ray microscopy revealed an improvement in the tensile strength, hardness and wear resistance in the composites with 10–25 wt% clays. The best values were obtained at 15 wt%. Wear rate was highly influenced by applied load and sliding speed. The developed composites with 15–25 wt% clay addition were similar to conventional semi metallic brake pad in terms of wear and friction properties.

© 2017 Production and hosting by Elsevier B.V. on behalf of King Saud University. This is an open access article under the CC BY-NC-ND license (<http://creativecommons.org/licenses/by-nc-nd/4.0/>).

## 1. Introduction

Aluminium based composites are gaining increased applications in the transport, aerospace, marine, oil and gas, automobile and mineral processing industries, due to their excellent strength, stiffness and wear resistance properties. However, their widespread adoption for engineering applications has been hindered by the high cost of producing components (Burkinshaw et al., 2012). Hence much effort has been geared toward the development of composites with reinforcements that are relatively cheap and can compete favourably in terms of strength and wear characteristics with composites reinforced with silicon carbide (SiC), aluminium oxide (Al<sub>2</sub>O<sub>3</sub>) and graphite. Clay could be a potential reinforcing component due to its availability and its major constituents such as alumina (Al<sub>2</sub>O<sub>3</sub>), silica (SiO<sub>2</sub>), oxides of iron (Fe<sub>2</sub>O<sub>3</sub>), titanium (TiO<sub>2</sub>), and sodium (Na<sub>2</sub>O).

Recently, great interest has been in the automobile and aviation industries and many other industries to reduce strength-to-weight ratio of components, improve the wear resistance of components, and or enhance fuel efficiency as evidenced by extensive research into aluminium-based composites (Rao et al., 2009; Rawal, 2001; Das, 2004). One of such area being considered for potential weight reduction is the brake system. Most cars today are built with disc brake which consists of the caliper and a ventilated rotor. The caliper and rotor are typically made from ductile cast iron and grey cast iron respectively. Cast aluminium and aluminium based metal matrix composites (MMC) brake rotors give as much as 45–61% weight reduction in the braking system (Sarip and Day, 2015; Huang and Paxton, 1998; Macke and Rohatgi, 2012; Miracle and Donaldson, 2001; Maleque et al., 2010). However, the major limitation of the use of aluminium alloys is its soft nature, hence the need for its reinforcement with high strength-stiffness materials such as SiC, TiC, TiB<sub>2</sub>, B<sub>4</sub>C, Al<sub>2</sub>O<sub>3</sub>, and Si<sub>3</sub>N<sub>4</sub> (Jimoh et al., 2012). Clay contains reinforcing materials such as Al<sub>2</sub>O<sub>3</sub>, SiO<sub>2</sub> and Fe<sub>2</sub>O<sub>3</sub> with trace presence of other materials (Esezobor et al., 2014) making it a potential candidate as a reinforcing agent for the production of metal matrix composite for wear applications. Wear is one of the most commonly encountered industrial problems that leads to the replacement of components and assemblies in engineering. When two solid surfaces are placed in solid-state contact, it is not easy to envision the absence of some wear even in the most

\* Corresponding author at: Metallurgical and Materials Engineering Department, University of Lagos, Lagos, Nigeria.

E-mail address: [aagbeleye@unilag.edu.ng](mailto:aagbeleye@unilag.edu.ng) (A.A. Agbeleye).

Peer review under responsibility of King Saud University.



Production and hosting by Elsevier

efficiently lubricated systems because of asperity contact (Narayanasamy and Selvakumar, 2016).

During the sliding action, the hard ceramic particles detached from the composite surface constitute a resisting barrier in reducing the wear rate of the composite material. The sliding wear resistance of the composites with respect to that of alloy varies with the process parameters (Al-Qutub, 2009; Alpas and Zhang, 1993; Balakumar, 2013). The three distinct regions of wear reported by Alpas and Zhang, 1993 are dependent of load, which include oxidative wear in which the oxide aluminium surface layer is removed during sliding process. Other regions include the mild wear in which the loss of material is dictated by asperity-to-asperity contact and the wear that is controlled essentially by subsurface deformation and fracturing of the surface (Suh and Saka, 1980). These regions occur at low, medium and high load regimes.

The braking system of a vehicle is usually subjected to a complex state of stress which includes mechanical and thermal stresses (Choudhury et al., 2014). The material used in brake rotors should, therefore be able to bear thermal fatigue and should absorb and quickly dissipate heat generated during braking (Esposito and Thrower, 1999). In a typical braking process, the hydraulic pressure could be in the range of 2 to 4 MPa. The rotors could reach at a very small duration, temperatures as high as 800 °C due to friction,

which could result to a thermal gradient up to 500 °C between the surface and the core of the rotors (Macnaughta, 1998).

Friction materials for brake systems comprise metallic components to improve their wear resistance, thermal stability and strength. Metals such as copper, steel, iron, brass, bronze, and aluminium have been used in the form of fibres or particles in the friction materials. The friction and wear of these materials depend mainly on the type, morphology, and hardness of the metallic ingredients (Jang et al., 2004). A commercial brake lining usually contains more than 10 different constituents categorized into four classes of ingredients: binders, fillers, friction modifiers and reinforcements. The choice of the constituents is often based on individual experience or a trial and error method to make a new formulation (Hee and Filip, 2005).

The incorporation of clay particles in aluminium alloy will harness the potential of its constituents (mainly  $\text{Al}_2\text{O}_3+\text{SiO}_2$ ) forming multi-reinforcements composite with the prospect of it a suitable substitute in wear resistant applications, in place of the monolithic reinforcements such as SiC,  $\text{Al}_2\text{O}_3$ , etc. currently in use.

Therefore, this paper will investigate the influence of various weight fractions of aluminosilicate clay on the mechanical, friction and wear properties of Al-clay composites for brake disc rotor applications. The results will be compared with the results obtained with a semimetallic brake pad (SMBP).

**Table 1**  
Optical Emission Spectrometric analysis of AA6063.

Element	Si	Mg	Fe	Cu	Mn	Zn	Cr	Ti	Al
% composition	0.429	0.425	0.225	0.004	0.026	0.002	0.006	0.033	98.850

**Table 2**  
Atomic Absorption Spectroscopy (AAS) analysis of clay sample.

Parameters	$\text{SiO}_2$	$\text{Al}_2\text{O}_3$	$\text{Fe}_2\text{O}_3$	MnO	MgO	$\text{Na}_2\text{O}$	CaO	$\text{K}_2\text{O}$	BaO	$\text{SO}_3$	LOI
Level detected (%)	45.62	33.74	0.43	0.01	0.06	0.05	0.04	0.63	0.01	0.03	4.545

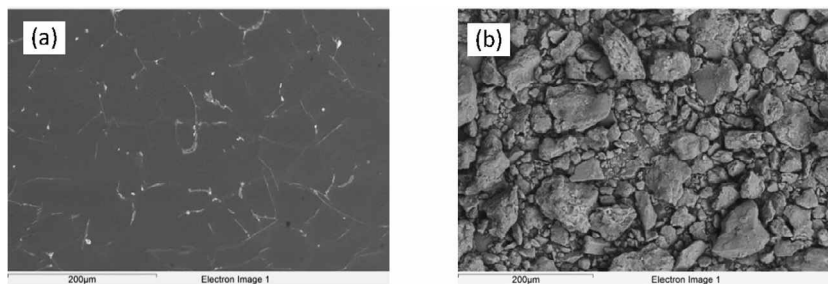


**Fig. 1.** SEM micrographs of: (a) As - cast AA6063 and (b) Clay particles.

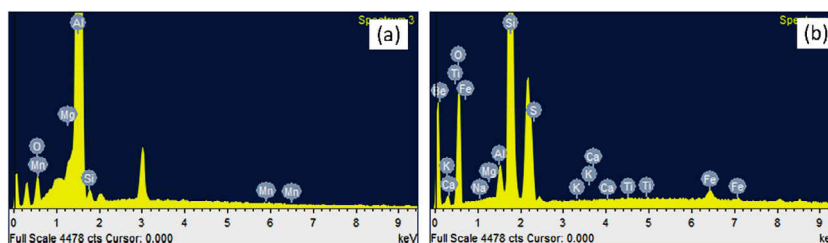


**Fig. 2.** EDX analysis of (a) As - cast AA6063 and (b) Clay particles.



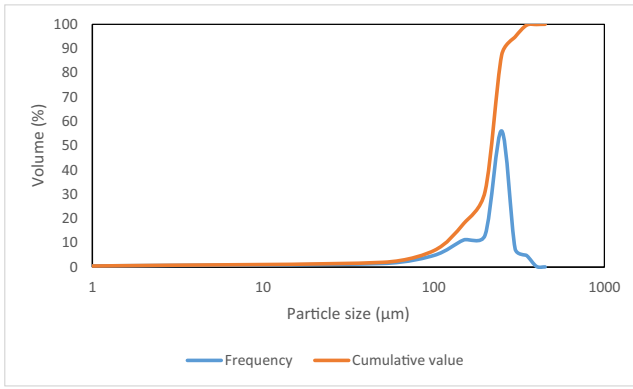


Fig. 3. Particle size distribution of clay sample (Narayanasamy and Selvakumar, 2017).

## 2. Experimental

The Al-clay composites which consist of aluminium alloy (AA6063) and 5–30 wt% of clay particles of grain size of 60 BSS (250 microns) were developed through liquid metallurgy stir casting route. The AA6063 was supplied by Nigerian Aluminum Extrusion Company (NIGALEX), Oshodi, Lagos, and the clay was obtained from Ikorodu town in Lagos State, Nigeria.

The tensile and Vickers hardness tests of samples were conducted using respectively 50 kN Instron 3369L3477 machine and Mitutoyo micro-hardness tester HM-122 in accordance with the ASTM E8/E8M-13 standards. The Metallographic examination was carried out using Zeiss EVO MA-15 Scanning Electron Microscope (SEM)/Energy Dispersive Xray (EDX). The sample surfaces were ground, polished using alumina suspension, and etched in Weck's reagent for 20 s as well as dried in still air. The microstruc-

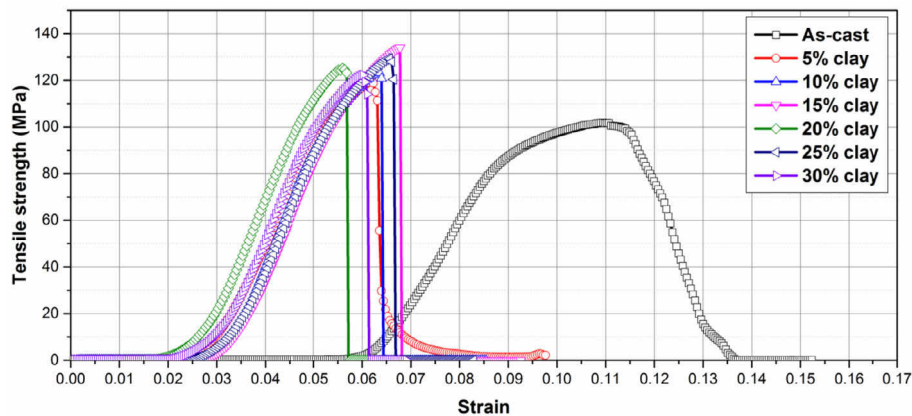


Fig. 4. Tensile strength against strain.

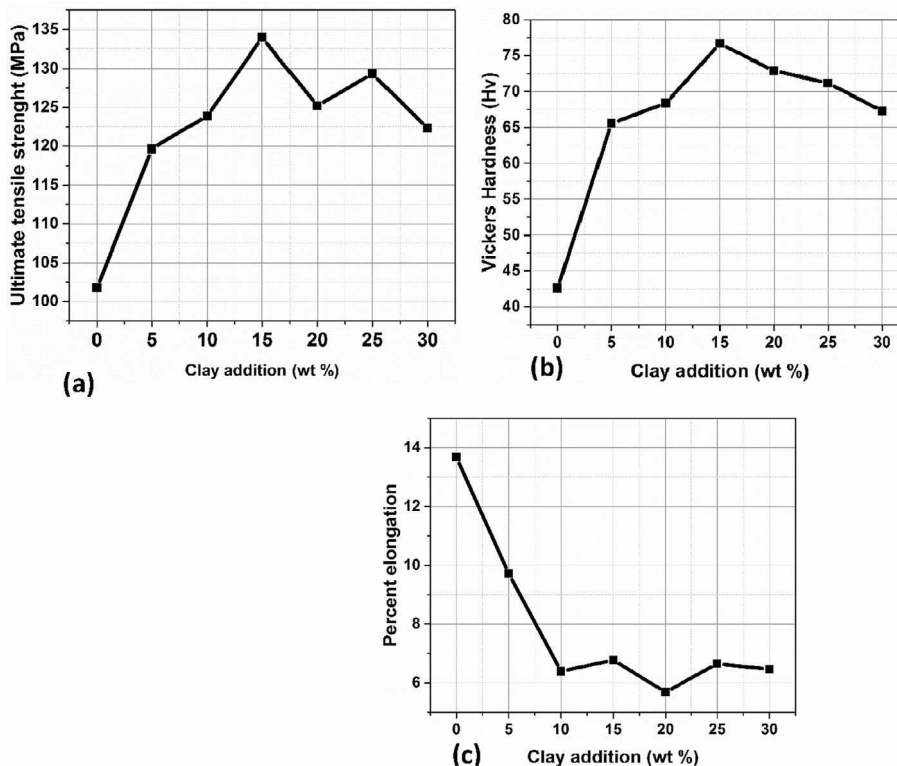


Fig. 5. Mechanical properties of test samples: UTS, (a) Vickers hardness, (b) and Percent elongation, (c).

ture of each samples were also examined with a digital Leica CTR6000 metallurgical microscope at 50  $\mu\text{m}$  magnification.

The wear characteristics of Al-clay and SMBP in dry sliding conditions were subjected to a series of Denison T62 HS pin-on-disc wear tests. Cylindrical pins of 5 mm diameter were made from the Al-Clay composite and SMPD. The action of two different loads (4 and 10 N), on AISI stainless steel disc at three sliding speeds of 1.05, 2.62 and 5.24 m/s were investigated as per ASTM: G99-05 standard. The wear was measured by weighing the pins before and after the test.

The volumetric wear rate was estimated by measuring the mass loss,  $\Delta m$  in the sample after each test. The volumetric wear rate  $W_r$ , which relates to the mass loss to the composite density,  $\rho$  and the sliding time,  $t$  was evaluated using the expression in Eq. (1):

$$W_r = \frac{\Delta m}{\rho t} \quad (1)$$

However, it is more appropriate to express the wear results in terms of wear constant  $K$  as extracted from Archard's law. For known values of wear volume  $V$ , Vickers hardness  $H$  of the softer component, sliding distance  $S$ , and normal load  $L$ , the wear coefficient is given in Eq. (2):

$$K = \frac{VH}{LS} \quad (2)$$

### 3. Results

#### 3.1. Mechanical properties

The results of the analysis of the aluminium alloy and the clay are presented in Tables 1 and 2 respectively. Figs. 1 and 2 show the SEM images and the EDX analysis of the AA6063 and clay samples used in this study respectively.

The results of the SEM/EDX (Figs. 1 and 2) revealed the as cast sample contains proportion of Al, Si and Mg in the range expected in AA6063, while clay sample contains the right proportion of Si, Al, Fe, O, Mg, Na, Ca and K that placed it in the range of aluminosilicate clay group as classified by Chesti, 1986. The size distribution of the clay particles is shown in Fig. 3.

The UTS of the composite samples increases as the addition of clay increases to a peak value of 133.98 MPa at 15 wt% clay particle addition over the conventional AA6063 of 104 MPa. Further increase in clay particle addition to 30 wt% clay resulted in a decline in the UTS to 122.29 MPa (Fig. 4).

The Vickers hardness values of the Al-clay composite are presented in Fig. 5. The increase in the percentage of clay particle addition was accompanied with corresponding increase in the hardness values and it reached a maximum value of 76.7 HV at 15 wt% after which the hardness value declined to 67.3 at 30 wt%. The percent elongation (ductility) values of the Al-Clay compos-

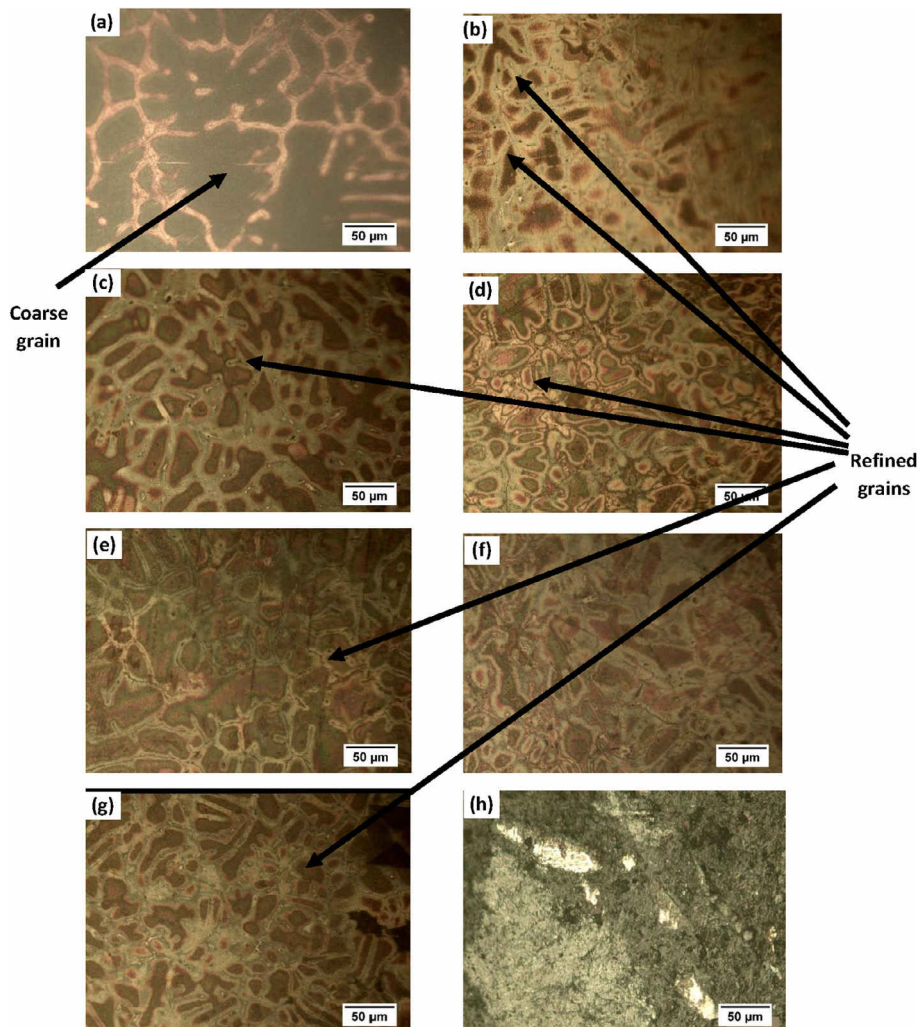


Fig. 6. Optical microstructure of the samples (a) As cast AA6063, (b) 5% clay, (c) 10% clay, (d) 15% clay, (e) 20% clay, (f) 25% clay, (g) 30% clay, (h) SMBP.

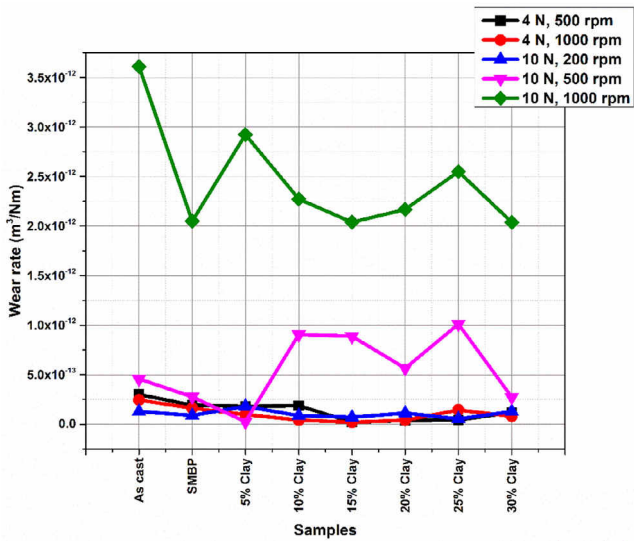


Fig. 7. Dimensional wear coefficient of test samples at varied loads and sliding speeds.

ites as presented in Fig. 5(c) show appreciable response to increase in clay particle addition. Strain values generally decrease with increase in clay particle addition with the minimum value of 5.7% attained at 20 wt.%.

3.2. Microstructure

The results of the metallographic examination of all the samples are displayed in Fig. 6. The clay particles are fairly distributed along the grain boundaries of the AA6063 matrix. The addition of the clay particles is observed to have enhanced the formation of finer grains (Fig. 6(b-h)) as compared to the as-cast AA6063 (control sample) (Fig. 6a).

3.3. Wear characteristics

The result of the wear test of the composites with various weight fractions of clay particles is displayed in Fig. 7.

The wear rate decreases with increase in the weight fraction of the reinforcing agent (clay) as compared to conventional AA6063. The lower wear rate observed at optimum condition between 15–20 wt% clay is due to enhanced hardness by the dispersion of the hard intermetallics over the AA6063 matrix, which acted as load supporting elements (Essam et al., 2010; Devaraju et al., 2013a,b; Kumar and Balasubramanian, 2008).

The wear behaviour of the developed composites is similar to the SMBP at lower sliding speed of 200 rpm for all samples. In some cases, the composites have enhanced wear properties. This behaviour can be attributed to the release of the clay particles on the surface during wear process, which to an extent may prevent metal to metal contact and also serve as solid lubricants (Tjong et al., 1999). On the other hand, the wear rate increases with

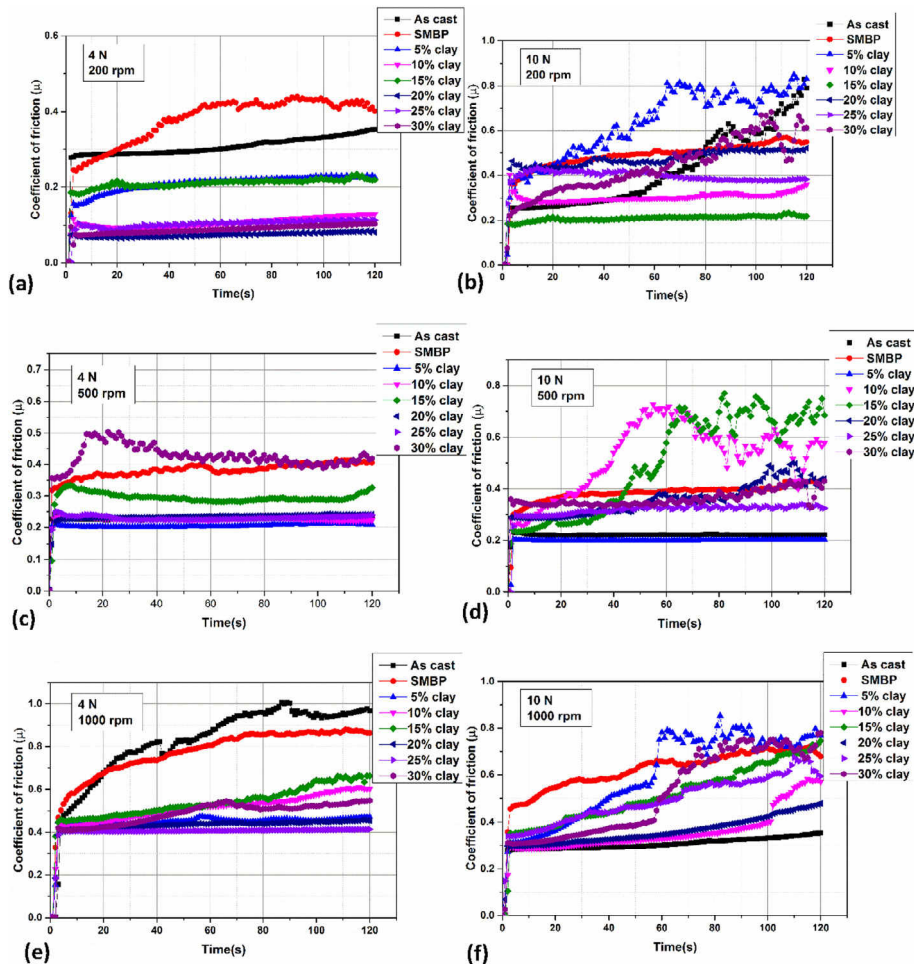


Fig. 8. Coefficient of friction (a) 4 N at 200 rpm, (b) 10 N at 200 rpm, (c) 4 N at 500 rpm, (d) 10 N at 500 rpm, (e) 4 N at 1000 rpm, (f) 10 N at 1000 rpm under ambient and dry conditions.

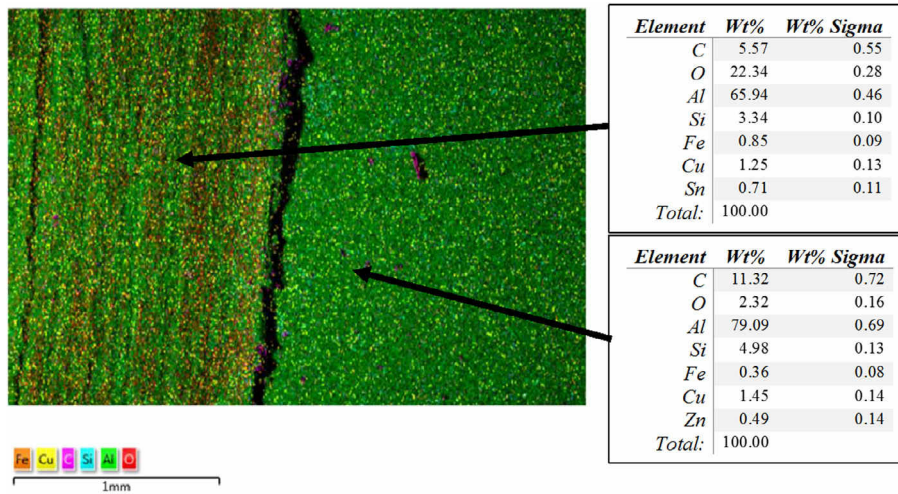


Fig. 9. EDS layered image of wear track.

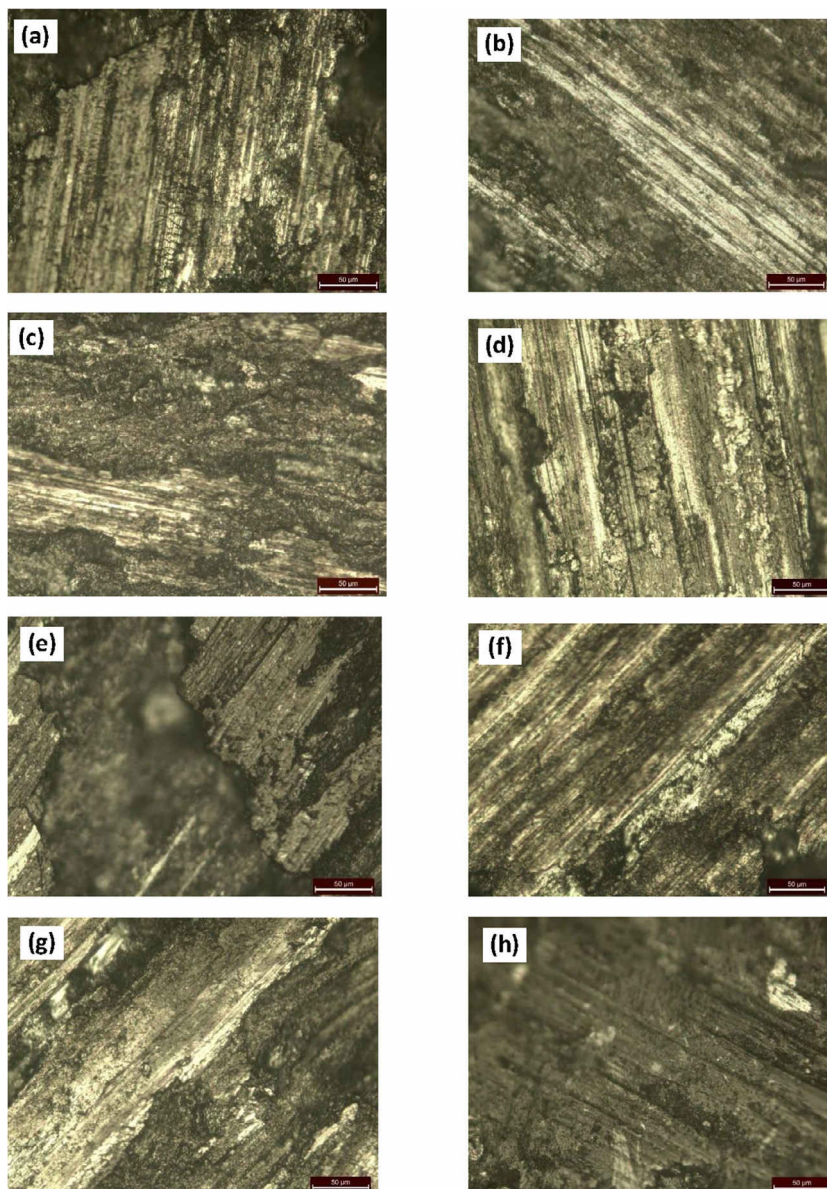


Fig. 10. Optical microstructure of worn surfaces of samples (a) As cast AA6063, (b) 5% clay, (c) 10% clay, (d) 15% clay, (e) 20% clay, (f) 25% clay, (g) 30% clay, (h) SMPB.

increase in the normal load and sliding speed. This trend was also observed in the work of Devaraju et al., 2013b. However 10–25% weight fraction at 10 N and 500 rpm show increase in the wear rate of the composite. This shows the dependence of load and the weight fraction of clay particle on the wear behaviour of the composite over conventional AA6063.

#### 3.4. Friction characteristics

The variation of coefficient of friction (CoF) of the test samples with the sliding time with respect to the various sliding load and the rotating speeds in dry conditions is presented in Fig. 8. It was observed that the CoF increased sharply in the first few seconds and then attained a nearly steady value with the sliding time. The initial high value of the CoF can be attributed to the roughness at the surface of the specimen (Sharma et al., 2012). However, the CoF value increases with increase in load at low rotating speed.

However, at higher speed the average CoF is found to be independent of load during the first few seconds of the experiment. After a while, the amplitude of CoF increases at high load, producing fluctuating values of CoF. This could be due to the presence of higher volume of wear debris trapped at the contact zone creating a third body effect within the contact surface, resulting in decrease in metal removal during the wear test (Devaraju et al., 2013b).

#### 3.5. Worn surface morphology

The morphology of the worn test samples showed in Fig. 10 indicate that there exist three microstructurally distinct areas with the wear tracks. These areas include: bright coloured area with scratches (part of the based metal), light grey areas, and dark grey areas.

The bright coloured area on the micrographs is the uncovered metal surface. This appears smooth, indicative of mild oxidational type of wear with no or minimal cracks. The grey area on the other hand, appear to be consisting of smaller compacted particles and with considerable cracks appearing on the surface. The oxidation of ruptured particle during sliding is called fragmented oxide particle. When this small particles were oxidized and emitted during sliding, they reduced the sliding contact surfaces. The fragmented oxide particle acts as a lubricating agent, and it may reduce wear. Consequently, no plastic deformation will occur on the worn surface of the Al-Clay composite (Narayanasamy and Selvakumar, 2017).

## 4. Discussion

The improvement of the UTS and microhardness with the increment in the weight fraction of clay particles may be due to the presence and pinning effect of the clay particles (Khraisat and Abu Jadayil, 2010; Essam et al., 2010; Devaraju et al., 2013a,b), which serve as impingement for the movement of dislocations and as a result restrict the sliding of the grain boundaries. The results of the mechanical property tests also indicate that ductility of the AA6063 was influenced by the amount of clay particles addition. This is evident with a decrease in percent elongation, which dropped to its minimum at 20 wt% clay particle addition.

The improved mechanical properties of the composite (Fig. 5) can be attributed to the combined effect of grain refinement propelled by increase in clay content and the formation, precipitation, and distribution of hard intermetallic compounds (Khraisat and Abu Jadayil, 2010). Previous studies (Marioara et al., 2003; Kuijpers et al., 2003; Miao and Laughlin, 1999) have shown that the mechanical properties are highly influenced by the precipitates

of hardening  $\beta$ (Mg<sub>2</sub>Si) phase. The strength is also influenced by the intermetallic phases formed during solidification of the alloys.

The Compositional variations of wear track as presented in Fig. 9 shows higher oxygen content of tribo-layer. This might be due to presence of oxides of elements (such as Al, Si, Cu, Sn, and Fe) present in the test materials.

Wear debris is attributed to delamination and fatigue wear of tribo-layers. Other sources of debris formation were identified as pin material fractured particles mostly at edges, and formation of third body abrasive particles during the test by tribo-oxidation and mechanical mixing of test products.

## 5. Conclusions

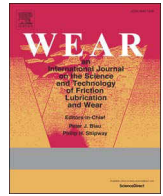
It can be concluded that:

- (i). The addition of clay particles generally improved the mechanical properties, wear resistance and CoF of the AA6063.
- (ii). The wear behaviour of the developed composite is dependent on the applied load, sliding speed and the weight fraction of clay particle additive.
- (iii). The wear and friction properties of the developed composite with 15–30 wt% clay particles addition are similar to that of SMBP and therefore can be substituted.
- (iv). The low wear rate exhibited at the surface of the developed composite occurred as a result of the presence of fractured particles between the composite pin and steel disc surfaces. The particles served as load bearing elements as well as solid lubricant.

## References

- Alpas, A.T., Zhang, J., 1993. Wear regimes and transitions in Al<sub>2</sub>O<sub>3</sub> particulate-reinforced Al alloys. *Mater. Sci. Eng. A* 161, 273.
- Al-Qutub, A.M., 2009. Effect of heat treatment on friction and wear behaviour of Al-6061 composite reinforced 10% submicron Al<sub>2</sub>O<sub>3</sub> particles. *Arab. J. Sci. Eng.* 24, 205–215.
- Balakumar, G., 2013. Tensile and wear characterisation of aluminium alloy reinforced with nano-ZrO<sub>2</sub> metal matrix composites (NMMCs). *Int. J. Nano Sci. Nanotechnol.* 4 (1), 121–129.
- Burkinshaw, M., Neville, A., Morina, A., Sutton, M., 2012. Calcium sulphate and its interactions with ZDDP on both aluminium-silicon and model silicon surfaces. *Tribol. Int.* 46, 41–51.
- Chesti, A.R., 1986. *Refractories, Production and Properties*. The Iron and Steel Institute, London, p. 3–13, 295–314.
- Choudhury, P., Singh, R.K., Panda, P., 2014. Thermal and structural analysis of a ceramic coated Fsa brake rotor using 3D finite element method for wear resistance and design optimisation. *IOSR J. Mech. Civ. Eng.* 11 (2), 143–149.
- Das, S., 2004. Development of aluminium alloy composites for engineering applications. *Trans. Indian Inst. Met.* 57, 325–334.
- Devaraju, A., Kumar, A., Kumsrswamy, A., Kotiveerachari, B., 2013a. Influence of reinforcements (SiC and Al<sub>2</sub>O<sub>3</sub>) and rotational speed on wear and mechanical properties of aluminium alloy 6061–T6 based surface hybrid composites produced via friction stir process. *Mater. Des.* 51, 331–341.
- Devaraju, A., Kumar, A., Kumsrswamy, A., Kotiveerachari, B., 2013b. Wear and mechanical properties of 6061–T6 aluminium alloy surface hybrid composites [(SiC+Gr) and (SiC+ Al<sub>2</sub>O<sub>3</sub>)] fabricated by friction stir processing. *J. Mater. Res. Technol.* 2 (4), 362–369.
- Esezobor, D.E., Obidiegwu, E.O., Lawal, G.I., 2014. The influence of agro-forestry waste additive on the thermal insulating properties of Osiele clay. *J. Emerg. Trends Eng. Appl. Sci.* 5 (5), 305–311.
- Esposito, A., Thrower, J., 1999. *Machine Design*. Delmar Publishers Inc.
- Essam, R.I., Makoto, T., Toshiya, S., Kenji, I., 2010. Wear characteristics of surface hybrid MMCs layer fabricated on aluminium plate by friction stir processing. *Wear* 268, 1111–1121.
- Hee, K.W., Filip, P., 2005. Performance of ceramic enhanced phenolic matrix brake lining materials for automotive brake linings. *Wear* 259, 1088–1096.
- Huang, S.X., Paxton, K., 1998. A macro-composite Al brake rotor for reduced weight and improved performance. *JOM* 50 (8), 26–28.
- Jang, H., Koa, K., Kim, S.J., Basch, R.H., Fash, J.W., 2004. The effect of metal fibers on the friction performance of automotive brake friction materials. *Wear* 256, 406–414.
- Jimoh, A., Sigalas, I., Hermann, M., 2012. In Situ synthesis of titanium matrix composite (Ti-TiB-TiC) through sintering of TiH<sub>2</sub>-B<sub>4</sub>C. *Mater. Sci. Appl.* 3, 30–35.

- Khraisat, W., Abu Jadayil, W., 2010. Strengthening aluminium scrap by alloying with iron. *Jordan J. Mech. Ind. Eng.* 4 (3), 372–377.
- Kuijpers, N.C.W., Kool, W.H., Koenis, P.T.G., Nilsen, K.E., Todd, I., Van der Zwaag, S., 2003. Assessment of different techniques for quantification of  $\alpha$ -Al(FeMn)Si and  $\beta$ -AlFeSi intermetallics in AA 6xxx alloys. *Mater. Charact.* 49, 409–420.
- Kumar, S., Balasubramanian, V., 2008. Developing mathematical model to calculate wear rate of AA7075/SiC<sub>p</sub> powder metallurgy composite. *Wear* 264, 1026–1034.
- Macke, A., Rohatgi, P., 2012. Metal Matrix Composites offer the automotive industry opportunity to reduce vehicle weight, improve performance. *Adv. Mater. Proc.* 170 (3), 19–23.
- Macnaughta, M., 1998. Cast iron brake discs—a brief history of their development and metallurgy. Technical Report, Foundryman. p. 321.
- Maleque, M.A., Dyuti, S., Rahman, M.M., 2010. Materials selection method in design of automotive brake disc. In: *Proceedings of the World Congress on Engineering*, June 30–July 2; London, UK (vol. 3, ISBN 978-988-18210-8-9).
- Marioara, C.D., Andersen, S.J., Jansen, J., Zandbergen, H.W., 2003. The influence of temperature and storage time at RT on nucleation of the  $\beta''$  phase in a 6082 Al-Mg-Si alloy. *Acta Mater.* 51, 789–796.
- Miao, W.F., Laughlin, D.E., 1999. Precipitation hardening in aluminium alloy 6022. *Scr. Mater.* 40 (7), 873–878.
- Miracle, D.B., Donaldson, S.L., 2001. *ASM Handbook*, Vol. 21: Composites. ASM International, Materials Park, OH.
- Narayanasamy, P., Selvakumar, N., 2016. Tensile, compressive and wear behaviour of self-lubricating sintered magnesium based composites. *Trans. Nonferrous Met. Soc. China.* 27, 312–323.
- Narayanasamy, P., Selvakumar, N., 2017. Effect of hybridizing and optimization of tic on the tribological behaviour of mg-mos<sub>2</sub> composites. *J. Tribol.* 139 (5), 051301–051311.
- Rao, R.N., Das, S., Mondal, D.P., Dixit, G., 2009. Dry sliding wear behaviour of cast high strength aluminium alloy (Al-Zn-Mg) and hard particle composites. *Wear* 267, 1688–1695.
- Rawal, R.S., 2001. Metal matrix composites for space applications. *JOM* 53, 14–17.
- Sarip, S., Day, A.J., 2015. An experimental study on prototype lightweight brake disc for regenerative braking. *Jurnal Teknologi (Sci. Eng.)* 74 (1), 11–17.
- Sharma, N., Kumar, N., Dash, S., Das, C.R., Subba Rao, R.V., Tyagi, A.K., Raj, B., 2012. Scratch resistance and tribological properties of DLC coatings under dry and lubricated conditions. *Tribol. Int.* 56, 129–140.
- Suh, N.P., Saka, N., 1980. In: Suh, N.P., Saka, N. (Eds.), *Fundamentals of Tribology*. The MIT Press, Cambridge, p. 443.
- Tjong, S.C., Lau, K.C., Wu, S.Q., 1999. Wear of Al-based hybrid composites containing BN and SiC particulates. *Metall. Mater. Trans.* 30A, 2551–2555.



# Tribocorrosion evaluation of hydrogenated and silicon DLC coatings on carbon steel for use in valves, pistons and pumps in oil and gas industry

A.H.S. Bueno<sup>a,\*</sup>, J. Solis<sup>b</sup>, H. Zhao<sup>c</sup>, C. Wang<sup>c</sup>, T.A. Simões<sup>a,d</sup>, M. Bryant<sup>c</sup>, A. Neville<sup>c</sup>

<sup>a</sup> Mechanical Engineering Department, Universidade Federal de São João Del Rei, 170 Praça Frei Orlando, 36307-352 São João Del Rei, Brazil

<sup>b</sup> SEP/SES/TECNM, IT de Tlalnepantla, 54070, Estado de México, México

<sup>c</sup> Institute of Functional Surfaces, University of Leeds, LS2 9JT, Leeds, England, UK

<sup>d</sup> Institute for Materials Research, University of Leeds, LS2 9JT, Leeds, England, UK

## ARTICLE INFO

### Keywords:

Carbon-based coatings  
PVD coatings  
Steel  
Sliding wear  
Corrosion-wear  
Electrochemistry

## ABSTRACT

Several components in the oil and gas industry are subjected to wear and corrosion. This work evaluated the feasibility of using Diamond-Like Carbon (DLC) coatings in Subsea Safety Control Valves (SSCV), piston and pumps. These are made from API X65 carbon steel and are subjected to wear and corrosive/saline environments. Coatings were deposited using Plasma Enhanced Chemical Vapour Deposition (PECVD). The electrochemical behaviour of Silicon-doped and Hydrogenated DLC films was evaluated before and after wear tests. Film characterisation included nano-indentation, surface roughness, micro-abrasion testing, Raman spectroscopy, atomic force microscopy and scanning electron microscopy. Electrochemical tests and electrochemical impedance was also measured. Sliding wear tests against silicon nitride were conducted with a maximum initial Hertz stress of 150 and 400 MPa under dry and wet conditions. The H-DLC had better wear performance than Si-DLC. The advantages of H-DLC were related to higher hardness increasing the wear resistance; small galvanic coupling between DLC and steel, inhibiting the localised corrosion into the DLC defects; lowest anodic current, suggesting high resistivity to use as a corrosion barrier for steel and the corrosion process on the substrate that did not affect DLC properties (adhesion and wear/ corrosion resistance).

## 1. Introduction

The recent interest and great challenges for oil and gas companies are to improve the efficiency and viability of crude oil recovery. However, there are some barriers related to the viability for commercial extraction, such as the water/ oil that contains high salinity and sand particles. Therefore, DLC films can be a good candidate for protection of carbon steel used in critical equipment of oil transportation that need to preserve its structural integrity. For example, Subsea Safety Control Valves (SSCV), pistons and pumps. DLC coatings could improve the oil carriage by reducing friction, wear and corrosion inside the pipelines and their components.

Currently, the main methods used to avoid internal scale corrosion are inhibitors due to the fact that they promote adsorption of films on the surface, and as a result, enhance the corrosion resistance by forming a compact protective layer [1–3]. However, there are a number of conditions that can affect the efficiency of these inhibitors, such as fluid (composition, temperature, flow velocities, pressure of CO<sub>2</sub> gas, wettability of the fluid, fluid density and types of crude oil), solid particles

(sand contents, size, attack angle of the particles, density and velocity) and steel (hardness, microstructure, strength, ductility and toughness) [1,2]. Seamless steels coated with resin are used to improve the wear and corrosion resistance in pipelines and drills [4]. However, polymeric coatings lack hardness and can be degraded. Because of this, DLC coatings could be applied on internal parts of pipelines providing good corrosion resistance for oil and gas applications [5,6].

DLC coatings are designed to have a combined resistance to wear and corrosion in automotive and biomedical areas [7–13]. However, DLC has not been widely studied and used in some parts of the crude oil exploration, such as SSCV, pistons and pumps. For the above reason, the study to evaluate the feasibility of using this coating for surface modification of carbon steel is very interesting for the oil and gas corporations.

The properties of DLC could improve the efficiency for the transport of oil by reducing the friction, wear and corrosion inside the equipment [3], such as: amorphous and inertness structure, hydrophobic, low coefficient of friction (CoF), high corrosion resistance, high hardness, high Young's modulus and good wear/abrasion resistance

\* Correspondence to: Head of Mechanical Engineering Department - DEMEC, MCL – Materials and Corrosion Laboratory, Federal University of São João del-Rei – UFSJ, Praça Frei Orlando, 170 – Centro, 36.307–060 São João del-Rei, MG, Brazil.

E-mail address: [alyssonbueno@ufsj.edu.br](mailto:alyssonbueno@ufsj.edu.br) (A.H.S. Bueno).

<http://dx.doi.org/10.1016/j.wear.2017.09.026>

Received 21 June 2017; Received in revised form 28 September 2017; Accepted 30 September 2017

Available online 03 October 2017

0043-1648/ Crown Copyright © 2017 Published by Elsevier B.V. All rights reserved.

[7–10,14–16]. Then, PECVD could be a good option to create an internal scale corrosion barrier for a carbon steel to avoiding the precipitation of salt scales. However, the main results in the literature are associated with defects and microstructure. Only few papers have been postulated to corrosion resistance for DLC coatings [1,2,5,14,17].

Manhabosco *et al.* [10] reports that the main problem for DLC coatings is associated with failure and delamination of the film. Defects are related to poor adhesion of the film, plastic deformation of the bulk material and cracking on the surface coating, which could be linked to chemical and mechanical properties between the film and substrate [18]. Therefore, adhesion layers and surface treatments are being studied to improve the mechanical properties, like load bearing capacity, hardness and tension distribution between the film and bulk material. According to Hadinata *et al.* [17], there is an extremely high mechanical resistance in DLC coatings mainly associated with wear/corrosion resistance, despite some electrochemical parameters involved in the process were not completely explained.

There are several studies related to tribocorrosion of stainless steel coated with a-C:H films. However, literature reporting the combined effect of the tribological conditions in a corrosive medium for a-C:H and a-C:H:Si using carbon steel as a substrate is scarce [1,2,5,7–9,14,17]. The behaviour of these materials subjected to tribocorrosion can be very complex owing to many parameters involved in the process, but sliding testing simultaneously with the use of electrochemical techniques could contribute to better understand the deterioration effect that takes place.

In this work, the tribological and electrochemical performance of two different functional layers on carbon steel was studied, namely amorphous hydrogenated DLC and silicon doped DLC.

## 2. Experimental details

### 2.1. Materials

The H-DLC and Si-DLC coatings were deposited on API  $\times$  65 carbon steel discs of dimensions 25 mm in diameter and 6 mm in thickness. The substrates were mechanically polished using 1  $\mu$ m diamond paste with a maximum roughness of  $R_a = 0.08 \mu$ m. After polishing, the specimens were ultrasonically cleaned in acetone (10 min) followed by rinsing in deionised water and dried in air jet. The substrates were first cleaned inside the chamber with sputter-etch in argon prior to any deposition. The coatings were produced using the PECVD technology, and the  $C_2H_2$  gas was selected for the reaction gases at a pressure of 0.3 Pa. The substrate was maintained at the temperature of less than 200  $^{\circ}C$ , the pulsed bias was a voltage of 780 V with a frequency of 40 kHz for the plasma. The deposition rate was about 0.8  $\mu$ m  $min^{-1}$  for hydrogenated DLC and 0.6  $\mu$ m  $min^{-1}$  for Si-DLC. The deposition time is about 126 min for the interlayer and 138 min for the DLC films. The deposition procedure included an adherent Cr interlayer (by DC magnetron sputtering) followed by the DLC coating, namely, Cr/WC/a-C: H, with 20–40 at% of H content and Si-DLC.

### 2.2. Characterisation of the DLC coatings

The roughness of surfaces was evaluated using two-dimensional contacting profilometry (Talysurf5, Taylor-Hobson, UK). Surface roughness data of 8 mm trace was analysed to the least square line, with Gaussian filter, 0.25 mm upper cut-off and bandwidth  $100 \pm 1$ .

The hardness and elastic modulus values were measured by depth-sensing Nano indentation (MicroMaterials, Wrexham UK). The diamond indenter was a Berkovich tip. The load was incremental with depth from 1 to 100 mN and a matrix of 50 indents was used. The maximum penetration was of 10% of the film thickness to avoid the influence of substrate.

Atomic Force Microscopy (AFM, Bruker, ICON dimension with scan assist) was used to analyse the surface topography before and after

tribology tests (outside and inside the wear scar). The surfaces were cleaned with acetone before analyses. The scan images were obtained using a silicon tip (cantilever stiffness  $\sim 0.4$  N/m and tip radius of  $\sim 10$  nm) in contact mode and a scan area of  $10 \mu$ m  $\times$   $10 \mu$ m.

A Renishaw Raman spectrometer was used to characterise the bonding structure of the DLC films. The extended and static modes were used to detect chemical compound formation and the carbon peaks (disorder D and amorphous graphitic G peaks), both for the coating structure before and after wear tests. All measurements were carried out in air at room temperature ( $20 \pm 2$   $^{\circ}C$ ), 35–50% RH, with a wavelength of 488 nm and 2 mW power. Data was fitted with a Gaussian Line shape to show the G and D peaks positions and the ratio of peak intensities. The  $I_D/I_G$  ratio was considered as an indicator of the carbon  $sp^2/sp^3$  structure. Curve fitting was done considering full-width at half-maximum (FWHM) as constraint.

Scanning Electron Microscopy (Zeiss EVO MA15 Variable Pressure and field emission SEM) was used to evaluate the surface morphology and cross section microstructure to examine the multilayers (adhesion and DLC layers), before and after wear tests. Assessment of the surface chemical composition and cross section of the coating was carried out with the energy dispersive spectroscopy (EDS). Hydrogen element ( $Z = 1$ ) do not have characteristic X-rays and therefore it is not shown both in the corresponding EDX analysis and the composition profiles.

White light interferometry (NPFLEX Bruker) was employed after tribology test to determine the volume and area of the worn track. Optical microscopy (LEICA DM 6000 M) was utilised to analyse the diameter of wear scars on the balls after tribology tests.

### 2.3. Mechanical tests

The scratch test is an effective method to obtain critical load and to identify the beginning of failure along the film. The tests were carried out using progressive loads from 0.1 to 80 N with a load rate of 100 N/min and for a transverse scratch length of 8 mm in dry condition. The scratch tester was equipped with an acoustic emission monitoring sensor.

The tribological tests of H-DLC and Si-DLC were carried out with a ball-on-plate tribometer. The horizontal frictional force is measured by the load cell which is a piezo-electric transducer that converts the analogue signal into a digital one to be then processed by Labview software. Steel balls are often used as a counter body to study only tribology aspects [19]. However, tribocorrosion is the aim of this study, which uses more complex parameters to analyse. In this study, we simulate extreme wear conditions by using  $Si_3N_4$  balls as high hardness counter body. These also own to have a good chemical stability and avoid galvanic coupling between both surfaces during tribocorrosion experiments. Ceramic balls used were composed by Si (62.0 wt%) and N (37.5 wt%) with a 12 mm diameter, 0.02  $\mu$ m surface roughness and hardness of  $HV_{50g} 1600$ . These were used in a reciprocating movement against stationary DLC coated steel. The maximum Hertzian contact pressures ( $P_{max}$ ) were of 150 MPa and 400 MPa for 6 h, at a frequency of 1 Hz, sliding velocity of 0.02  $ms^{-1}$  and 10 mm sliding stroke. These contact pressures were defined to simulate real conditions where equipment for oil and gas can be subjected. The tests were carried out at room temperature of 18–23  $^{\circ}C$  in dry condition with relative humidity approximately of 25% RH and in wet condition with a solution of 3.5% NaCl at pH 6.5.

### 2.4. Electrochemical tests

A computer-controlled potentiostat (Solartron potentiostat/galvanostat) was used for the electrochemical tests. In this study two methods were used: Potentiodynamic and EIS. Potentiodynamic polarization curves, naturally aerated with scan rate of 30 mV/min and in a range from  $-1.8$  V up to  $+0.5$  V, performed separately. Electrochemical impedance spectroscopy (EIS):



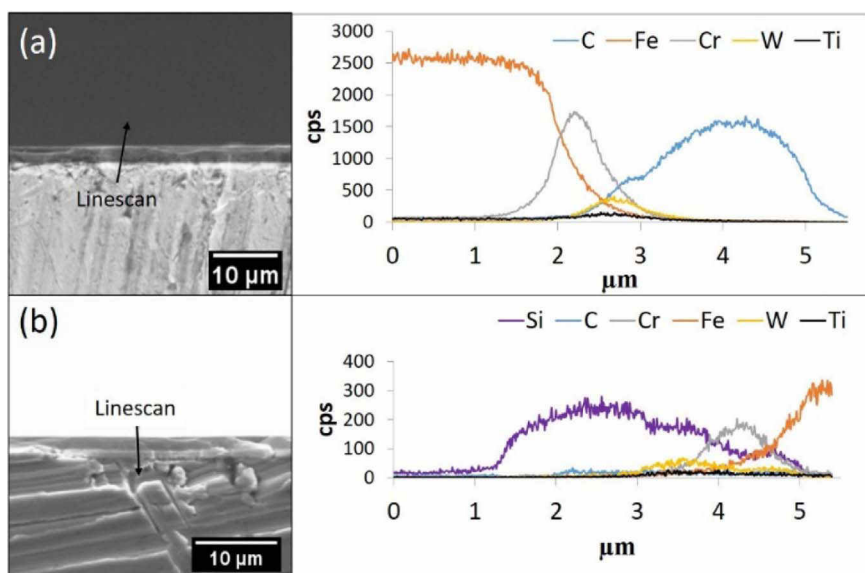


Fig. 1. Backscattering SEM images of cross section and linear EDS scan of: (a) H-DLC and (b) Si-DLC films.

Amplitude of 5 mV (Ag/AgCl/KCl) with the frequency of 30 kHz–10 MHz. For the polarization and impedance tests were carried out before and after the tribology tests with the solution of 3.5% NaCl, pH: 6.5 and at room temperature of 18–23 °C. Prior the tests, the samples were immersed in the solution for 30 min to stabilize the open circuit potential (OCP). The conventional three electrodes cell was used with an Ag/AgCl/KCl (Thermo Scientific) as reference and counter electrode, and DLC films as a working electrode.

### 3. Results and discussion

#### 3.1. Characterisation of DLC films

Fig. 1 shows SEM backscattering images of adhesion layers of Cr/WC for H-DLC and Cr/WSi for Si-DLC; and EDS line scan spectra of cross sections. H-DLC (Fig. 1a) exhibited a surface layers composed of iron (carbon steel), adhesion layers of Cr (1.7 µm), W (1 µm) and a final layer of H-DLC (2.7 µm). Si-DLC (Fig. 1b) presented adhesion layers of Cr (1 µm), W (1 µm) and a final layer of Si-DLC (3 µm). The interface between both films and bulk material showed to be homogeneous all over the surface analysed and without the presence of defects. An interlayer of W was detected in both subtract. Literature [20,21] shows that the interlayer WC and H forms a non-stoichiometric hydrogenated tungsten carbide WC:H, also known as W-C:H or as W-DLC.

Literature [5,8,14,17,22] shows that the Raman spectrum of the coating has two types of C-C bonding structure, where diamond-like ( $sp^3$  – D band) is found between 1200 and 1450  $cm^{-1}$  and graphite-like structure ( $sp^2$  – G band) between 1500 and 1700  $cm^{-1}$ . Raman spectrum of DLC films before and after wear tests are presented in Fig. 2, exhibiting D (Diamond-like) and G (Graphite-like) bands. Both DLC coatings showed peak of G higher than D, indicating graphite-like structure as predominant in both films. The spectrum of H-DLC (Fig. 2a) shows D and G bands with peaks (Raman shifts) of 1365  $cm^{-1}$  and 1549  $cm^{-1}$ , respectively. Hence, the ratio of D and G peaks ( $I_D/I_G$ ) was 0.42. Si-DLC (Fig. 2c) spectra shows D and G bands with peaks of 1321  $cm^{-1}$  and 1501  $cm^{-1}$ , respectively and with ratio of D and G peaks as  $I_D/I_G = 0.24$ .

AFM images of surface topography, before wear tests, are presented in Fig. 3a–b. H-DLC film (Fig. 3a) shows a roughness surface containing large and small grains, compact and homogeneous. A maximum roughness ( $R_y$ ) of 3.10 µm was obtained calculated from an area of 10 × 10 µm. The maximum roughness of H-DLC was 0.13 µm slightly smoother surface than Si-DLC (Fig. 3a), with  $R_y = 0.27$  µm, which also

held large and small grains with compact and homogeneous characteristics.

After wearing of the H-DLC surfaces, an increase of roughness was generally observed. This indicates that when the contact pressure increased, the plastic deformation of the surface asperities also increased. The samples under dry environment at 400 MPa (Fig. 3e) were the worst condition due to film delamination. Therefore, bits of H-DLC coating were emerged off the surface of API × 65 carbon steel, as SEM images shows (see Fig. 4c). The best lubricated conditions were shown to H-DLC coating under wet condition submitted to 150 MPa contact pressure. The results presented the lowest roughness change and surface degradation, as SEM EDS linescan detected very low variation of carbon across the wear track (see Fig. 4b).

The Si-DLC (Fig. 4e) had the largest wear track and wear rate when compared to H-DLC which presented total delamination. It probably occurred because Si-DLC presented lower hardness than H-DLC, promoting less resistance to wear. Nano indentation results demonstrated hardness values of 20.4 and 14.1 GPa for H-DLC and Si-DLC, respectively. In addition, according to Jellesen et al. [23], the amount of  $sp^3$  bonding and hydrogen are important to improve the hardness and wear properties. Thus, H-DLC presented more hardness and more wear resistance than Si-DLC.

The DLC film presents a meta-stable structure that is formed by an amorphous carbon with some crystalline phases and fractions of  $sp^3$  and  $sp^2$  bonds. The characteristics of the  $sp^3$  bonds are associated with mechanical (hardness, rigidity, fracture toughness, wear and friction), chemical and electrochemical properties (corrosion resistance). In addition, the  $sp^2$  controls the electronic properties [15].

Liu and Kwek [14] have shown that the formation of  $sp^3$  bonds occurs when the bulk surface received the carbon ions in higher kinetic energy, which can be produced by increasing the pulse bias during the deposition process of the DLC film. Therefore, the kinetic energy of the carbon ion tends to increase when there is a high voltage applied on DLC film deposition process, causing the formation of diamond-like ( $sp^3$  – D band) by the bombardment of carbon ions on the bulk surface. However, when there is a high value of bulk bias, a high energy of carbon ions, applied by a pulse bias above 500 V, promotes the graphitization by the formation of a DLC film with graphitic clusters spread, causing a roughness on the surface of the DLC coating. This explains the results obtained in this work, i.e. since the DLC films were deposited at 780 V, it presented high concentration of graphite-like structures ( $sp^2$  – G band, Fig. 2a and c) and high roughness (observations through AFM, Fig. 3a and b).

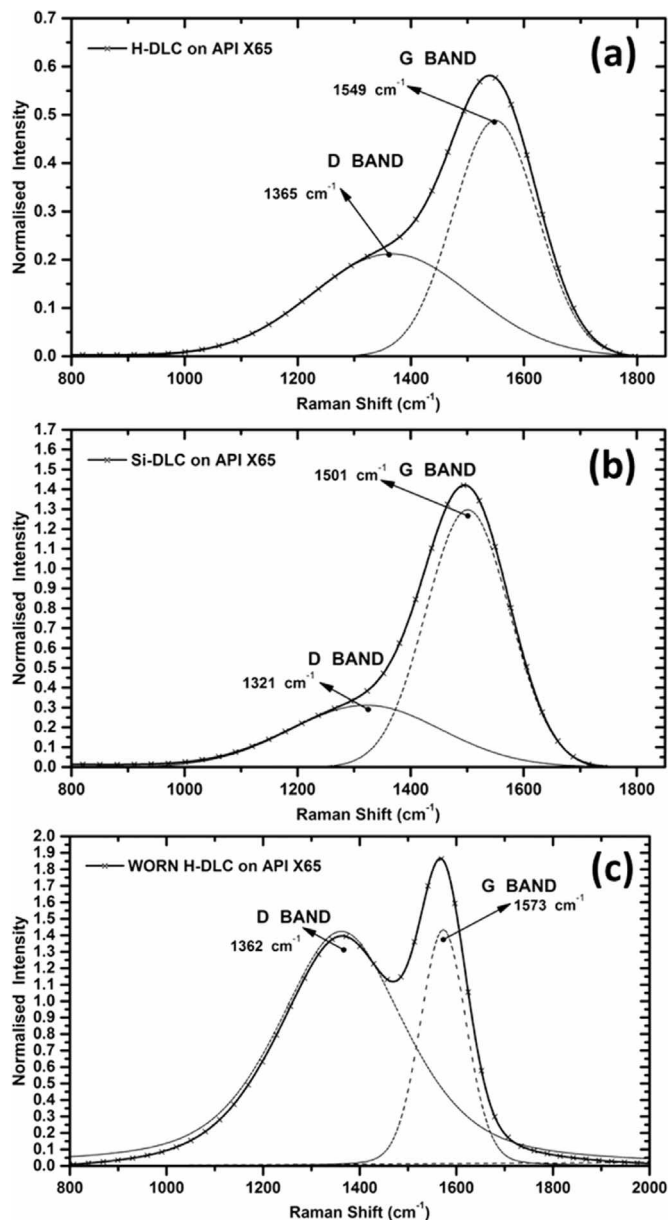


Fig. 2. Raman spectra (a) H-DLC before wear test, (b) H-DLC after wear test and (c) Si-DLC before wear test.

### 3.2. Mechanical properties

H-DLC presented Young's modulus, hardness and roughness of  $181.2 \pm 7$  GPa,  $20.4 \pm 3$  GPa and  $0.02 \pm 0.005$   $\mu\text{m}$ . Si-DLC had  $132.6 \pm 9$  GPa,  $14.1 \pm 4$  GPa and  $0.002 \pm 0.0005$   $\mu\text{m}$ , respectively. The scratch tests on Si-DLC (Fig. 5b) revealed good adhesion to carbon steel substrate with a critical load of 23 N of the incremental load (2.3 mm depth) with no signal of cracking. Point A (Fig. 5b) indicates the onset of angular cracks at the edge of the groove caused by a higher load of almost 40 N at the rear of the contact end but with no evidence of adhesive failure. The high amplitude of acoustic emission (AE) peaks at point B, namely, penetration depth of 4.8 mm and a load of 50, 31 N, are evidence of material activity and with the aid of the images, the presence of transverse semi-circular cracks in the bulk material can be observed. This situation is sustained until the test was completed. From all the above, it can be considered critical load  $> 23$  N for the present coating without any interfacial fracture or adhesive failure. Unlike Si-DLC, the H-DLC coating revealed weaker coating resistance since the beginning of the test as shown in Fig. 5a. From the evident small peaks,

there is a possible premature failure which could be due to microscopic interfacial fractures with a critical load of 5.3 N. This behaviour could also be indicative of insufficient adhesion. However, as the indenter advances forward and penetration depth gradually increases with the scratch load and there is no evidence of flaking and/or delamination into the groove or by the edges of it. Therefore, it clearly establishes that H-DLC coating is less ductile than the Si-DLC. Thus, H-DLC presented better mechanical resistance, probably due to higher hardness. There was no evidence of adhesive failure.

Fig. 6 shows the variation of coefficient of friction (CoF) with contact pressures of 150 e 400 MPa and in dry and wet conditions. A summary of CoF values at the end of sliding test are given in Table 1. H-DLC exhibited lower levels of CoF than Si-DLC for all test conditions.

The highest CoF of Si-DLC occurred in dry conditions. Unlike the Si-DLC, a better adhesive strength was observed on the H-DLC, i.e. its surface did not undergo adhesive failure after the wear test under wet conditions at the lower contact pressures. This results are confirmed by SEM EDS linescan (Fig. 4), in which carbon and silicon are the trace element that confirm the presence of H-DLC and Si-DLC coatings, respectively.

The borderline difference of CoF between Si-DLC results is associated with the solution, while for H-DLC the contact pressure played more important role. As shown in Fig. 6 and Table 1, the H-DLC and Si-DLC coatings undergo a reduction in friction under wet conditions. The literature [24,25] describes that DLC films do not undergo elastic and plastic deformation under the metal substrate submitted to high loads. Therefore, lubricants are used to reduce the wear and friction on DLC films, such as ionic liquids that reduce the friction and increase the load carrying capacity. Based on this researches, it is evident that NaCl solution can also reduce the friction. However, this solution is rather aggressive and capable of attacking the metal substrate at the localised defects in the coating.

H-DLC tested with a contact pressure of 400 MPa in dry conditions presented a decrease of CoF during test. According to Manhabosco et al. [10], such reduction is linked to the roughness and hardness of the H-DLC coating. The contact pressure is mostly concentrated at the top of the material crests when the sliding starts, and this small contact area induces higher shear stress.

The variation of CoF with sliding distance with respect to loading in H-DLC tested under both conditions, clearly shows a decrease in the steady state values of CoF when the contact pressure is augmented. In general, this reduction occurs when the contact pressure of some carbon layers of the H-DLC film are transferred to the ball creating a lubricious graphite-like or amorphised transfer layer at the interface of coating and counterpart. This is graphitization process that develops on the H-DLC surface. These results are also in agreement with [10,26] where the CoF of the H-DLC is attributed to the high coating hardness. It was also demonstrated by Costa et al. [4] that the CoF of the DLC in 3% NaCl after 1000 cycles reached 0.11.

The graphitization of the wear track was confirmed by Raman spectroscopy (Fig. 2b). Raman spectroscopic measurements were performed at several locations of the wear track at the end of the sliding test of the H-DLC coating. The spectra have D and G peaks of  $1362$   $\text{cm}^{-1}$  and  $1573$   $\text{cm}^{-1}$ , respectively. The ratio of D and G peaks ( $I_D/I_G$ ) is 0.82. Therefore, comparing the Raman spectroscopies (Fig. 2a and b), the ratio of D and G peaks  $I_D/I_G$  increased from 0.42 for the virgin coating to 0.82 after the wear test. According to Costa et al. [4], the increase of  $I_D/I_G$  ratio indicates the formation of a graphite layer over H-DLC surface during the tests. The phase of diamond-like ( $\text{sp}^3$  – D band) transformed in graphite-like structures ( $\text{sp}^2$  – G band) because of the stress-strain state imposed by the sliding friction of the tribo pair.

It should be noted that the above analyses were done only for H-DLC coating because Si-DLC coating exhibited significant spalling and delamination in all test conditions. Therefore, the coefficient of friction values with contact pressure of 150 and 400 MPa (see Table 1) are almost the same to Si-DLC coating. It probably occurred because with

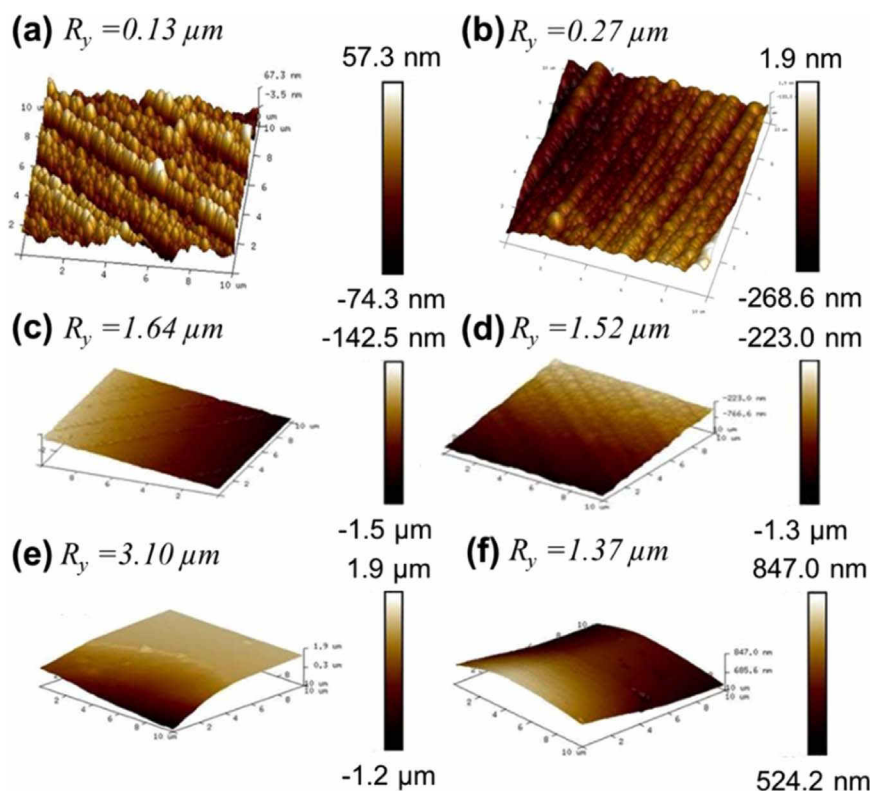


Fig. 3. AFM images: (a) H-DLC before wear tests, (b) Si-DLC before wear tests, (c) H-DLC - Dry condition at contact pressures of 150 MPa, (d) H-DLC - Wet condition at contact pressures of 150 MPa, (e) H-DLC - Dry condition at contact pressures of 400 MPa and (f) H-DLC - Wet condition at contact pressures of 400 MPa.

contact pressure of 150 MPa was already sufficient to cause damage on the coating surface.

The measurements of wear scars diameter on the silicon nitride balls and the wear rate are shown in Table 2. The largest diameter of wear scars, for each coating, correspond to the highest load under dry conditions. The wear scar diameters and wear rate for Si-DLC were consistently higher than H-DLC; this seems linked to the Si-DLC having a higher CoF compared to H-DLC under all conditions (Table 1). The mass loss of DLC surfaces occurred in all tested conditions, being less for the contact pressures of 150 MPa and wet conditions.

A comparison between the wear rates of the coatings tested at different conditions and contact pressures is also shown in Table 2. Dry conditions (high friction) with higher contact pressures as expected was the most severe test. Si-DLC showed the widest wear tracks and highest wear rates due to an adhesive failure. This result could be likely attributed to the resistance to wear in terms of the hardness, ductility and stiffness of the coatings. As previously determined, the hardness and elastic modulus of Si-DLC coating were 30% and 26% respectively; noticeably inferior to H-DLC coating.

Table 2 shows that H-DLC presented consistently lower wear than Si-DLC. Results are proved by SEM micrographs and EDS (Fig. 4). A better adhesive strength was observed on H-DLC, i.e. its surface did not undergo adhesive failure after wear test under dry and wet conditions at lower contact pressures (Fig. 4a and b). However, when increased the contact pressure occurred detachment of the coating (Fig. 4c and d). Si-DLC did not exhibited sufficient adhesion under both dry and wet conditions at lower contact pressure (150 MPa) (Fig. 4e). The detachment occurred along the wear track after sliding.

Despite knowing that higher stresses in the contact promoted graphitisation of the H-DLC, particularly under dry conditions, it should be noted that the carbon transfer weakens the coating structure and above some critical point when coating cannot withstand higher loads and failures arose from the detachment of the coating by interfacial fractures with the consequent increase of wear (Fig. 4c). Conversely, the H-DLC under wet conditions appears to be that graphitisation promoted by the impinging stresses in the contact is not completely suppressed

since the carbon contents remain as graphically shown in Fig. 4b and d. Analogously, it is also in agreement with behaviour of the CoF, where the variations of the CoF are scarce (Fig. 6). For Si-DLC coating, the lacking of adherence of the coating was observed in all test conditions. Analyses by EDS linescan shows enough evidence of the delamination failures, as can be seen in Fig. 4e.

Fig. 3c-f shows AFM analysis of H-DLC worn coatings under dry and wet conditions at contact pressures of 150 and 400 MPa. In both conditions, an increase in the surface roughness was identified, although, as expected to a lesser extent for the lowest loads. Again, no measurable features are given for Si-DLC coating because of the delamination failures throughout the tests.

### 3.3. Electrochemical properties

Fig. 7 shows anodic polarization curves obtained in naturally aerated 3.5% NaCl solution and Table 3 shows the polarization curves data. Tests were carried out on H-DLC and Si-DLC coatings before wear test and H-DLC film after wear test with 150 MPa of contact pressure and wet condition. This latter condition was selected because it was the only condition found without any substantial adhesive failure on the coating surface, as demonstrated by SEM/EDS examinations (see Fig. 4b).

H-DLC film (before wear test) had an initial OCP of  $-0.543$  mV and after wear test of  $-0.496$  mV, indicating that after wear test approximated to the OCP of carbon steel ( $-0.477$  mV). It probably happened because of the presence of Nano-defects on the H-DLC surface provoked by wear test. Plus, the galvanic couple formed between the H-DLC coating and the surface of carbon steel is very low because of the narrow difference between these OCP values. These results are in agreement with the literature [1,5]. Wang et al. [5], claim that if there is a failure on the surface of the DLC film exposing the metal surface, the localised corrosion could be easily inhibited by virtue of the DLC film and carbon steel have almost the same OCP. Consequently, the H-DLC provide a good improvement on the integrity against internal corrosion in carbon steel, given the protective barrier of the film and by

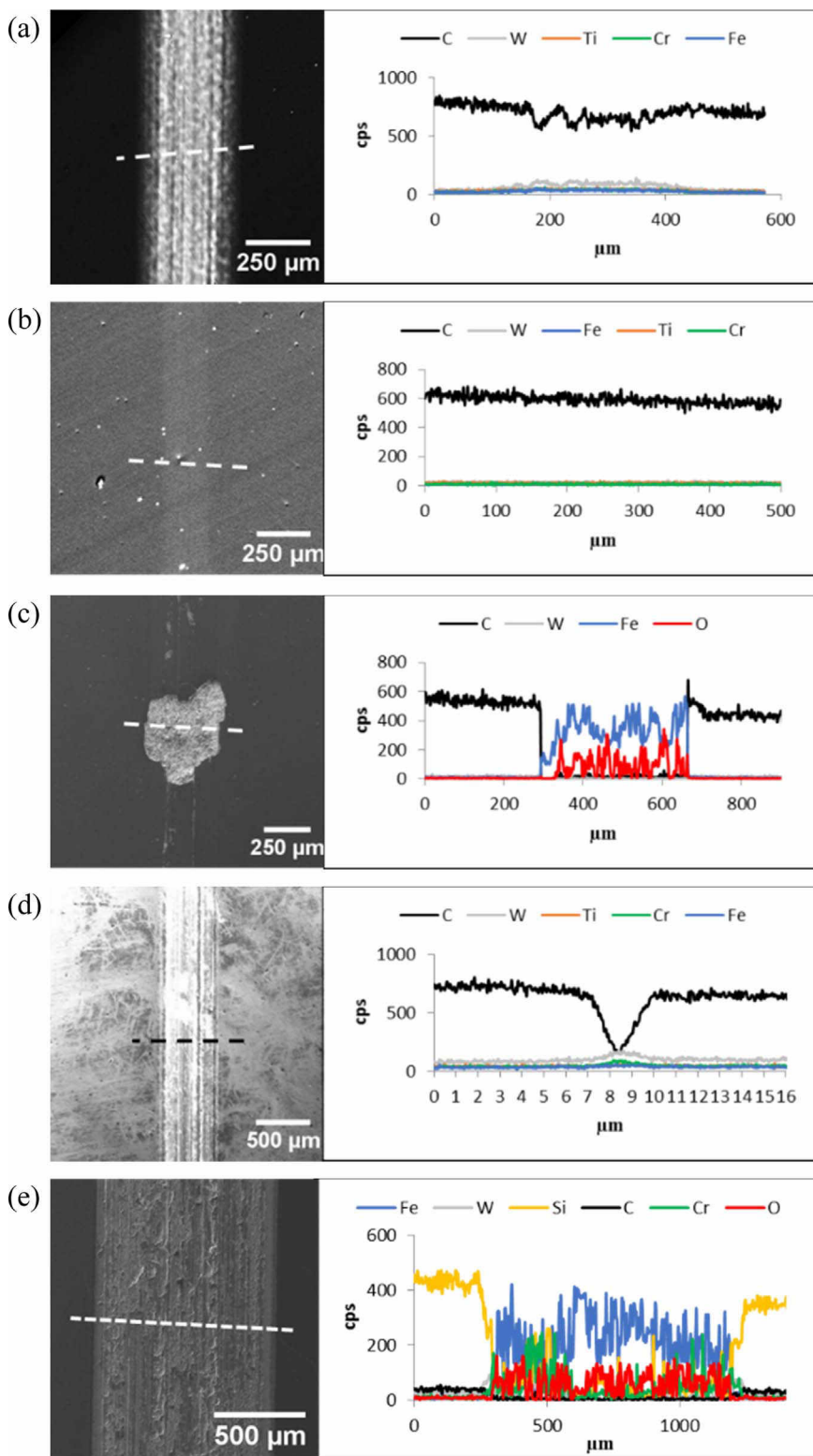


Fig. 4. SEM secondary electron images and EDS linescan composition profiles of cross worn track for (a) H-DLC - Dry condition at contact pressure of 150 MPa, (b) H-DLC - Wet condition at contact pressure of 150 MPa, (c) H-DLC - Dry condition at contact pressure of 400 MPa, (d) H-DLC - Wet condition at contact pressure of 400 MPa and (e) Si-DLC - Dry condition at contact pressure of 150 MPa.

obstructing the pitting corrosion process on the bulk carbon steel. These results are in accordance with Hadinata *et al.* [17], where the coated samples without defects and with defects had similar OCPs in relation to the OCP of the carbon steel. The Si-DLC revealed a more negative OCP ( $-0.676$  mV) than the H-DLC. Thus, the galvanic couple between this Si-DLC film and carbon steel is larger.

The H-DLC and Si-DLC coatings prior the wear assessment, revealed an increased corrosion resistance compared to the carbon steel as

expected. The carbon steel, in turn, exhibited active dissolution in the solution (Fig. 7). The corrosion current density measured at 200 mV above OCP (Table 3 and Fig. 7) was 2 orders of magnitude higher on carbon steel than DLC coating. Before wear tests, H-DLC was around  $10^{-9}$  A cm $^{-2}$  and after wear tests were around  $10^{-7}$  A cm $^{-2}$ . For Si-DLC, corrosion current density was  $10^{-5}$  A cm $^{-2}$ . Comparing these values with the corrosion current density of carbon steel ( $10^{-2}$  A cm $^{-2}$ ), even with defects DLC films presented less anodic current

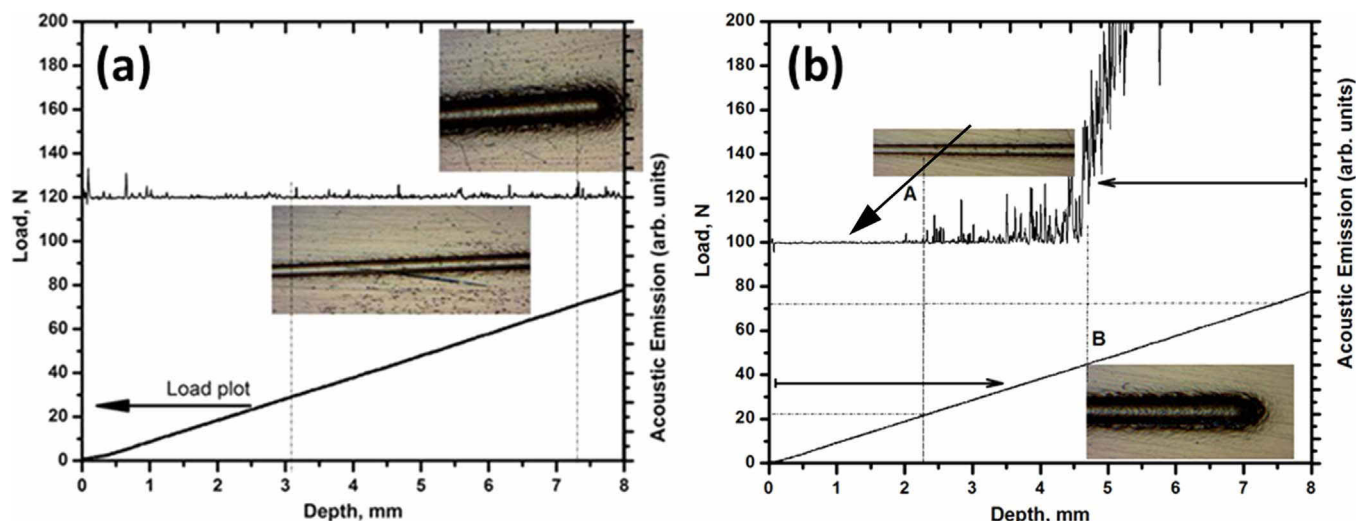


Fig. 5. Scratch induced acoustic emission of the (a) H-DLC and (b) Si-DLC coatings.

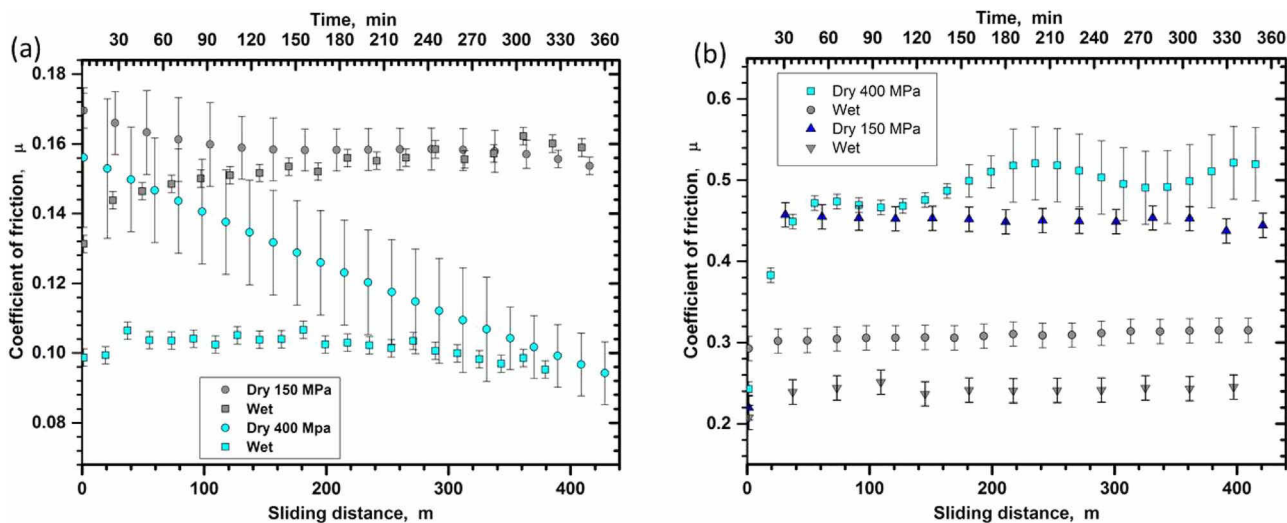


Fig. 6. CoF curves under dry and wet conditions for (a) H-DLC and (b) Si-DLC.

Table 1  
Comparison of CoF at the end of rubbing test for H-DLC and Si-DLC.

Coating	Contact pressure (Mpa)			
	150		400	
H-DLC	Dry	Wet	Dry	Wet
Si-DLC	0.16	0.15	0.10	0.09
	0.43	0.24	0.48	0.31

Table 2  
Diameter of wear scars on the counterparts (Si<sub>3</sub>N<sub>4</sub>) and wear rate for different environments and contact pressures.

Contact Pressure (MPa)	Condition	Diameter (mm)		Wear Rate (mm <sup>3</sup> /N.m)	
		Si-DLC	H-DLC	Si-DLC	H-DLC
150	Dry	0.987	0.429	1.30E-07	5.57E-09
	Wet	0.790	0.328	1.72E-07	4.60E-10
400	Dry	1.302	0.770	1.03E-06	5.83E-09
	Wet	1.197	0.665	3.29E-06	5.54E-09

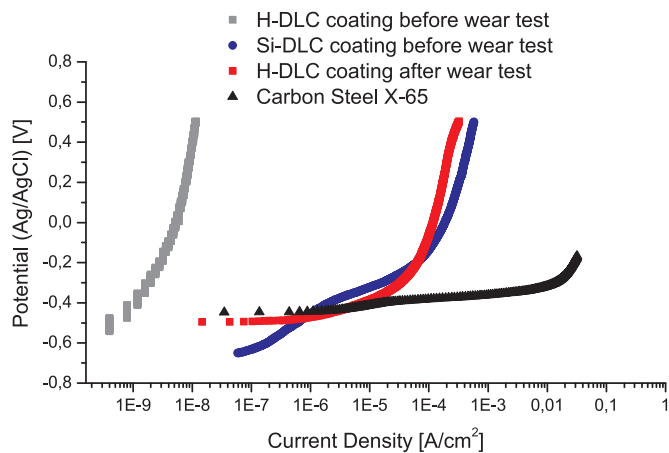


Fig. 7. Anodic polarization curves of H-DLC and Si-DLC coatings and bare steel in 3,5% NaCl, naturally aerated, pH 7.

density than carbon steel. This occurs probably because the exposed area of carbon steel due to nano defects of DLC after wear tests were much smaller than the area of carbon steel specimen. Therefore, these values are important to compare results of each condition, showing that

**Table 3**  
Open circuit potential (OCP), current density values measured at 200 mV above the OCP.

Sample	OCP (V) (Ag/AgCl/KCl)	Pot. (V) 200 mV above OCP	Log i (A/cm <sup>2</sup> ) 200 mV above OCP
Steel	−0.477	−0.247	2.21E−02
H-DLC –Before wear test	−0.543	−0.343	1.60E−09
H-DLC –After wear test	−0.496	−0.296	3.44E−05
Si-DLC –Before wear test	−0.676	−0.476	7.67E−07

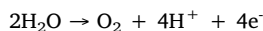
anodic current density increased on DLC coatings with defects. However, to measurement the corrosion rate underneath the porous regions of the DLC film is difficult due to the need of measure the exposed area of the bulk into the DLC defects.

Galvanic couple formed between DLC films and carbon steel surface can be influenced by two factors: OCP and conductivity [1,5,27]. H-DLC film before wear test had an initial OCP of −0.543 mV and after wear test of −0.496 mV, which was close to the OCP of carbon steel (−0.477 mV). This behaviour could be a secondary effect related to nano-defects imposed on H-DLC by the wear test. Plus, galvanic couple formed is very low due to the slight difference between OCP values.

Si-DLC OCP was more negative than the H-DLC. Thus, galvanic couple between Si-DLC film and carbon steel is higher. These results are in agreement with the literature [1,5]. Wang *et al.* [5] claim that if there is a failure on the surface of the DLC film exposing the metal surface, the localised corrosion could be easily inhibited due to DLC film and carbon steel to have similar OCP. Hadinata *et al.* [17] reported that the coated samples with and without defects presented similar OCP to carbon steel. However, conductivity could decrease corrosion resistance of the DLC film and affect negatively galvanic couple DLC/Fe. According Miyagawa *et al.* [27], DLC coatings present high electrical resistivity, around 10<sup>2</sup> to 10<sup>6</sup> Ω cm. The wide range of values are associated with the deposition technique and conditions.

It has been reported [7–10,14–17] that the DLC has a lower anodic density current than the carbon steel, around nA/cm<sup>2</sup>, but they do not correlate this DLC density current with dissolution processes of the DLC coating or bulk material. In fact, two factors need to analysed in this context. The first one is that this small current density could be associated to pores in the DLC film. Plus, according to Reisel *et al.* [8] the DLC is inert, amorphous and does not corrode, so this anodic current is not associated to the passivation process; and the amorphous structure of the DLC coating reduces or halts the electron transport over the DLC surface. Therefore, this low anodic density current is probably associated to two facts, being nano-pores on the DLC films and the ion flow.

Films with nano-pore defects can easily be penetrate by the solution. By this mechanism, the solution could reach the carbon steel surface (inner layer) and trigger the corrosion process on the bulk material. However, films free of nano defects effectively protect the carbon steel inner layer from fluid ingress. The ionic transportation process on the substrate (under DLC surface) is related to water dissolution as the following reaction:



The Si-DLC begun with a low anodic current but it increased after applying some anodic potential (Fig. 7). This is likely to be because some defects and the anodic polarization on the surface. The process of film deposition could create some nano scale defects and then, during the anodic polarization, high imposed anodic potentials could promote the diffusion of ions inside these defects, commencing the corrosion process on the metal surface [5]. From the mentioned, it is need to study if nano defects on the film could resist to ionic diffusion forces during long periods of exposition to a corrosive environment.

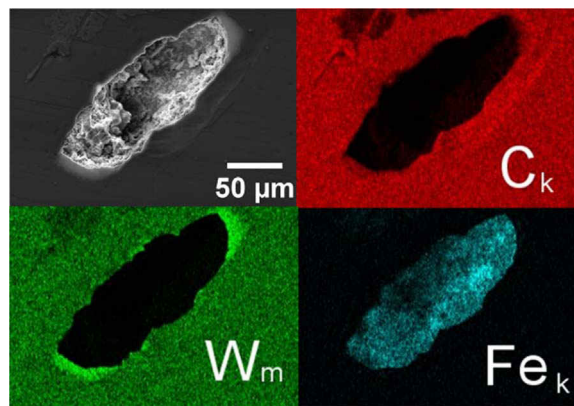


**Fig. 8.** H-DLC – SEM secondary image and EDS mapping of the defect caused by wear test (400 MPa and wet condition).

The lowest anodic current of the H-DLC coating (before wear testing) suggests that this film has excellent resistivity to be used as a corrosion barrier in oil and gas equipment made of carbon steel, which is a good property against corrosion process in saline solution (see Table 3). In addition, it proves that the film was deposited without a significant defect on the carbon steel, as indicated in Fig. 2, where it is clear the excellent adhesion of the coating to the substrate and exhibiting a structure without adhesive failures, i.e. with an interface of high quality with respect to the carbon steel.

The only wear test that did not show evidence of coating damage was that of 150 MPa contact pressure and in wet conditions. However, the anodic current of the H-DLC (post wear test) increased in relation to the H-DLC (before wear test), indicating that the wear test produced some nano defects on the H-DLC film surface. Nonetheless, these Nano defects were not observed by SEM/EDS (Fig. 1). Therefore, this ramp up on the anodic density current could be associated with the process of substrate anodic dissolution. It means that 150 MPa was sufficient contact load to produce nano defects on the H-DLC surface and to expose the substrate to the corrosive solution.

Fig. 8 shows the H-DLC film surface after the wear test in wet condition and with contact pressure of 400 MPa. From the SEM secondary electron image, it was noticed a hole of around 200 μm, in the multi-layered H-DLC film. The hole exposed the carbon metal causing the corrosion process. It may be inferred that this delamination of the H-DLC film occurred during the wear test. However, the good information is that the corrosion process occurred only at the location where wear test promoted the defects and it did not propagate between the interface of H-DLC film and substrate. Even with some defects, the H-DLC is a good option to reduce the corrosion rate of the carbon steel to prolong the service life of the equipment utilised in oil industry. According to Sharma, Barhai and Kumari [15], the DLC coatings are chemically inert, at room temperature, for almost all acid, alkalis and organic solutions and solvents. Because of its good corrosion resistance and excellent adherence to the carbon steel substrate, the H-DLC has a strong potential to be used for important parts and equipment of the oil and gas industries for instance, the SSCV, pistons and pumps, associated to pipelines.

In medical applications like ankles, wear-corrosion solicitations caused failure on the DLC film [3], demonstrating that the DLC film did not have good results with regard to wear and corrosion processes acting together for this environment. Conversely, the results in this work elucidated that the resistance of the H-DLC film, applied over carbon steel, had better performance than Si-DLC in situations where the equipment are subject to conditions of wear and corrosion acting together in saline environments.

DLC films have poor adhesion on carbon steel that contributes to the spontaneous debonding effects. A variety of metallic and intermetallic interlayers (Al, Cr, W, Ti, Si) are used to improve the adhesion

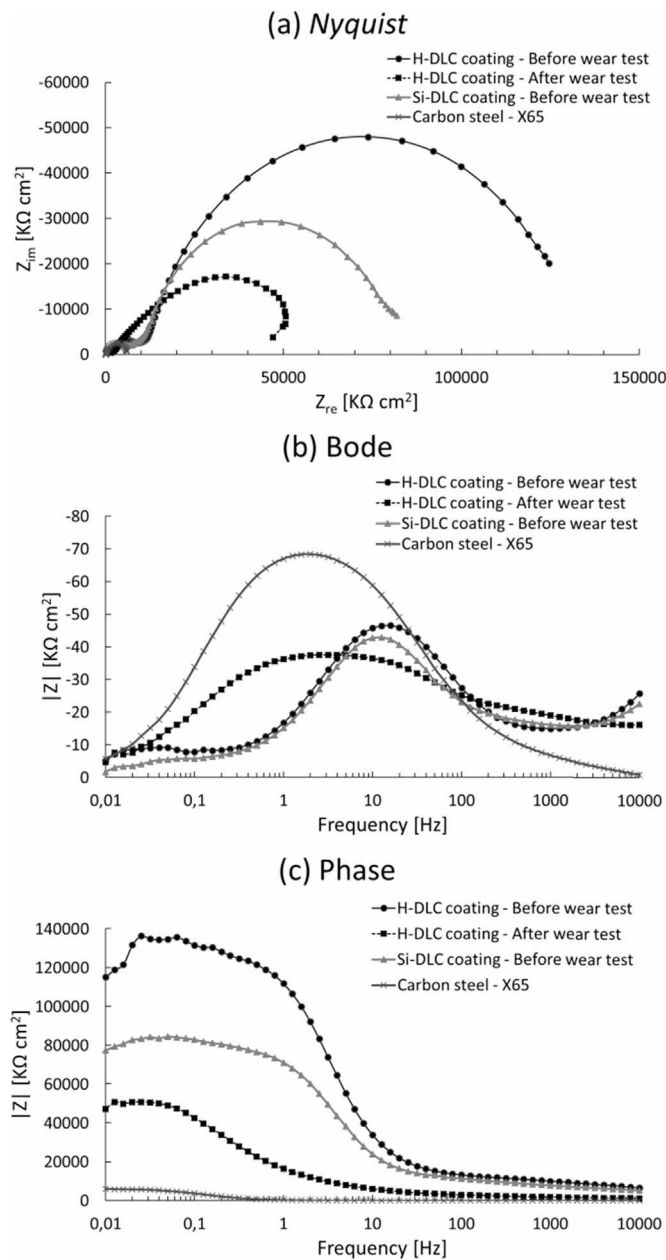


Fig. 9. EIS behaviours for carbon steel, HDLC and Si-DLC films. (a) Nyquist plots, (b) Bode plots and (c) Phase plots.

properties, corrosion resistance and reduce the number of critical film defects of DLC on carbon steel. This prevents premature delamination under both higher loads and contact pressure during tribocorrosion conditions [28–30]. Reisel *et al.* [8] showed that the electron transport through the diamond-like carbon coating is reduced or even stopped by

the amorphous structure of the layer. The fraction of metallic layers could lead to increase electron conductivity. Multi layers and single layers coatings presented different behaviour in relation to electrochemical behaviour, being better for multi layers coatings than single layers. In the present work, the interlayer of Cr/W could improve the electrical conductivity on the defects. However, further investigation is need, once it was not possible to evaluate the influence of Cr/W interlayer in wear and electrochemical tests for both films had the same interlayer.

Fig. 9 shows the EIS curves obtained at the open circuit potentials of the steel, H-DLC and Si-DLC coatings before wear test and H-DLC film after wear tests with 150 MPa of contact pressure and wet condition.

The Nyquist plot (Fig. 9a) shows different behaviours of carbon steel, H-DLC and Si-DLC coatings at locations of high frequencies, with values of imaginary and real components of  $M\Omega\text{cm}^2$  for both DLC coatings and  $K\Omega\text{cm}^2$  for the carbon steel. The same performance is observed in intermediary and small frequencies, where both DLC coatings presented higher values of  $Z_{real}$  and  $Z_{imag}$ . These results suggest that both DLC films have a higher capacitance than carbon steel. It occurred due to the carbon steel had activated dissolution without presenting any passivation process, as showed in the polarization curves (Fig. 7). Therefore, the capacitive arc of both DLC coatings is so much higher that the carbon steel, showing the good polarization resistance and high resistivity of the coatings. The Si-DLC presented a capacitive arc smaller than H-DLC. These results agree with the polarization curves (Fig. 7) where the Si-DLC had more anodic density current than the H-DLC coating.

Impedance module Bode plots shows at high frequencies (1 kHz until 100 kHz) that the Z module is almost constant and phase angle  $\phi$  are near to zero for the carbon steel. This characteristic represents the resistive behaviour of the solution. However, the phase angle of both DLC films is higher, where the resistive behaviour of the solution is associated with the inert conditions of both DLC films.

It should be noted for low frequencies that both DLC films had higher Z module than the carbon steel (Fig. 9c), showing the excellent corrosion resistance of the DLC films. Therefore, the electrochemical corrosion reactions followed between the interface of DLC films and metal substrate as it had a very small contact time. Thus, the ions transport related to the corrosion process at the metal substrate could hardly be avoid because of the layer of DLC film [5]. The reduction of Z module of the H-DLC before wearing test to H-DLC after wearing test and Si-DLC coating can be associated to Nano defects on the films surfaces.

Bode plots (Fig. 9b) shows that the impedance process moves from Ohmic to capacitance dominance. The phase shift moves from 0 to  $-68^\circ$  to carbon steel, 0 to  $-38^\circ$  to the H-DLC film before wearing test, 0 to  $-42^\circ$  to the H-DLC after wearing test and 0 to  $-45^\circ$  to the Si-DLC coating. Plus, it also shows that there is one constant time or maximum angle for the carbon steel, while there are two constant times or two maximum angles for both DLC coatings. This angle at high frequencies could be associated to the inert property of the DLC films, acting as a barrier to the process of charge transfers (electrochemical reactions) at the interface of DLC films and electrolyte. The angle in intermediary

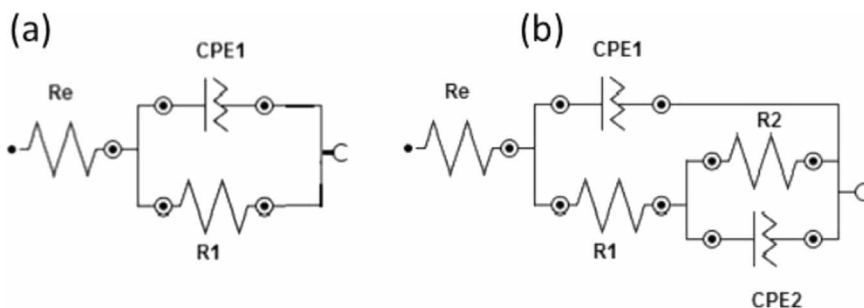


Fig. 10. Equivalent circuit of (a) carbon steel and (b) DLC films coatings.

frequencies could be associated to the capacitance of the DLC films (CPE<sub>1</sub>).

The equivalent circuits (Fig. 10) of the EIS were used to assess the mechanisms of corrosion process that ensued at the interface of electrolyte/carbon steel and electrolyte/DLC coating systems. The equivalent circuit of both DLC coating has been used [5,7,14] to explain the AC response of the DLC coating on a metallic bulk material. Thus, the DLC equivalent circuit is composed by: Tested electrolyte resistance (R<sub>e</sub>); capacitance of the DLC coating, being a constant phase element (CPE<sub>1</sub>); resistance to charges transference at the interface of DLC film and electrolyte, external layer of the DLC film associated to some areas of the surface film that has ionic conduction, named porous resistance (R<sub>1</sub>); the elements R<sub>2</sub> and CPE<sub>2</sub> represent the polarization resistance of charge transfer and capacitance of interface of the DLC film and metal substrate, which means that is the internal layer of the DLC film. The carbon steel equivalent circuit is composed by: Tested electrolyte resistance (R<sub>e</sub>); capacitance of the carbon steel, being a constant phase element (CPE<sub>1</sub>) and resistance to charges transference between the carbon steel and solution (R<sub>1</sub>).

In high frequencies, the impedance of the DLC films has a dominating Ohmic behaviour, being controlled by Ohmic of the electrolyte resistance (R<sub>e</sub>). In intermediary frequencies, the system is controlled by the capacitance of the DLC coatings (CPE<sub>1</sub>) and the resistance to charges transference at the interface of DLC films and electrolyte (R<sub>1</sub>). Moreover, in low frequencies (10<sup>-3</sup> to 10<sup>-1</sup> Hz), the impedance is managed mainly by the polarization resistance of charges transfer between the interface of the DLC films and metal substrate (R<sub>2</sub>) and by capacitance of interface of the DLC films and metal substrate (CPE<sub>2</sub>). This results are in accordance with Liu and Kwek [14].

#### 4. Conclusion

The purpose of this research was to evaluate tribocorrosion behaviour of hydrogenated and silicon DLC coatings on carbon steel. The approach used to investigate the problem was sliding wear test on pin on plate machine, plus electrochemical and electrochemical impedance experiments. As a result of this work, the following main findings concerning the nature of wear were:

- 1) Tribology tests showed poor performance of Si-DLC coating, which presented total delamination in all contact pressure applied. H-DLC exhibited high incidence of coating damage under the conditions tested, except when applied a contact pressure of 150 MPa in wet condition. Although there is an absence of visible defects on H-DLC coatings under these conditions, electrochemical tests showed an increase of corrosion. It means that 150 MPa was enough pressure to produce nano defects on the H-DLC surface, exposing carbon steel substrate to the corrosive solution.
- 2) The lowest anodic current of the H-DLC coating suggests that this film has excellent resistivity to use as a corrosion barrier in oil and gas equipment made of carbon steel. It was proved to have an excellent adhesion of the coating to the substrate and to be effective against the corrosion process in saline solution.

#### Acknowledgement

This work was supported by CNPq (grant number 249193/2013-2), UFSJ (Brazil) and University of Leeds (UK).

#### References

[1] X. Hu, A. Neville, CO<sub>2</sub> erosion–corrosion of pipeline steel (API X65) in oil and gas conditions—A systematic approach, *Wear* 267 (2009) 2027–2032, <http://dx.doi.org/10.1016/j.wear.2009.07.023>.  
 [2] R. Barker, X. Hu, A. Neville, The influence of high shear and sand impingement on preferential weld corrosion of carbon steel pipework in CO<sub>2</sub>-saturated environments, *Tribol. Int.* 68 (2013) 17–25, <http://dx.doi.org/10.1016/j.triboint.2012.11.015>.

[3] T.M. Manhabosco, I.L. Müller, Tribocorrosion of diamond-like carbon deposited on Ti6Al4V (229–229), *Tribol. Lett.* 34 (2009), <http://dx.doi.org/10.1007/s11249-009-9417-7>.  
 [4] R.P.C. Costa, F.R. Marciano, D.A. Lima-Oliveira, E.J. Corat, V.J. Trava-Airoldi, Tribological effect of iron oxide residual on the DLC film surface under seawater and saline solutions, *Surf. Sci.* 605 (2011) 783–787, <http://dx.doi.org/10.1016/j.susc.2011.01.018>.  
 [5] Z.M. Wang, J. Zhang, X. Han, Q.F. Li, Z.L. Wang, R. Wei, Corrosion and salt scale resistance of multilayered diamond-like carbon film in CO<sub>2</sub> saturated solutions, *Corros. Sci.* 86 (2014) 261–267, <http://dx.doi.org/10.1016/j.corsci.2014.05.015>.  
 [6] R. Wei, Development of new technologies and practical applications of plasma immersion ion deposition (PIID), *Surf. Coat. Technol.* 204 (2010) 2869–2874, <http://dx.doi.org/10.1016/j.surfcoat.2010.01.046>.  
 [7] P. Papakonstantinou, J. Zhao, P. Lemoine, E.T. McAdams, J.A. McLaughlin, The effects of Si incorporation on the electrochemical and nanomechanical properties of DLC thin films, *Diam. Relat. Mater.* 11 (2002) 1074–1080, [http://dx.doi.org/10.1016/S0925-9635\(01\)00656-2](http://dx.doi.org/10.1016/S0925-9635(01)00656-2).  
 [8] G. Reisel, G. Irmer, B. Wielage, A. Dörner-Reisel, Electrochemical corrosion behavior of carbon-based thin films in chloride ions containing electrolytes, *Thin Solid Films.* 515 (2006) 1038–1042, <http://dx.doi.org/10.1016/j.tsf.2006.07.063>.  
 [9] M. Pourbaix, J. Burbank, Atlas D-equilibres électrochimiques, *J. Electrochem. Soc.* 111 (1964) 14C, <http://dx.doi.org/10.1149/1.2426051>.  
 [10] T.M. Manhabosco, A.P.M. Barboza, R.J.C. Batista, B.R.A. Neves, I.L. Müller, Corrosion, wear and wear–corrosion behavior of graphite-like a-C:H films deposited on bare and nitrided titanium alloy, *Diam. Relat. Mater.* 31 (2013) 58–64, <http://dx.doi.org/10.1016/j.diamond.2012.11.005>.  
 [11] D. Vouagner, A.M. de Becdelievre, M. Keddad, J.M. Mackowski, The electrochemical behaviour in acidic and chloride solutions of amorphous hydrogenated carbon thin films deposited on single crystal germanium slices (n-type) by plasma decomposition of methane, *Corros. Sci.* 34 (1993) 279–293, [http://dx.doi.org/10.1016/0010-938X\(93\)90007-4](http://dx.doi.org/10.1016/0010-938X(93)90007-4).  
 [12] G. Dearnaley, J.H. Arps, Biomedical applications of diamond-like carbon (DLC) coatings: a review, *Surf. Coat. Technol.* 200 (2005) 2518–2524, <http://dx.doi.org/10.1016/j.surfcoat.2005.07.077>.  
 [13] S.J. Bull, A. Matthews, Diamond for wear and corrosion applications, *Diam. Relat. Mater.* 1 (1992) 1049–1064, [http://dx.doi.org/10.1016/0925-9635\(92\)90075-Y](http://dx.doi.org/10.1016/0925-9635(92)90075-Y).  
 [14] E. Liu, H.W. Kwek, Electrochemical performance of diamond-like carbon thin films, *Thin Solid Films.* 516 (2008) 5201–5205, <http://dx.doi.org/10.1016/j.tsf.2007.07.089>.  
 [15] R. Sharma, P.K. Barhai, N. Kumari, Corrosion resistant behaviour of DLC films, *Thin Solid Films.* 516 (2008) 5397–5403, <http://dx.doi.org/10.1016/j.tsf.2007.07.099>.  
 [16] J. Robertson, Diamond-like amorphous carbon, *Mater. Sci. Eng. R. Rep.* 37 (2002) 129–281, [http://dx.doi.org/10.1016/S0927-796X\(02\)00005-0](http://dx.doi.org/10.1016/S0927-796X(02)00005-0).  
 [17] S.-S. Hadinata, M.-T. Lee, S.-J. Pan, W.-T. Tsai, C.-Y. Tai, C.-F. Shih, Electrochemical performances of diamond-like carbon coatings on carbon steel, stainless steel, and brass, *Thin Solid Films.* 529 (2013) 412–416, <http://dx.doi.org/10.1016/j.tsf.2012.05.041>.  
 [18] J. Solis, H. Zhao, C. Wang, J.A. Verdusco, A.S. Bueno, A. Neville, Tribological performance of an H-DLC coating prepared by PECVD, *Appl. Surf. Sci.* 383 (2016) 222–232, <http://dx.doi.org/10.1016/j.apsusc.2016.04.184>.  
 [19] M. N. R. G, Effect on lubrication regimes with silicon nitride and bearing steel balls, *Tribol. Int.* 116 (2017) 403–413, <http://dx.doi.org/10.1016/j.triboint.2017.06.043>.  
 [20] M. Kalin, J. Vižintin, A comparison of the tribological behaviour of steel/steel, steel/DLC and DLC/DLC contacts when lubricated with mineral and biodegradable oils, *Wear* 261 (2006) 22–31, <http://dx.doi.org/10.1016/j.wear.2005.09.006>.  
 [21] C. Strondl, N.M. Carvalho, J.T.M. De Hosson, T.G. Krug, Influence of energetic ion bombardment on W-C:H coatings deposited with W and WC targets, *Surf. Coat. Technol.* 200 (2005) 1142–1146, <http://dx.doi.org/10.1016/j.surfcoat.2005.02.182>.  
 [22] H. Pang, X. Wang, G. Zhang, H. Chen, G. Lv, S. Yang, Characterization of diamond-like carbon films by SEM, XRD and Raman spectroscopy, *Appl. Surf. Sci.* 256 (2010) 6403–6407, <http://dx.doi.org/10.1016/j.apsusc.2010.04.025>.  
 [23] M.S. Jellesen, T.L. Christiansen, L.R. Hilbert, P. Møller, Erosion–corrosion and corrosion properties of DLC coated low temperature gas-nitrided austenitic stainless steel, *Wear* 267 (2009) 1709–1714, <http://dx.doi.org/10.1016/j.wear.2009.06.038>.  
 [24] Z. Jia, Y. Xia, J. Li, X. Pang, X. Shao, Friction and wear behavior of diamond-like carbon coating on plasma nitrided mild steel under boundary lubrication, *Tribol. Int.* 43 (2010) 474–482, <http://dx.doi.org/10.1016/j.triboint.2009.07.012>.  
 [25] G. Dumitru, V. Romano, H. Weber, S. Pimenov, T. Kononenko, J. Hermann, S. Bruneau, Y. Gerbig, M. Shupegin, Laser treatment of tribological DLC films, *Diam. Relat. Mater.* 12 (2003) 1034–1040, [http://dx.doi.org/10.1016/S0925-9635\(02\)00372-2](http://dx.doi.org/10.1016/S0925-9635(02)00372-2).  
 [26] Z.F. Zhou, K.Y. Li, I. Bello, C.S. Lee, S.T. Lee, Study of tribological performance of ECR–CVD diamond-like carbon coatings on steel substrates, *Wear* 258 (2005) 1589–1599, <http://dx.doi.org/10.1016/j.wear.2004.10.005>.  
 [27] S. Miyagawa, S. Nakao, J. Choi, M. Ikeyama, Y. Miyagawa, Effects of target bias voltage on the electrical conductivity of DLC films deposited by PBIID with a bipolar pulse, *Nucl. Instrum. Methods Phys. Res. Sect. B Beam Interact. Mater. At.* 242 (2006) 346–348, <http://dx.doi.org/10.1016/j.nimb.2005.08.051>.  
 [28] F. Cemin, C.D. Boeira, C.A. Figueroa, On the understanding of the silicon-containing adhesion interlayer in DLC deposited on steel, *Tribol. Int.* 94 (2016) 464–469, <http://dx.doi.org/10.1016/j.triboint.2015.09.044>.  
 [29] H. Decho, A. Mehner, H.W. Zoch, H.R. Stock, Optimization of chromium nitride



(CrNx) interlayers for hydrogenated amorphous carbon (a-C:H) film systems with respect to the corrosion protection properties by high power impulse magnetron sputtering (HiPIMS), Surf. Coat. Technol. 293 (2016) 35–41, <http://dx.doi.org/10.1016/j.surfcoat.2016.01.037>.

[30] F. Cemin, L.T. Bim, C.M. Menezes, M.E.H. Maia, da Costa, I.J.R. Baumvol,

F. Alvarez, C.A. Figueroa, The influence of different silicon adhesion interlayers on the tribological behavior of DLC thin films deposited on steel by EC-PECVD, Surf. Coat. Technol. 283 (2015) 115–121, <http://dx.doi.org/10.1016/j.surfcoat.2015.10.031>.



**SEP**

**DIRECCIÓN GENERAL DE EDUCACIÓN SUPERIOR TECNOLÓGICA  
INSTITUTO TECNOLÓGICO DE TLALNEPANTLA**



# Reconocimiento

*a José Solís Romero*

Por su participación como Instructor en el curso  
“Computational tools for writing a technical paper”,  
realizado del 18 al 22 de Junio de 2012  
con una duración de 30 horas.

Tlalnepantla de Baz, Edo. de Méx., a 22 de Junio, 2012.



*Oscar Castellanos Hernández*  
Ing. Oscar Castellanos Hernández  
DIRECTOR

S. E. P.  
D. G. E. S. T.  
I. T. DE TLALNEPANTLA  
DIRECCION



INSTITUTO TECNOLÓGICO DE  
TLALNEPANTLA



RSSC 610



UNIVERSITY OF LEEDS

Jose Solis Romero

attended

41<sup>st</sup> Leeds-Lyon Symposium on  
Tribology

**'INTEGRATED TRIBOLOGY'**

JoseSolis Romeroon

Tuesday 2 – Friday 5 September 2014

*Martin Priest*

Martin Priest, Jost Chair of Engineering Tribology  
Chairman of the 41<sup>st</sup> Leeds-Lyon Symposium on Tribology



SECRETARÍA DE EDUCACIÓN PÚBLICA

SUBSECRETARÍA DE EDUCACIÓN SUPERIOR

México, D.F. a 22 de noviembre del 2007

Oficio No. 103/2007- 026

ASUNTO: DICTAMEN LICENCIA BECA-COMISION

Ing. José Fausto León Jacobo  
Director del I. T. de Tlalnepantla  
PRESENTE

De conformidad con lo establecido en el "Manual para el Otorgamiento de Licencias por Becas-Comisión a Servidores Públicos para efectuar Estudios de Posgrado en Instituciones Educativas Nacionales", se emite:

DICTAMEN: SE AUTORIZA LICENCIA POR BECA-COMISION INICIAL AL  
C. SOLIS ROMERO JOSE

FILIACION: SORJ630126781

CLAVE (S): E386300/141033

ADSCRIPCION: I.T. TLÁLNEPANTLA

INSTITUCION: INSTITUTO TECNOLOGICO Y DE ESTUDIOS SUPERIORES DE MONTERREY (EDO. MEX.)

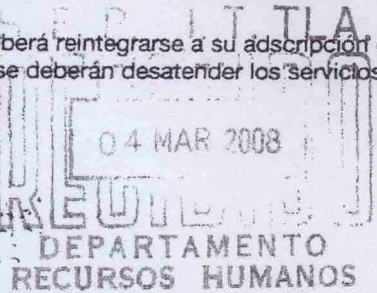
MOTIVO: REALIZAR ESTANCIA POSDOCTORAL (CARACTERIZACION MECANICA Y ESTRUCTURAL DE COMPUESTOS MANOESTRUCTURADOS EN PELICULAS DELGADAS) (Primer año)

PERIODO: 15 DE ENERO DEL 2008 AL 15 DE ENERO DEL 2009

Al término de este período el profesor deberá reintegrarse a su adscripción original a prestar sus servicios. Al otorgar esta beca, por ningún motivo se deberán desatender los servicios educativos de su Institución.

ATENTAMENTE

DR. RODOLFO TUIRÁN  
SUBSECRETARIO



C.C.P.- ING. HÉCTOR ARREOLA SORIA.- DIRECTOR GENERAL DE EDUCACIÓN SUPERIOR TECNOLÓGICA  
LEOPOLDO ALEJANDRO CAMPOS MORENO.- COORDINADOR SECTORIAL DE ADMINISTRACIÓN  
Y FINANZAS DE LA DGEST  
EXPEDIENTE  
INTERESADO



SECRETARÍA DE EDUCACIÓN PÚBLICA

SUBSECRETARÍA DE EDUCACIÓN SUPERIOR

México, D.F. a 22 de noviembre del 2007

Oficio No. 103/2007- 026

ASUNTO: DICTAMEN LICENCIA BECA-COMISION

Ing. José Fausto León Jacobo  
Director del I. T. de Tlalnepantla  
PRESENTE

De conformidad con lo establecido en el "Manual para el Otorgamiento de Licencias por Becas-Comisión a Servidores Públicos para efectuar Estudios de Posgrado en Instituciones Educativas Nacionales", se emite:

DICTAMEN: SE AUTORIZA LICENCIA POR BECA-COMISION INICIAL AL  
C. SOLIS ROMERO JOSE

FILIACION: SORJ630126781

CLAVE (S): E386300/141033

ADSCRIPCION: I.T. TLALNEPANTLA

INSTITUCION: INSTITUTO TECNOLOGICO Y DE ESTUDIOS SUPERIORES DE MONTERREY (EDO. MEX.)

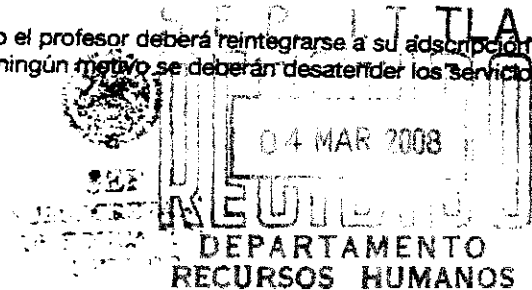
MOTIVO: REALIZAR ESTANCIA POSDOCTORAL (CARACTERIZACION MECANICA Y ESTRUCTURAL DE COMPUESTOS MANOESTRUCTURADOS EN PELICULAS DELGADAS) (Primer año)

PERIODO: 15 DE ENERO DEL 2008 AL 15 DE ENERO DEL 2009

Al término de este período el profesor deberá reintegrarse a su adscripción original a prestar sus servicios. Al otorgar esta beca, por ningún motivo se deberán desatender los servicios educativos de su Institución.

ATENTAMENTE

DR. RODOLFO TUIRÁN  
SUBSECRETARIO



C.C.P. - ING. HÉCTOR ARREOLA SORIA.- DIRECTOR GENERAL DE EDUCACIÓN SUPERIOR TECNOLÓGICA  
LEOPOLDO ALEJANDRO CAMPOS MORENO.- COORDINADOR SECTORIAL DE ADMINISTRACIÓN  
Y FINANZAS DE LA DGEST  
EXPEDIENTE  
INTERESADO



4<sup>th</sup> July 2013

To whom it may concern:

RE: Jose Solis-Romero

This is to confirm that we will gladly welcome Dr Jose Solis-Romero on his sabbatical leave to our Institute.

The main objectives of the study period will be:

- to advance the understanding of the microwave PVD technique as a means of depositing tribological coatings on to steels
- to establish long term relationships between iETSI and ITTLA
- to contribute to the scientific literature in this area.

Jose will have access to our laboratory facilities and in particular he will work on the Hauzer Flexicoat 850 PVD instrument with a unique microwave capability integrated within the conventional PVD system. Also all of the required surface analysis equipment, TEM, SEM, SIMS will be accessible.

We would invite Jose to also take part in our seminar programme for our postgraduate and MSc students and will fully integrate him in the research group.

If you require any further information, please don't hesitate to contact me.

Yours sincerely

A handwritten signature in cursive script that reads "Anne Neville".

Professor Anne Neville

# TECNOLÓGICO NACIONAL DE MÉXICO

EL INSTITUTO TECNOLÓGICO DE TLALNEPANTLA

OTORGA EL PRESENTE

# RECONOCIMIENTO

A

## JOSÉ SOLÍS ROMERO

POR SU PARTICIPACIÓN COMO PONENTE DE LA CONFERENCIA  
“IMPORTANCIA DE LA INVESTIGACIÓN EN EL SIGLO XXI”  
EN EL MARCO DEL 45 ANIVERSARIO DEL INSTITUTO

TLALNEPANTLA DE BAZ, EDO. DE MÉXICO A 7 DE SEPTIEMBRE DE 2017



DR. GUSTAVO FLORES FERNÁNDEZ  
DIRECTOR



SEP  
INSTITUTO TECNOLÓGICO DE TLALNEPANTLA  
DIRECTOR



08 December 2014

**Dear Mtra. Lorena Archundia Navarro**  
Directora de Planeación de Ciencia  
Dirección Adjunta de Desarrollo Científico  
CONSEJO NACIONAL DE CIENCIA Y TECNOLOGÍA (CONACYT)

**Atn':** Ing. Humberto Pineda  
Alegria

Jefe de Departamento de  
Evaluación de Revistas  
Científicas y Tecnológicas.

I have analysed the final report on "The deposition and tribological behaviour of hydrogenated diamond like-carbon coatings on steel by Microwave Plasma Enhance Chemical Vapour Deposition". I totally agree with the report and I am pleased by the work that was carried out during the period of visiting.

Some required data by Conacyt are as follows:

---

NOMBRE DEL VISITANTE:	JOSE SOLIS ROMERO
ESTANCIA SABÁTICA:	SEGUNDO PERÍODO DE LA CONVOCATORIA 2013.
TIÍTULO DEL PROYECTO:	<b>Estancia Sabática en <i>The University of Leeds</i>. "Deposición de revestimientos tribológicos nanoestructurados por medio de CVD y combinaciones de procesamiento sobre acero".</b>
No. PROPUESTA:	207502
ÁREA DE CONOCIMIENTO:	7. Cs. DE LA INGENIERÍA
FECHA DE INICIO:	01 DE ENERO DE 2014
FECHA DE TÉRMINO:	31 DE DICIEMBRE 2014

---

Should you have any queries on the above or any other information regarding the José Solis Romero visiting please do not hesitate to contact me.

Yours sincerely

Professor Anne Neville



## Tribological evaluation of plasma nitride H13 steel

\*Solis Romero J., Medina Flores A., Roblero Aguilar O.

SEP-DGEST-Instituto Tecnológico de Tlalnepantla

Av. Tecnológico s/n, Col. la Comunidad, Tlalnepantla de Baz, Edo Mexico, 54070. Mexico

Oseguera Peña J.

Instituto Tecnológico y de Superiores de Monterrey campus Estado de México

Carretera a Lago de Guadalupe km 3.5, Atizapán Edo. Méx., 52926 México.

(Recibido: 29 de septiembre de 2013; Aceptado: 2 de diciembre de 2013)

The influence of nitriding time and applied load in the friction-wear behaviour of an H13 steel has been studied. Weakly ionised plasma unit and a postdischarge plasma reactor were used for nitriding the H13 die steel with variations of nitriding time from 5h to 9h (at 500 °C). Optical microscopy and microhardness deep profiles of the nitrided layer were obtained for each nitriding time. Standard pin-on-disc wear test were conducted at ambient temperature (18-23 °C) and dry sliding. It was observed that the higher the nitriding time, the lower the friction coefficient variations and wear rate varied as a function of the applied load. Plastic deformation and abrasion wear resulted to be the main wear mechanism for short sliding distances, while for long sliding distances plastic deformation dominated the wear mechanism and to some extent oxidative wear. The compound layer (white layer) was central for wear and load capacity.

*Keywords:* Plasma nitriding; H13 steel; Wear; Pin-on-disc; Tribology

### 1. Introduction

The aim of achieving materials with better lifetime has given impetus to the emergence of new technologies and consequently to developments in the understanding of, among others, tribological properties. These challenges have attracted a considerable number of scientists and engineers. Plasma nitriding has been a successfully surface hardening process employed to enhance the fatigue strength, wear and corrosion resistance of bulk materials [1]. This thermochemical treatment involves diffusional addition of nitrogen into the surface of metallic materials. Two different structures are formed from surface to core, namely, a compound layer (white layer) and a diffusion layer. In the former layer generates as epsilon phase ( $\epsilon$ - $Fe_2N$ ,  $\epsilon$ - $Fe_3N$ ), gamma phase ( $\gamma'$ - $Fe_4N$ ), or mixed phase ( $\epsilon + \gamma'$ ) whereas in the diffusion zone, N atoms are dissolved interstitially in excess in the ferrite lattice to give rise to formation of nitride precipitates (CrN) [2, 3]. These compound layers are, generally, hard and brittle but the thin monophase  $\gamma'$  produced by plasma nitriding is extremely ductile and wear resistant according to the  $\epsilon$  phase. Thus, wear characteristics of the compound layer depend on several factors, namely, compound layer composition ( $\epsilon/\gamma'$ ), its thickness, loading type, etc. [4, 5]. From the different nitriding techniques available such as liquid nitriding, gas nitriding and plasma-assisted nitriding; nitriding in the post-discharge flow of microwave generated plasma has proven to reach higher values of nitrogen potential than those achieved in other plasma nitriding treatment [6]. Accordingly, the nitrogen surface concentration can quickly reach the value corresponding to the equilibrium between the atmosphere and the  $\gamma'$  or  $\epsilon$  nitride phases. The process has been successfully applied on H13 steel to improve surface mechanical properties [3].

In particular, although higher hardness levels in shorter nitriding times were obtained respect to other plasma methods, tribological properties were not assessed. It entails the characterisation of tribological properties in terms of friction and wear behaviour.

Wear of extrusion dies has an important technological and economic significance due to cost in order to prevent die failure from thermal cracking, erosive wear, soldering and corrosion or a combination of these processes. H13 die steel is characterised by its high hardenability and toughness, but a relatively low wear resistance. The savings that result from increasing the lifetime of the dies by the enhancements of its tribological properties have motivated researchers to optimise surface treatments suitable to these materials. Therefore, the purpose of the present work is to investigate the influence of a plasma nitriding time on the friction and wear behaviour of H13 steel. To accomplish this undertaken, evaluation of dry friction and wear mechanism at ambient temperature as a function of nitriding time and sliding distance during pin-on-disc wear tests was carried out.

### 2. Materials and Experimental Methods

Nitriding of an H13 die steel was performed in a dual plasma reactor which incorporates a weakly ionised plasma unit that provides continuous cleaning of the sample by sputtering plus heating by ion bombarding and a post-discharge plasma reactor that supplies a highly reactive atmosphere. The apparatus used for the nitriding treatment is shown in Fig.1.

The substrate of the samples in this study was H13 die steel with the following nominal chemical composition (wt. %): 0.32-0.45% C, 0.20-0.50% Mn, 0.80-1.20% Si, 4.75-5.50% Cr, 1.10-1.75% Mo, and 0.8-1.20% V. The samples

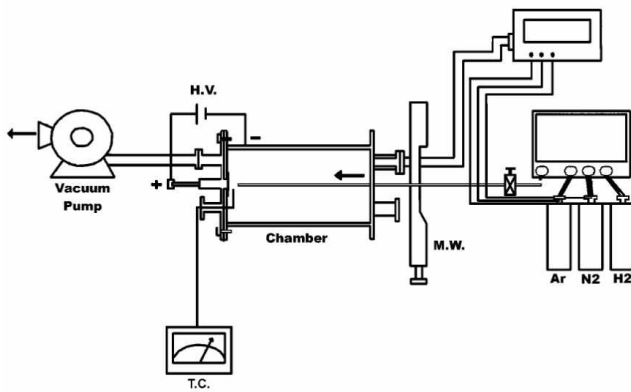


Figure 1. Schematic of the dual plasma reactor showing its main parts. The sample is placed inside the chamber

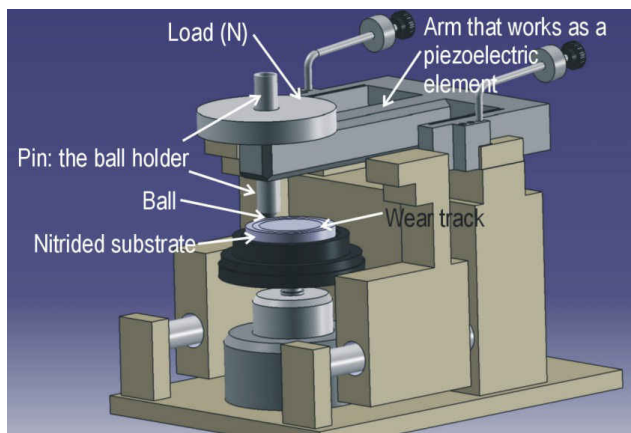


Figure 2. Schematic representation of the pin-on-disc test rig.

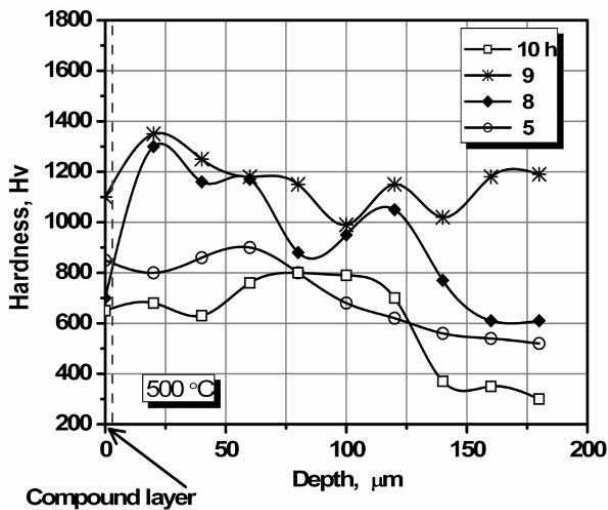


Figure 3. Microhardness profiles as a function of depth for samples nitrided for 5, 8, 9, and 10 h at 500 °C.

with size of 3cm long, 2cm wide, and 2.5 cm thick were first quenched (austenizing at 1020 °C for 2 h, cooling in forced air to room temperature) and two tempering treatments (at 540 °C for 2 h each, followed by forced convection cooling). The hardness of the resulting microstructure was 560 HV<sub>0.1</sub>. The decarburized layer that formed at the surface during heat treatment was removed by grinding. The surface of the sample exposed to the nitriding atmosphere was polished with silicon carbide emery papers and diamond paste to mirror finish (Ra = 0.1±0.02 µm). Nitriding temperature was 500 °C and the nitriding times were 5 h and 9 h, all selected by virtue of minimum and maximum hardness response, respectively as well as the large variation of these as a function of time, as put forward in previous work [3]. Specimens were obtained for cross-sectional analysis by optical microscope. The samples surface was examined by means of X-ray diffraction (XRD), both with and without the surface compound layer (white layer). The compound layer was carefully removed by controlled polishing with 6 µm diamond paste. For microscopic observation, the microstructures of the case depth and substrates were revealed on polished and etched cross sections in a 2% nital solution.

The pin-slid-on-disc (see Fig.2) wear experiments against AISI 52100 (100Cr6) steel ball with 6mm in diameter, 800±40 HV<sub>0.1</sub> hardness and Ra of 0.013 µm were performed in ambient environment with temperature 20-25 °C, humidity 44±5% and no lubricant. Friction force is determined by direct measurement (with a piezoelectric element) of the tangential force applied on the flexible arm. The friction coefficient is given by the ratio between the friction force and the normal force (applied load). The vertically applied loads at the top of the specimens were selected to 2, 5, 7 and 10N; the sliding speed maintained 0.02m s<sup>-1</sup>, and the diameter of the wear track circle slightly varied from 12 to 14mm. The experimental procedure was undertaken according to ASTM G99-95a [7]. Wear losses were determined by wear track measurements and by weight-loss method. Volume loss from flat disc was worked out, assuming no significant pin wear, by means of [7]:

$$V = 2\pi R \left( r^2 \sin^{-1} \frac{d}{2r} - \left( \frac{d}{4} \right) \left( 4r^2 - d^2 \right)^{\frac{1}{2}} \right) \quad (1)$$

where  $R$  denotes the wear track radius;  $r$  represents pin sphere radius (3mm);  $d$  the track width.

Analogously, volume loss from a spherical ended pin was determined by:

$$V = \frac{\pi h}{6} \left( \frac{3d^2}{4} + h^2 \right) \quad (2)$$

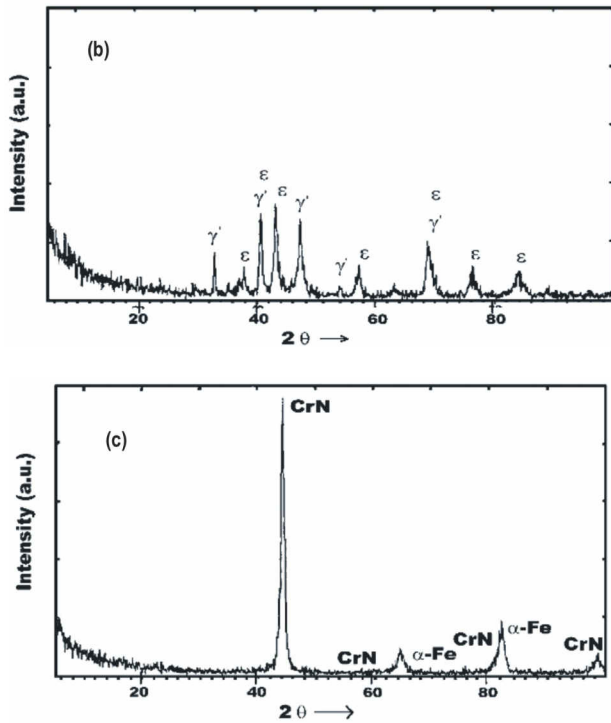
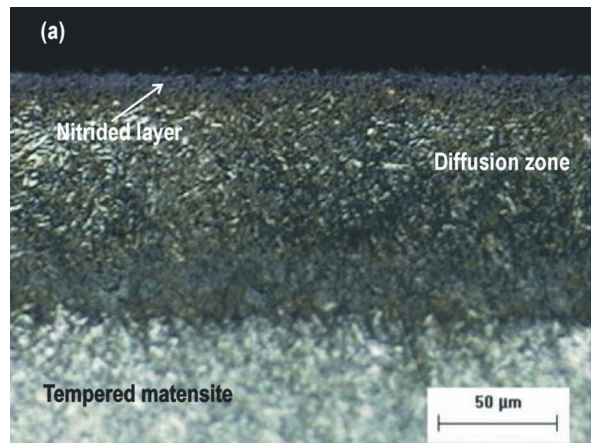


**Figure 4.** (a) Cross sectional microstructure without white layer after 9 h nitriding. XRD diffraction pattern of H13 steel nitrided at 500 °C for 9 h: (b) from the original surface and (c) after the compound layer was removed.

where  $h = r - \left[ r^2 - \frac{d^2}{4} \right]^{\frac{1}{2}}$ ,  $r$  represents pin end radius (3mm) and  $d$  is the wear scar diameter.

Disc wear tracks and pin wear scars were measured by image analysis with an Olympus metallographic light microscope connected to an Image-Pro image analyser. Track widths are the mean values after 12 measurements performed along the pin trails. Mass loss was measured using an electronic balance with precision of 0.1 mg.

For determining the wear rate, typically denoted by  $K$ , the Holm/Archard's relationship was used [8]:

$$K = \frac{\Delta V}{w \cdot s} \quad (3)$$

where  $V$  ( $\text{mm}^3$ ) is the worn volume,  $w$  (N) is the normal force applied and  $s$  (m) is the total sliding distance. For this research, however, the wear volume divided with the sliding distance was defined as the wear rate because the normal force applied was the variable parameter. To identify the wear mechanisms, worn surfaces were observed through the scanning electron microscopy plus energy dispersive X-ray spectroscopy (SEM + EDS) both on top surfaces and also on polished and etched cross sections. The  $HV_{0.05}$  microhardness profiles of the nitrided layers were obtained in the cross section by means of a Shimadzu MMV-2 instrument.

### 3. Results and Discussions

#### 3.1. Surface hardness and microstructure

The hardness evolution for a choice of nitriding times at 500 °C is depicted in Fig.3. There can be seen a significant increase in both a compound layer and a diffusion zone over the matrix hardness. Maximum hardness of the compound layer reached values on the order of 1100  $HV_{0.1}$ . It is also observed that the maximum hardness of the nitrided layer (1350  $HV_{0.1}$ ) was located near to 20  $\mu\text{m}$  below the surface. After these subsurface peaks, hardness exhibited a monotonic decrease in depth, although hardness for 9 h nitriding showed a flatter profile from which the hardness values were as high as 1200  $HV_{0.1}$  at 180  $\mu\text{m}$  depth. Castro *et al.* [9] achieved hardness values on the order of 1100  $HV_{0.05}$  for H13 nitrided in a salt bath activated with sulphur (sursulf nitriding) after 9 h treatment and with a diffusion layer of 110-140  $\mu\text{m}$  depth. For longer nitriding times the surface hardness converged into 1100  $HV_{0.05}$ . There was only a case for the 15 h (190-240  $\mu\text{m}$ ) in which a hardness of 1150  $HV_{0.05}$  was reached. It is interesting to note that whereas for the Castro *et al.* research no compound layer grew before a nitriding time of 7 h at 580 °C, in this work, such layer growth was observed from nitriding times of 5 h upwards and at 500°C. Their previous heat treatment condition to the nitriding treatment was quite similar to heat treatment condition carried out in the present study, which demonstrates that the present method offers some improvement over other nitriding methods, especially in the attainment of flatter hardness profiles which do not favour the development of residual stresses in the hardened layer.

The microstructure for the 9 h nitriding, shown in Fig.4a consists of an internal nucleus of tempered martensite and a nitrided layer in the external surface. The nitrided layer consists of a nitrogen diffusion region with fine elongated nitride plates precipitated and a shallow compound layer on the outside part. In the X-Ray diffraction pattern of Fig. 4b it is indicated that the compound layer consisted mainly of  $\epsilon$ -nitride together with rich  $\gamma'$ -nitride and a mixed phase ( $\epsilon+\gamma'$ ) on the diffusion zone of the nitrided surface. Below the compound layer, the presence of CrN with a small amount of ferrite appears in the diffractogram of Fig. 4c. Generally speaking, at short nitriding times (5 h), there is not enough of the CrN phase to result in a high value of

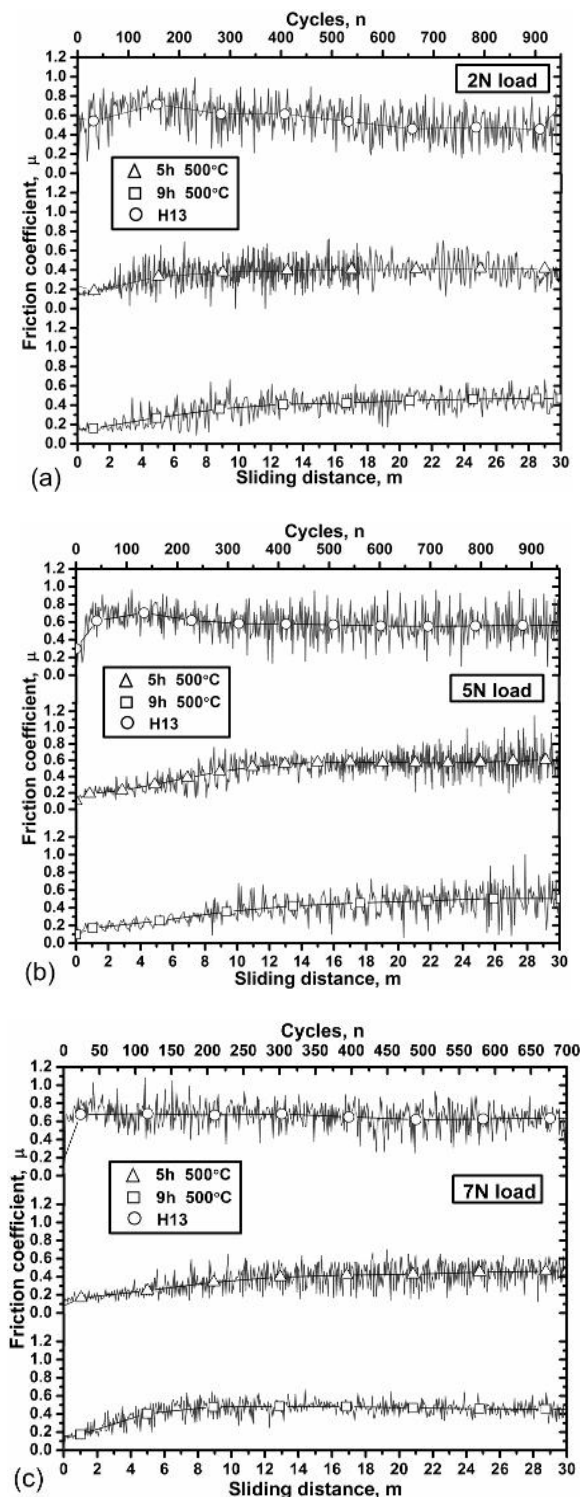


**Figure 5.** Friction coefficient variations of nitrided and non-nitrided H13 steel as a function of sliding distance/cycle for: (a) 2 N sliding load and 12 mm diameter of the wear track circle; (b) 5 N sliding load and 12 mm diameter of the wear track circle; (c) 7 N sliding load and 14 mm diameter of the wear track circle.

hardness, however, at intermediate times (8-9 h); there is an optimum amount, size, and distribution of CrN, which after longer times ( $> 10$  h), it coarsens and as a result, a drop of hardness occurs (see Fig. 3).

### 3.2. Tribological properties

The measurements of the coefficient of friction for plasma nitrided and non-nitrided H13 steel samples as a function of sliding distance/cycles at 2N and 5N sliding loads and 12 mm diameter of the wear track circle are shown in Fig. 5a-b. The friction coefficient variations for a load of 7N and 14 mm diameter of the wear track circle are given in Fig. 5c. The coefficient of friction for the non-nitrided H13 steel for all different loads changed as a function of the distance slid, particularly in the early stages of sliding. It usually exhibited a low initial value (in the range of 0.1-0.2) but rapidly increases until reaching a steady state value. The substantial augment of the frictional force is in turn, a result of the rapid increase in the number of wear fragments entrapped between the sliding surfaces, where some of them, mainly from the disc material, plough such surfaces as can be seen in Fig. 6a. Worn surface consist of ploughed grooves and plastically deformed regions in the sliding direction. These fragments are generated by subsurface deformation, crack nucleation and crack propagation [10]. This can be confirmed by taking a closer look as shown in Fig. 6b. The frictional force is also affected by the escalation in adhesion due to the increase in clean interfacial area as observed by the large variations in the friction coefficient from 0.2 to 0.8 all along the steady state. After a maximum value was reached, the friction coefficient slightly drops to an average value of 0.6 (see Fig. 5). The drop in the friction coefficient is associated with mutual polishing of the mating surfaces and such behaviour results principally when the hardness of the pin is greater than that of the moving disc [10]. Comparable friction coefficient values, and in general, analogous tribological behaviour from *pin-on-disc* tests with a steel ball dry sliding on a steel disc has been previously reported by H. Czichos *et al.*[11].

In the case of longer sliding distance, the friction coefficient does not exhibit any substantial change, i.e. an average value of 0.6 is sustained as well as high friction coefficient variations. Nevertheless, while part of the removed material remains in the contact between pin and disc generating the thin abrasion grooves as observed in Fig. 6, some transfer of material from steel counterbody to H13 steel non-nitrided was exhibited in the form of located heaps on the wear track of the H13 steel. Wear rate of steel counterbody for sliding distance of 30 m was  $3.69 \text{ (mm}^3 \text{ N}^{-1} \text{ m}^{-1} \times 10^{-5})$ , whereas for sliding distance of 100 m was  $8.26 \text{ (mm}^3 \text{ N}^{-1} \text{ m}^{-1} \times 10^{-5})$ . This substantial ball wear increase suggest that large debris particles might have formed causing thick wear tracks with the evident surface penetration. Majority of the removed particles accumulated were pushed through the worn surface of the wear track and during testing deposited on the side of the wear track in the sliding direction. Therefore, large friction coefficient

variations are attributed to hard particles ploughing the sliding pair and to some extent the adhesion between smashed substances coming from the pin.

The nitrided steel, in turn, exhibited a similar friction coefficient pattern for all loads and nitriding times, characterised by the initial running-in period followed by a gradual increase until reaching a gradual steady state. A low initial value of 0.1 was recorded but in this case, there was a gradual ramp up until reaching a steady state value whose range oscillated from 0.4 - 0.5. The initial running-in corresponds to the contact of the disc highest asperities and the ball surface. The gradual increase of the friction coefficient shown in Fig. 5(a-c) can be associated to the real contact between the thin compound layer and the steel ball surface as this leads to an increase of the applied stress on the wear surface and, thus, to the plastic deformation of material. This friction coefficient behaviour also suggests some similitude in hardness both the pin and the disc. On the other hand, for 30 m sliding distances, the compound layer begins to wear out, as seen in Fig. 7. From this figure, the compound layer is being both plastically deformed and partly removed from the wear track. Furthermore, it is observed some degree of compound layer detachment, which can be attributed either the higher contact pressure than the pressure capacity of such layer or the inherent brittleness of such compound layer. In this respect, it is well known the fact that a mixed phase ( $\gamma' + \epsilon$ ), typically observed in gas nitriding, can be prone to spalling since it is brittle and breaks down during the early stage of wear tests [12-13]. In addition, the brittleness of the compound layer is influenced by the  $\epsilon/\gamma'$  phase ratio [5].

A detailed examination of the mildly worn surface of H13 steel nitrided for 9 h is shown in Fig. 8. The higher magnification in Fig. 8 depicts the plastically deformed layer and also it can be seen part of the compound layer underneath this smashed layer. This degraded surface consists of shallow ploughed formations, where a new compacted surface in the valleys can be distinguished as a result of the plastically deformed material and the agglomerated wear debris. The wear rate of steel counterbody at this stage was  $1.223 \text{ (mm}^3 \text{ N}^{-1} \text{ m}^{-1} \times 10^{-5})$ . It thus appears that small debris particles were formed with faint surface penetration. These observations are consistent with friction coefficient variations of H13 steel nitrided, and in particular for 9 h nitriding and sliding distance of 30 m, since it exhibited the smallest variations as seen in Fig. 5 (a-c). In general, it is observed that plasma nitriding and specifically the compound layer has effect on the friction coefficient variations: the higher the nitriding time, the lower the friction coefficient variations. As expected, dry sliding resulted in larger friction coefficient variations for the non-nitrided H13 steels.

The aforementioned observations are also consistent with the wear behaviour of tested steels, as graphically presented in Fig. 9. From this figure, independently of the non-nitrided alloy results, two major observations are underlined and hence, to be analysed. The first one is associated with the applied load, i.e., it is observed that for a given nitrided time, the wear rate increases as a function

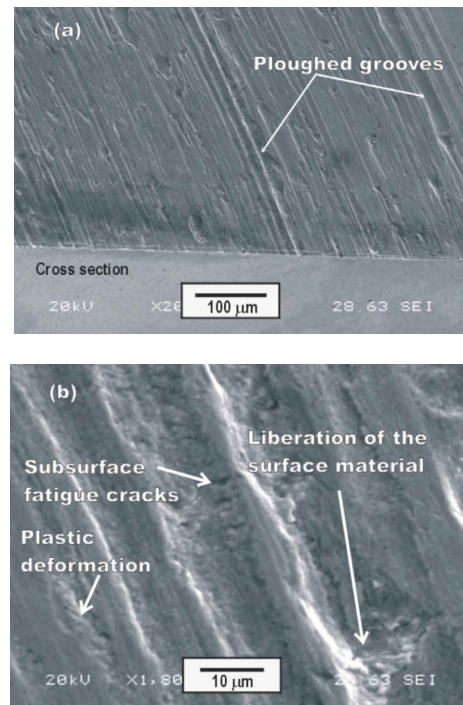


**Figure 6.** Non-nitrided H13 steel tested during a sliding distance of 100 m and 2 N normal load. (a) Worn surface showing the abrasion grooves. (b) A detailed examination of worn surface showing surface fatigue wear and plastic deformation.

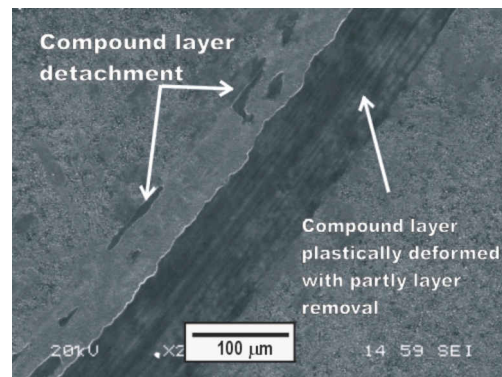


**Figure 7.** Partly worn compound layer of the H13 steel nitrided for 9 h tested during a sliding distance of 30 m and 2N normal load.

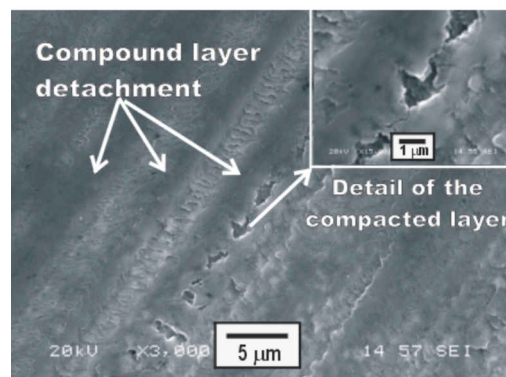


**Figure 8.** The mildly degraded surface of the H13 nitrided steel for 9 h. In the picture of the right up corner, an amplification of a ploughed zone is shown.

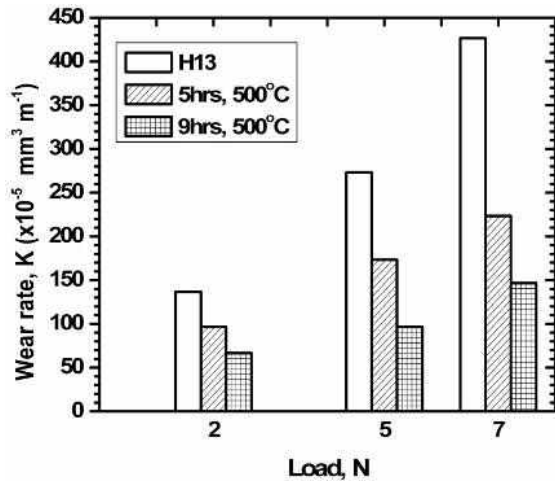


Figure 9. Wear rate behaviour vs. applied load of H13 steel nitrided during selected times compared to that non-nitrided for a sliding distance of 30 m.

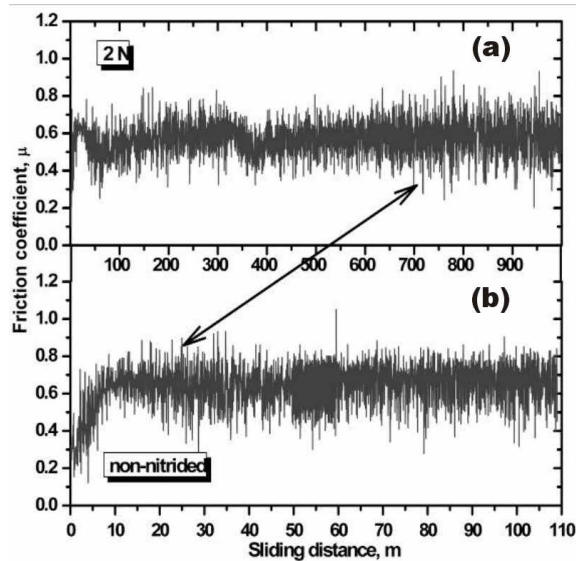


Figure 10. Friction coefficient variations versus the sliding distance of: (a) H13 steel nitrided during 9 h and 2 N applied load and (b) H13 steel non-nitrided with the same applied load. The arrow indicates the beginning of large friction coefficient variations for the nitrided and non-nitrided steel.

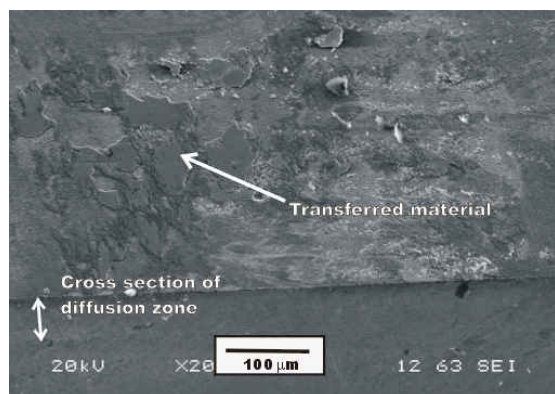


Figure 11. Transferred pin material on the worn surface for a sliding distance of 95 m and 7N applied load.

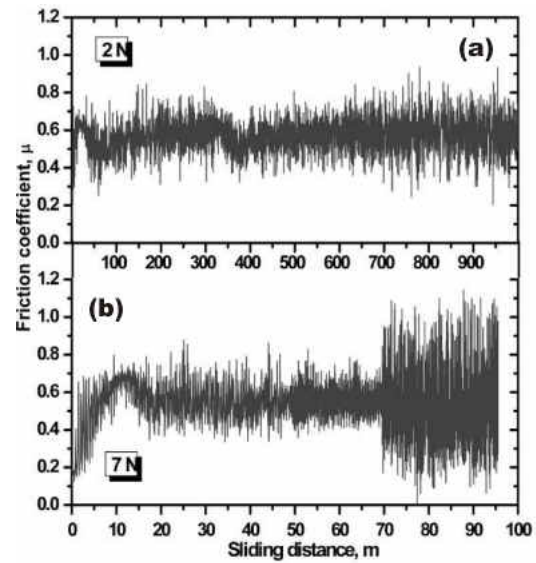


Figure 12. A comparison of the friction coefficient behaviour of: (a) H13 steel nitrided during 9 h and 2 N applied load; (b) H13 steel nitrided during 9 h and 7 N applied load. For this latter load, seizure was observed at 95 m.

of the applied load. This can be ascribed to the mildly removal of the compound layer with the progression of the test. The increment of the normal applied load leads to a rise of the applied shear stress on the wear compound layer resulting in the eventual removal of metal slivers. The second one is related to the nitriding time, i.e., a correlation between surface hardness-appearance-thickness and wear resistance of the compound layer. The H13 steel nitrided during 9 h exhibited the lowest wear rate values clearly manifested at all tested loads, whereas for the H13 steel nitrided during 5 h, higher worn volumes were observed. The local pressures at the points of asperity contacts forge metallic junctions between surfaces. At a given load, friction coefficient ( $\mu$ ) strongly depends on the real contact area which it can be associated with its appearance and surface hardness corresponding to the deformation resistance of the contact area, according to the well known relationship  $\tau = \frac{F\mu}{A} \Rightarrow H = \frac{F}{A}$ , where  $A$  would be the real contact

area,  $\tau$  the shear strength of the junction,  $F$  the applied normal load and  $H$  the mean pressure on an asperity or simply the local hardness of the material. The hardness of the compound layer for 9h and 5 h nitrided steels was recorded to be  $1100 \pm 100 \text{ HV}_{0.1}$  and  $850 \pm 100 \text{ HV}_{0.1}$  respectively. Shallow wear tracks as well as relatively large wear scars on the steel counterbody ( $800 \pm 40 \text{ HV}_{0.1}$ ) were also observed. Therefore, it is clear that the harder surface often corresponds to the higher deformation resistance to prevent the particles, adhered to the softer surface, from pressing into it and protect it from being worn out. Thickness of the compound layer, in turn, influences the wear rate behaviour, i.e. thicker compound layer and nitride layer may provide higher load capacity and deformation resistance, which again, prevents the compound layer from being worn out. Wear rate discrepancies in Fig. 9 may also be attributed to shuffling

off the compound layer by the trackside. As the test progresses the ball scar grows up due to the large-scale wear and consequently it cuts off the trackside, widening the disc wear track.

In order to reach a clearer insight into the behaviour of friction coefficient for nitrided H13 steel alloys sliding against steel, friction variations of H13 nitrided during 9 h and H13 non-nitrided, tested at 2 N applied load for longer sliding distances were attained as shown in Fig. 10. It was observed that in H13 steel nitrided, large friction coefficient variations took place up to sliding distances above 700 m whereas for the non-nitrided steel, comparable variations were observed at sliding distances of 25 m onwards. These findings reveal that the growth of a compound layer (white layer) on top of nitrided layer (nitrogen diffusion zone), for the actual nitriding process, hinders the generation of hard particles or fragments due to the sliding and therefore, slows down ploughing on the sliding disc. This particular behaviour may be interpreted in terms of the  $\epsilon/\gamma'$  phase ratio, i.e. the presence of copiously  $\gamma'$ -nitride (Fig. 3b) in the compound layer increases ductility and wear resistant according to  $\epsilon$  phase [14].

For longer sliding distance and larger applied load, the friction behaviour exhibited the expected features of large plastic deformation followed by a substantial material transfer. Material transfer was mainly observed from the counter-body deposited in the form of patches and to some extent of heaps on the compound layer surface. Those patches and heaps appear as add-on substances both for 2 N and 7 N applied load as shown in Fig. 11. Energy dispersive X-ray analysis (EDS) of the add-on substances obtained in the worn surface of H13 nitrided for 9h and at 2N described a low percentage of chromium and high percentage of carbon and iron, in addition to silicon and oxygen but no nitrogen. It indicated that the transferred material corresponded to the pin.

On the other hand, the friction behaviour for such longer distances can be appreciated in Fig. 12. A comparison between 2N load and 7N clearly shows the shear and transfer effects. Accordingly, highest friction variations are observed above 700m for 9h steel nitrided subjected to 2N applied load. In the case of the 9h steel nitrided with a 7N applied load, massive friction variations come out early around 70m, however, interestingly in this later case, the tribometer suddenly stopped itself by 95 m sliding distance. Evidently, the machine did not manage to carry on due to the frictional forces arisen as a consequence of the larger load. In this respect, under large enough loads the local pressures at the asperity contacts junctions are sheared and therefore, both the real contact area and the nominal area grow because of plastic indentation, mass flow and metallic transfer. These latter effects have been identified as the basis of catastrophic junction growth mainly caused by shear. Following that large-scale mass flow and metallic transfer, the real contact area is.

This condition was identified and modelled as the wear mechanism of seizure [15]. Thus, the 9h steel nitrided seized at about 95 m under 7N applied load.

#### 4. Conclusions

In the present work, the AISI H13 hot work steel was ion nitrided with a dual plasma reactor and surface analysed to measure the frictional and wear characteristics. Pin-on-disc wear tests have been conducted at ambient temperature and dry sliding in both short and long sliding distances. The following conclusions can be derived from the results.

Nitriding of H13 die steel by using a dual plasma reactor offers a substantial advantage over conventional gas nitriding as it provides higher hardness levels in shorter nitriding times.

At short nitriding times (5 h), there is not enough of the CrN phase to result in a high value of hardness. At intermediate times (8-9 h) there is an optimum amount, size, and distribution of CrN which provides the highest hardness values as well as the best hardness profiles. For longer times (> 10 h), CrN coarsens and a reduction of hardness occurs.

The friction coefficient of the nitrided steel under this plasma method increase in the early stage of the wear tests up to a steady state value of 0.4-0.5, regardless the applied load. A steady state friction coefficient of 0.6 for the non-nitrided steel was obtained, also regardless the applied load. At early stages, asperity deformation was identified as the friction-generating mechanism for nitrided steel. For the subsequent stages ploughing showed to be the friction mechanism. Adhesion was significantly increased for long distances, particularly due to the material transfer.

The compound layer has effect on the friction coefficient variations: the higher the nitriding time, the lower the friction coefficient variations.

Wear behaviour on the short sliding distance test was characterised by the influence of two wear mechanisms: plastic deformation and abrasive wear. For long sliding distances the wear mechanism controlling the wear rate was the plastic deformation and to some extent, the oxidative wear. Wear rates of 9h nitrided steel were lowest for all applied loads.

For long sliding distances and large applied loads, the contact area of the counter-body eventually equals the worn surface area and, as a result, the condition of seizure ensues. Due to the latter, the frictional force becomes so high that the test is stopped since the device has not got the power to keep the specimen in rotation. The compound layer enriched with gamma nitride and epsilon nitride generated by the nitriding of H13 die steel in a dual plasma reactor hinders the generation of hard particles or fragments due to the sliding and therefore, slows down ploughing on the sliding disc. Therefore, this layer resulted to be beneficial in terms of wear and load capacity.

#### Acknowledgments

The authors gratefully acknowledge SEP-SES-DGEST-ITTLA and ITESM-CEM, for the support of this research project.

## References

- [1]. Mehmet Baki Karamış, Kemal Yıldızlı, Gamze Çarkıt Aydın. Sliding/rolling wear performance of plasma nitrided H11 hot working steel. *Tribology International*, **51**, 18 (2012).
- [2]. Shi Li and Rafael R. Manory. Comparison of compound layer nucleation mechanisms in plasma nitriding and nitrocarburizing: the effect of CHn species. *Journal of Materials Science*, **34**, 1045 (1999).
- [3]. O. Salas, J. Oseguera, N. García and U. Figueroa. Nitriding of an H13 die steel in a dual plasma reactor. *Journal of Materials Engineering and Performance*. ASM International, **10**, 649 (2001).
- [4]. M. Terčelj, A. Smolej, P. Fajfar and R. Turk. Laboratory assessment of wear on nitrided surfaces of dies for hot extrusion of aluminium. *Tribology International*, **40**, 374 (2007).
- [5]. P. Psyllaki, G.Kefalonikas, G. Pantazopoulos, *et al.*. Microstructure and tribological behaviour of liquid nitrocarburised tool steels. *Surface & Coatings Technology*, **162**, 67 (2002).
- [6]. J. Oseguera, O. Salas, U. Figueroa and M. Palacios. Evolution of the surface concentration during post-discharge nitriding. *Surface & Coatings Technology*, **94**, 587 (1997).
- [7]. Standard Test Method for Wear Testing with a Pin-on-Disk Apparatus ASTM G99 95a (2000).
- [8]. Kenneth Holmberg and Allan Matthews. *Coatings tribology: properties, techniques, and applications in surface engineering*, Elsevier Science B.V. ISBN: 0 444 88870 5 (Amsterdam, The Netherlands 1994).
- [9]. G. Castro, A. Fernández-Vicente and J. Cid. Influence of the nitriding time in the wear behaviour of an AISI H13 steel during a crankshaft forging process. *Wear*, **263**, 1375 (2007).
- [10]. Nam P. Suh and H.C. Sin. The genesis of friction. *Wear*, **69**, 91 (1980).
- [11]. Horts Czichos, Susanne Becker and Jurgen Lexow. Multilaboratory Tribotesting: Results from the Versailles Advanced Materials and Standards Programme on Wear Test Methods. *Wear*, **114**, 109 (1987).
- [12]. M. B. Karamis. An investigation of the properties and wear behaviour of plasma nitrided hot-working steel. *Wear*, **150**, 331 (1991).
- [13]. Yucel Birol, Analysis of wear of a gas nitrided H13 tool steel die in aluminium extrusion. *Engineering Failure Analysis*, **26**, 203 (2012).
- [14]. M. Terčelj, A. Smoleja, P. Fajfar and R. Turk. Laboratory assessment of wear on nitrided surfaces of dies for hot extrusion of aluminium. *Tribology International*, **40**, 374 (2007).
- [15]. S.C. Lim and M.F. Ashby. Wear-Mechanism Maps. *Acta Metallurgica*, **35**, 1 (1987).



**INSTITUTO TECNOLÓGICO DE TLALNEPANTLA**

**HORARIO DE ACTIVIDADES**

SECRETARÍA DE EDUCACIÓN PÚBLICA  
 INSTITUTO TECNOLÓGICO DE TLALNEPANTLA  
 HERNANDO CASTELLANO  
 DIRECTOR DEL INSTITUTO

INSTITUTO TECNOLÓGICO DE TLALNEPANTLA  
 C.C.T.: 16DT0825M  
 PERIODO ESCOLAR: ENERO-JUNIO-2013  
 CLAVE COMPLETA DE LA(S) PLAZA(S): 1103 1402 E3863 00.B 14-1033  
 NOMBRE COMPLETO: JOSE SOLIS ROMERO  
 R. F. C.: SORJ530126781  
 NO. DE HRS. DE NOMBRAMIENTO: 40  
 TITULADO: X  
 TIPO DE NOMBRAMIENTO: 10  
 PASANTE: X  
 NO. DE TARJETA DE CONTROL: 451  
 FECHA DE INGRESO A LA S.E.P.: 198617  
 FECHA DE INGRESO A LA INSTITUCIÓN: 198617

ASIGNATURA	CLAVE ASIGNATURA	GRUPO	AULA TALLER O LAB.	NIVEL	MODALIDAD	CARRERAS	HORARIO							TOTAL HRS SEMANALES						
							L	M	M	J	V	S	HT		HP					
INTRODUCCIÓN AL MET. DEL ELEM. FINITO	S/C	1	LC POSG	M	E	M. MECA.														
DISEÑO E ING. ASISTIDOS POR COMP.	EMC1010	L61	LCA	L	E	MECÁNICA	16-18	18-19	21-22	18-18	18-19									
DIRECCIÓN DE 4 TESIS DE MAESTRÍA																				
SUBTOTAL							0	3	4	3	0									
TOTAL							0	3	4	3	0									10

**II.- ACTIVIDADES DE APOYO A LA DOCENCIA**

NOMBRE DE LA ACTIVIDAD	METAS A ATENDER	HORARIO							TOTAL HRS SEMANALES												
		L	M	M	J	V	S	HORAS													
ACTIVIDADES DE CAPACITACIÓN Y SUPERACIÓN PROFESIONAL A ESTUDIANTES Y PASANTES	13																				
ELABORAR Y VALIDAR PROYECTOS Y PROGRAMAS DOCENTES																					
PREPARAR A LA DOCENCIA Y A LA INVESTIGACIÓN	8,9,10,11,14,17				11-19			11-16		11-18	11-19								30		
SUBTOTAL							8	5	4	5	8									30	
TOTAL							8	8	8	8	8										40

**III.- ACTIVIDADES EN LA ADMINISTRACIÓN**

PUESTO	UNIDAD ORGÁNICA DE ADSCRIPCIÓN	HORARIO (20)							TOTAL HRS SEMANALES											
		L	M	M	J	V	S	HORAS												
PREPARATORIA ( )																				
Secundaria ( )																				
Primaria ( )																				
Otro ( ) Especificar:																				
SUBTOTAL																				
TOTAL																				

PERSONAL NO DOCENTE:  
 PUESTO: DR. JOSE SOLIS ROMERO  
 UNIDAD ORGÁNICA DE ADSCRIPCIÓN: ENCARGADO DE LA DIVISIÓN DE ESTUDIOS DE POSGRADO E INVESTIGACIÓN  
 OBSERVACIONES: El presente horario aplicará a partir del 28 de enero de 2013. Para fines de carga académica, las materias de maestría cuentan doble y cada dirección de tesis de posgrado cuenta 2 horas (circular 018 de la DGEST)

FECHA DE ASESORIA DE LA INFORMACIÓN: 29-ENERO-2013  
 SELLO: M.C. GILBERTO PÉREZ LUQUE  
 SUBDIRECCIÓN ACADÉMICA

SECRETARÍA DE EDUCACIÓN PÚBLICA  
 D. G. A. E. S. T.  
 SUBDIRECCIÓN ACADÉMICA

PRESENTE ES COPIA FIEL DEL DOCUMENTO ORIGINAL QUE SE TUVO A LA VISTA.

*[Handwritten Signature]*  
 FIRMA

SECRETARÍA DE EDUCACIÓN PÚBLICA  
 INSTITUTO TECNOLÓGICO DE TLALNEPANTLA  
 DIRECCIÓN

C.c.p.- Subdirección Académica  
 ITLA-AC-PO-004-06

C.c.p.- Departamento de Planeación, Programación y Presupuestación  
 S. E. P. I. T. T. L. A.

**RECIBIDO**  
 11 FEB 2013  
 RECURSOS HUMANOS  
 SECCION CONTROL DE PERSONAL

## La Red Temática de Ingeniería de Superficies y Tribología (REDISYT)



Hace constar que el (la):

**C. Solis Romero José**

Es **MIEMBRO INVESTIGADOR**, con los derechos y obligaciones establecidos en los

Estatutos de la Red



Guadalajara, Jalisco, México a 18 de diciembre de 2015

Comité Técnico Académico de la REDISYT 2015-2017



Instituto Tecnológico Superior

**Dr. Martín Flores Martínez**

**Presidente**



Universidad Veracruzana



4<sup>th</sup> July 2013

To whom it may concern:

RE: Jose Solis-Romero

This is to confirm that we will gladly welcome Dr Jose Solis-Romero on his sabbatical leave to our Institute.

The main objectives of the study period will be:

- to advance the understanding of the microwave PVD technique as a means of depositing tribological coatings on to steels
- to establish long term relationships between iETSI and ITTLA
- to contribute to the scientific literature in this area.

Jose will have access to our laboratory facilities and in particular he will work on the Hauzer Flexicoat 850 PVD instrument with a unique microwave capability integrated within the conventional PVD system. Also all of the required surface analysis equipment, TEM, SEM, SIMS will be accessible.

We would invite Jose to also take part in our seminar programme for our postgraduate and MSc students and will fully integrate him in the research group.

If you require any further information, please don't hesitate to contact me.

Yours sincerely

A handwritten signature in cursive script that reads "Anne Neville".

Professor Anne Neville

SEP

SECRETARÍA DE EDUCACIÓN PÚBLICA



Subsecretaría de Educación Superior  
Dirección General de Educación Superior Tecnológica  
Instituto Tecnológico de Tlalnepantla

"2014, Año de Octavio Paz"

ASUNTO: CONSTANCIA DE ADSCRIPCIÓN

**SISTEMA NACIONAL DE INVESTIGADORES (CONACyT)  
PRESENTE**

El que suscribe, **DIRECTOR del INSTITUTO TECNOLÓGICO DE TLALNEPANTLA, CERTIFICA** y hace **CONSTAR** la **ADSCRIPCIÓN** y **ACTIVIDADES** que desarrolla en esta institución el DR.:

NOMBRE: SOLIS ROMERO JOSÉ  
 FILIACIÓN: SORI630126781  
 CLAVE(S) PRESUPUESTAL(ES): 14.02 E3863 00.0 141033  
 FECHA DE INGRESO ITTLA/SEP: 1° DE SEPTIEMBRE DE 1986  
 TIPO DE NOMBRAMIENTO ACTUAL: (10) BASE  
 CATEGORÍA(S) ACTUAL: PROFESOR INVESTIGADOR DE CARRERA TITULAR "C" (40 HRS., PTC)  
 DEPARTAMENTO DE ADSCRIPCIÓN: DIVISIÓN DE ESTUDIOS DE POSGRADO E INVESTIGACIÓN  
 PERÍODO DE LICENCIAS: AÑO SABÁTICO AUTORIZADO\* (13/01/2014-12/01/2015)  
 FUNCIONES DOCENTES:  
 FUNCIONES ADMINISTRATIVAS:  
 FUNCIONES DE INVESTIGACIÓN: PROYECTO EN PERÍODO SABÁTICO: EVALUACIÓN TRIBOLÓGICA DE SUPERFICIE DE ACERO MODIFICADA CON PELÍCULA DE CARBÓN TIPO DIAMANTE (DLC) POR MEDIO DE PLASMA FRÍO DE MICROONDAS (PECVD). REALIZANDO LA INVESTIGACIÓN EN LA UNIVERSIDAD DE LEEDS, UK

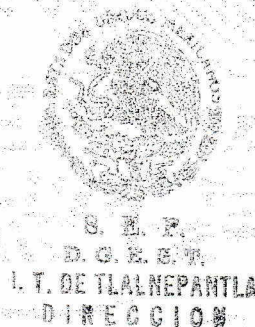
\*Nota: Se envió la notificación correspondiente a su debido tiempo al personal de la Subdirección de Seguimiento del SNI.

A petición del interesado, se extiende la presente en Tlalnepantla de Baz, Estado de México, a los nueve días del mes de Mayo del año dos mil catorce.

ATENTAMENTE

*"Por la Realización Tecnológica de mi Pueblo"*

  
ING. OSCAR CASTELLANOS HERNÁNDEZ  
DIRECTOR



c.c.p. Dirección, Recursos Humanos, División de Estudios de Posgrado  
Interesado.

CAMPUS TLALNEPANTLA  
OCTACZNS/VADE/mve Instituto Tecnológico S/N  
Col. La Comunidad C.P. 54070  
Tlalnepantla de Baz, México  
Tel: 5553900310 / 5553900209

CAMPUS ORIENTE  
Av. Hermilo Mena S/N,  
Col. Lázaro Cárdenas La Presa C.P. 54187  
Tlalnepantla de Baz, México  
Tel: 5553846464

